Title

Quantifying the Relationships Among Selective Motor Control, Brain Imaging, Biomechanics and Physical Therapy in Children with Spastic Bilateral Cerebral Palsy

Author

Vuong, Andy

Publication Date

2022

Peer reviewed|Thesis/dissertation

UNIVERSITY OF CALIFORNIA

Los Angeles

Quantifying the Relationships Among Selective Motor Control, Brain Imaging, Biomechanics and Physical Therapy in Children with Spastic Bilateral Cerebral Palsy

A dissertation submitted in partial satisfaction of the requirements for the degree of Doctor of Philosophy in Bioengineering

by

Andy Vuong

2022

ABSTRACT OF THE DISSERTATION

Quantifying the Relationships Among Selective Motor Control, Brain Imaging, Biomechanics and Physical Therapy in Children with Spastic Bilateral Cerebral Palsy

by

Andy Vuong

Doctor of Philosophy in Bioengineering

University of California, Los Angeles, 2022

Professor Eileen G. Fowler, Co-Chair

Professor Shantanu H. Joshi, Co-Chair

Cerebral palsy (CP) is a motor disorder caused by an injury to the developing fetal or infant brain. While the corticospinal tract (CST) is related to selective motor control (SMC) function, an underlying deficit in spastic CP, little is known about CST microstructural impairment, its relationship with motor function measures and neuroplasticity in response to a physical therapy intervention focused on intensive practice of lower extremity (LE) SMC exercises. The aim of this dissertation was to study the effect of Camp Leg Power, a novel LE SMC intervention in spastic CP, on measures of white matter (WM) motor tract microstructure and motor function measures.

Children with unilateral or bilateral spastic CP born premature were recruited for Camp Leg Power. Diffusion-weighted imaging scans were collected for participants with bilateral CP

and periventricular leukomalacia (PVL). Children with typical development (TD) were recruited as brain imaging controls. The Selective Control Assessment of the Lower Extremity (SCALE) and the gross motor function measure were collected for all participants with CP. Motor function measures analyzed included the 10-meter walk/run test, 6-minute walk test, stride length during gait and isokinetic knee joint torque.

Twenty-three children with spastic CP were enrolled (3 unilateral, 20 bilateral; mean age ± SD: 10.1 ± 2.8 years; age range: 5.6-16.6 years). Diffusion-weighted imaging scans were evaluated for a subset of 12 participants with spastic bilateral CP and PVL and 12 children with TD (mean age ± SD: 10.3 ± 1.5 years; age range: 7.5-12.8 years). The CP group exhibited lower anisotropy, damaged myelination, decreased axonal integrity and greater overall diffusivity throughout the whole brain including WM motor tracts relative to TD. The CP group improved their motor function following Camp Leg Power coinciding with improved myelination of brain motor regions suggesting neuroplasticity in response to intervention. SCALE is a strong clinical correlate of brain motor impairment, baseline motor function and post-intervention motor outcomes.

This work contributes to the overall understanding of neuroimaging, clinical correlates of impaired WM and biomechanics measures, neuroplasticity and motor function changes in response to a novel LE SMC intervention in spastic CP.

The dissertation of Andy Vuong is approved.

Katherine L. Narr

Alan Garfinkel

Rachel M. Thompson

Joyce H. Matsumoto

Eileen G. Fowler, Committee Co-Chair

Shantanu H. Joshi, Committee Co-Chair

University of California, Los Angeles

2022

This dissertation is dedicated to my loving partner Wendy Renteria.

Table of Contents

Chapter 1: Introduction……1

1.1 Cerebral Palsy……1

1.2 Periventricular Leukomalacia……2

1.3 Corticospinal Tracts……..……3

1.4 Selective Motor Control……..……...3

1.5 The Selective Control Assessment of the Lower Extremity……...…….4

1.6 Other Clinical Measures in CP……..…….5

1.7 Diffusion-Weighted Imaging…….6

1.8 Diffusion Tensor Imaging……..……7

1.9 Significance of the Study……..10

Chapter 2: Tractography of the Lower Extremity Corticospinal Tracts……..12

2.1 Introduction……..…12

2.2 Methods……14

2.2.1 Study Cohort……..14

2.2.2 Selective Control Assessment of the Lower Extremity (SCALE)……..15

2.2.3 MRI and Diffusion-Weighted Imaging Protocols……..15

2.2.4 Tractography of the Corticospinal Tracts……..16

2.2.5 Statistical Analysis……20

2.3 Results……..……21

2.4 Discussion. ……..28

Chapter 3: Selective Motor Control is a Clinical Correlate of Brain Motor Tract Impairment in Children with Spastic Bilateral Cerebral Palsy……..…….32

3.1 Introduction……..……32

3.2 Materials and Methods…….35

3.2.1 Participants……35

3.2.2 Clinical Assessments. ……...36

3.2.3 MRI Protocols……...36

3.2.4 Statistical Analysis……37

3.3 Results……..38

3.3.1 Group Differences..……...39

3.3.2 Correlation Analyses…….42

3.4 Discussion……47

3.5 Conclusions……..……52

Chapter 4: Improved Myelination Following Camp Leg Power, a Selective Motor Control Intervention for Children with Spastic Bilateral Cerebral Palsy: a Diffusion Tensor MRI Study...54

4.1 Introduction……..54

4.2 Materials and Methods…….57

4.2.1 Participants……57

4.2.2 Functional Outcome Measures.…….....58

4.2.3 Lower Extremity Selective Motor Control Intervention (Camp Leg Power).58

4.2.4 Image Acquisition Protocol……...……59

4.2.5 Statistical Analysis……....60

4.2.6 Region of Interest Parcellation……...60

4.3 Results……..61

4.4 Discussion……66

Chapter 5: Selective Motor Control is a Clinical Correlate of Baseline Motor Outcomes and Motor Outcome Changes Following Camp Leg Power……71

5.1 Introduction……..71

5.2 Methods……73

5.2.1 Participants……73

5.2.2 Clinical Assessments……74

5.2.3 Lower Extremity Selective Motor Control Intervention (Camp Leg Power).74

5.2.4 Motor Outcome Measures……76

5.2.5 Gait Analysis……76

5.2.6 Statistical Analysis……77

5.3 Results……..78

5.3.1 Baseline Motor Outcome Correlations with SCALE……79

5.3.2 Post-Camp Leg Power Motor Outcome Changes……..83

5.4 Discussion……89

Chapter 6: Post-Camp Leg Power Correlation Analyses Among Selective Motor Control, Brain Imaging and Biomechanics……92

6.1 The Relationship Between Selective Motor Control and Brain Imaging……..92

6.2 The Relationship Between Selective Motor Control and Biomechanics…….……..94

6.3 The Relationship Between Brain Imaging and Biomechanics……..95

Chapter 7: Summary and Future Directions……99

7.1 Summary……..99

7.2 Future Directions……100

List of Figures

Figure 1-1: T1-weighted image from an axial view……..6

Figure 1-2: Tensor examples of isotropic diffusion……..8

Figure 1-3: Equations for each DTI measure……9

Figure 2-1: Initial tract-specific ROI method……..16

Figure 2-2: Tractography ROI method for isolating……...18

Figure 2-3: Anatomical location of the CSTs……19

Figure 2-4: ROIs used to segment the "full CST" ……..20

Figure 2-5: Correlation graphs for DTI outcomes of LE CSTs……...23

Figure 2-6: Correlation graphs for DTI outcomes within the PLIC……25

Figure 2-7: Correlation graphs for DTI outcomes between the PLIC and CerPed……..27

Figure 3-1: Steps involved in the TBSS pipeline……34

Figure 3-2: TBSS results display significant differences……40

Figure 3-3: Mean differences in DTI measures……...42

Figure 3-4: TBSS results display significant correlations……...43

Figure 4-1: TBSS results show significant reductions……62

Figure 5-1: Camp Leg Power participants on the Biodex……75

Figure 5-2: The modified Helen Hayes marker set……77

Figure 5-3: Baseline correlation between 10mWRT times……79

Figure 5-4: Baseline correlation between 6MWT distances……...80

Figure 5-5: Baseline correlation between GMFM……..80

Figure 5-6: Baseline correlations between ankle plantar……81

Figure 5-7: Left and right KE torque correlations……...81

Figure 5-8: Left and right KF torque correlations……...82

Figure 5-9: Left and right normalized step lengths……82

Figure 5-10: Normalized stride length versus……83

Figure 5-11: 10mWRT times at pre, post and FU……...84

Figure 5-12: 6MWT distances at pre, post and FU……84

Figure 5-13: GMFM scores at pre, post and FU……84

Figure 5-14: Percent knees able to generate KE and KF torque……85

Figure 5-15: Left KE torque for high and low SCALE score groups……86

Figure 5-16: Left KF torque for high and low SCALE score groups……87

Figure 5-17: Right KE torque for high and low SCALE score groups……87

Figure 5-18: Right KF torque for high and low SCALE score groups……88

Figure 5-19: Normalized stride lengths for participants walking……89

Figure 6-1: Right PLIC RD and MD changes versus total SCALE score……...…93

Figure 6-2: Left fornix RD changes versus total SCALE score……...……93

Figure 6-3: Left KF changes at 180 and 240 deg/s versus left SCALE score……95

Figure 6-4: Right KF changes at 180 and 240 deg/s versus right SCALE score……95

Figure 6-5: Change in average KF torque at 120 deg/s versus CC genu RD changes……97

Figure 6-6: Change in right KF torque at 120 deg/s versus right ACR MD changes……98

Figure 6-7: Change in right KF torque at 120 deg/s versus left SFOF MD changes……98

List of Tables

Table 2-1: Demographics of participants with CP……..21

Table 2-2: Bilateral SCALE scores of each participant……...22

Table 2-3: Average DTI values for LE CSTs……..22

Table 2-4: Average DTI values within the PLIC……24

Table 2-5: Average DTI values between the PLIC and CerPed……..26

Table 3-1: Demographics of the CP and TD groups……39

Table 3-2: Correlations between clinical measures……45

Table 3-3: ROI correlation analyses comparing……46

Table 4-1: Average DTI decreases within WM ROIs……64

Table 4-2: Voxel counts of WM ROIs……65

Table 5-1: Demographics of all participants with spastic CP in Camp Leg Power……78

Acknowledgements

In completion of my graduate studies, I am greatly indebted to many people that form a caring community dedicated to serving people with disabilities at UCLA. First and foremost, I am forever grateful to have worked under the supervision of Dr. Eileen Fowler, my longtime mentor who has filled the role of advisor, teacher and role model. I am thankful that she presented me the opportunity to work in the Kameron Gait and Motion Analysis Laboratory and Center for Cerebral Palsy at UCLA/Orthopedic Institute for Children. Under her guidance, my expertise in the scientific process, pediatric neurological disorders, gait biomechanics, biomedical imaging and research has flourished as she provided the autonomy, intellectual guidance and community resources to help me grow. She has always encouraged me to be curious in the endless pursuit of problems, questions and answers. She taught me how to be the best version of myself that I can be, with confidence, integrity and purpose. I am so thankful and recognize how incredibly lucky I am to have joined her laboratory and research for my graduate studies.

I have also gained invaluable mentorship and insight from my committee members: Dr. Shantanu Joshi, Dr. Joyce Matsumoto, Dr. Rachel Thompson, Dr. Alan Garfinkel and Dr. Katherine Narr. I met Dr. Joshi and Dr. Matsumoto a year or so into my doctoral studies. They never hesitated to provide help and lend their knowledge and expertise in biomedical imaging and pediatric neurology, respectively. They helped me build a solid foundation for the major topics of my dissertation and have continuously offered assistance without fail. I met Dr. Garfinkel at the beginning of my graduate career as well and I have the highest regard for him being in the unique position of the best professor I have ever had in class. His teachings in his course on dynamical systems modeling of physiological processes still resonate with me today and his passion on the subject matter has greatly influenced me. I met Dr. Thompson in the latter years of my graduate

studies. Her knowledge, skill and confidence as an orthopedic surgeon and role as director for the Center for CP inspires me to hone my own skills as a researcher and to work extremely hard to become an expert in any future endeavor and career that I choose. I met Dr. Narr in the last year of my PhD and she gracefully accepted the role of serving on my committee. Her expertise in neurology has only improved my work at UCLA and having her constructive criticisms and curiosity on my side has been paramount to my growth as a researcher.

Dr. Bill Oppenheim, Loretta Staudt, Christy Skura, Marcia Greenberg and Dr. Kristen Reider were all integral parts of the Center for CP, aiding in its creation and continued growth in serving patients globally. I am thankful to have met and worked with every one of them and each person made significant contributions to my pleasant experience at UCLA. Undoubtedly, my PhD and the mountain of data collection, analysis and evidence would not have been possible without them.

I am incredibly humbled by and appreciative of every patient I have had the pleasure of crossing paths within the gait and motion analysis laboratory. It was truly an honor and my privilege to serve in their care, and their health and well-being has always and forever will be at the forefront of my mind. I am also forever grateful to have met and mentored the large number of students and volunteers through the Center for CP including Kate Christoferson, Vinh Nguyen, Priyanka Bhakta, Vivan Nguyen, Yuhang Cai, Isabel Chu, Rachel Hunsucker, Kevin Sullivan, Saskia van Ommeren-Egberts, Connie Lu, Israa Dahbour, Alex Seder and Ahan Agarwal. Every one of these students took the initiative and challenged themselves to advance their own education and assist underserved populations. Additionally, they all aided me with data collection, processing and analysis. I truly believe that all of our relationships were mutually beneficial and that the future of science and health care is in great hands.

Lastly, I would like to thank my family and friends. Without my parents, Xuan Huynh and Tri Vuong, I would not be the person I am today. I felt their sense of pride in this challenging journey I have taken and could not have done it without their support. Most importantly, I would like to thank my loving partner, friend and confidant, Wendy Renteria, without whom I would not have had the courage and strength to finish my doctoral degree. We met when I was just the naïve age of 14 years old and I consider myself the most fortunate person in the world to have had her in what is now the majority of my life.

Every person that I listed above has been so patient and understanding in this challenging process and I feel as though I am standing on the shoulders of giants. If every person in the world were granted access to the community I have had during these years, it would only be a kinder and more loving place. I am grateful for all the funding that has allowed me to pursue my PhD. Data acquisitions were funded by donations and grants from the UCLA Children's Discovery and Innovation Institute, Shapiro Family Foundation, United Cerebral Palsy of Los Angeles, Santa Barbara and Ventura Counties, Waters Foundation, California Community Foundation, Lena Longo Foundation and UCLA Brain Mapping Center. Additional support was received from the National Center for Advancing Translational Science of the National Institutes of Health under the UCLA Clinical and Translational Science Institute grant number UL1TR001881.

Chapter 3 is a version of: Vuong, A., Fowler, E.G., Matsumoto, J.H., Staudt, L.A., Yokota, H., Joshi, S.H. (2021). Selective Motor Control is a Clinical Correlate of Brain Motor Tract Impairment in Children with Spastic Bilateral Cerebral Palsy. *American Journal of Neuroradiology*, 42(11): 2054-2061. AJNR copyright agreement allows a journal author to retain proprietary rights such as the right to use all or part of this article in future works of their own.

Chapter 4 is a version of: Vuong, A, Joshi, S.H., Staudt, L.A., Matsumoto, J.H., Fowler, E.G. (2022). Improved myelination following Camp Leg Power, a selective motor control intervention for children with spastic bilateral cerebral palsy: a diffusion tensor MRI study. This work has not yet been published and was submitted to the *American Journal of Neuroradiology* for review.

Chapter 5 contains elements from a version of: Fowler, E.G., Staudt, L.A., Greenberg, M.B., Vuong, A., Reider, K.M. (2022). Selective voluntary motor control predicts the rate of torque development and knee joint torque across a range of speeds in children with spastic cerebral palsy. This work along with other data presented in Chapters 5 and 6 are in preparation for publication.

VITA

2015	B.S. in Biophysics with a double major in Mathematics
	Wake Forest University
	Winston-Salem, North Carolina
2017-2018	STEM Career Consultant
	UCLA Career Center
	University of California, Los Angeles
2019	M.S. in Bioengineering
	University of California, Los Angeles
	Los Angeles, California
2015-2022	Graduate Student Researcher
	Department of Orthopedic Surgery
	University of California, Los Angeles

PUBLICATIONS AND PRESENTATIONS

Vuong, A., Heberer, K., Greenberg, M., Bernthal, N., Yamaguchi, K., Eckardt, J., Fowler, E.G. (2017). "Gait outcomes post proximal tibial tumor resection and endoprosthetic reconstruction." In: Proceedings of the 21st Annual Meeting of the Gait and Clinical Motion Analysis Society (GCMAS). Salt Lake City, Utah. Presentation.

Fowler, E.G., Staudt, L., Greenberg, M., Kelley, C., Skura, C., Vuong, A. (2017). Camp leg power: intensive training of lower extremity motor control for children with spastic cerebral palsy. Developmental Medicine & Child Neurology, 59(S3): 48-49. Abstract.

Vuong, A., Fowler, E.G., Matsumoto, J., Staudt, L., Greenberg, M., Yokota, H., Joshi, S. (2019). Clinical correlates of impaired white matter tracts in children with spastic bilateral cerebral palsy. Developmental Medicine & Child Neurology, 61(S3): 51-52. Abstract.

Vuong, A., Fowler, E.G., Staudt, L., Greenberg, M., Yokota, H., Matsomoto, J., Joshi, S. (2020). Diffusion imaging shows improved myelination following an intervention targeting skilled lower extremity movement in children with spastic bilateral cerebral palsy. Developmental Medicine & Child Neurology, 62(S3): 27-28. Abstract.

Fowler, E.G., Eckardt, J.J., Vuong, A., Greenberg, M.B., Yamaguchi, K., Bukata, S.V., Bernthal, N. (2021). Gait outcomes following proximal tibial tumor resection and endoprosthetic reconstruction. Gait & Posture, 88:167-173.

Vuong, A., Fowler, E.G., Matsuomoto, J., Staudt, L.A., Yokota, H., Joshi, S.H. (2021). Selective Motor Control is a Clinical Correlate of Brain Motor Tract Impairment in Children with Spastic Bilateral Cerebral Palsy. American Journal of Neuroradiology, 42(11): 2054-2061.

Chapter 1: Introduction

1.1 Cerebral Palsy

Cerebral palsy (CP) is one of the most common childhood disabilities in the United Sates. In 1992, Rosen and Dickensen aggregated published research studies regarding CP and reported its incidence rate to be roughly 2.7 cases out of every 1,000 live births by the age of 5 to 7 years (Rosen and Dickinson, 1992). According to Rosenbaum et al., CP describes "a group of disorders of the development of movement and posture, causing activity limitation, that are attributed to non-progressive disturbances that occurred in the developing fetal or infant brain. The motor disorders of CP can be accompanied by disturbances of sensation cognition, communication, perception, and/or behavior, and/or by seizure disorder" (Bax et al., 2005). While the function deficit in those with CP ranges from slight coordination difficulties to total body involvement with sensorimotor and cognitive impairment, this study focuses primarily on participants who have either spastic unilateral (involving one arm and one leg on the same side of the body) or spastic bilateral (involving both legs) CP. Within spastic CP, there is a wide range of clinical outcomes and lower extremity (LE) function varies among individuals.

Spastic CP is one of three major types of CP (the others being athetoid and ataxic) and consists of the majority of diagnoses. One multisite study reported the prevalence of spastic CP as high as 77% among all cases, with bilateral spastic CP at 70% within the spastic group (Bass, 1999; Yeargin-Allsopp et al., 2008). Spasticity classifies those whom exhibit a form of hypertonia, a condition marked by an abnormal increase in muscle tension and a reduced ability of a muscle to stretch. In spastic CP, there is an increase in resistance to passive stretch that is dependent on velocity and direction of joint movement and/or resistance to an externally imposed movement

that increases above a threshold velocity or joint angle, and this resistance is associated with hyperactivity of deep-tendon stretch reflexes (Peacock and Staudt, 1990; Sanger et al., 2003).

As there is no cure for CP, the primary focuses are on prevention, early detection and physical rehabilitation. The standard of care for children with spastic CP typically ranges from orthopedic surgery, botulinum toxin (BTX) injections to culprit muscles, physical therapy (PT) regimens, foot, ankle and leg orthotics/splints and serial casting. Most ambulatory children with CP will likely undergo a multitude of treatments throughout their lives and the success of each treatment is dependent on a number of factors including underlying impairment of motor ability.

1.2 Periventricular Leukomalacia

Periventricular leukomalacia (PVL) is a magnetic resonance imaging (MRI) finding associated with perinatal injury to the cerebral white matter (WM) (Volpe, 2009; Lee et al., 2011; Ceschin et al., 2015). Children born prematurely are at higher risk of neurologic sequelae including spastic CP associated with PVL. It has been found that damage to WM of the brain, in particular focal necrotic lesions of PVL deep in cerebral white matter, in premature infants correlate well to the defective coordination of movements and/or regulation of muscle tone typically used to characterize spastic CP (Bax, Tydeman and Flodmark, 2006; Volpe, 2009). PVL is therefore linked to the motor impairment in spastic CP and damage to the motor tracts, specifically the corticospinal tracts (CSTs), in this area is a significant feature and focus of research. This damage is responsible for the inhibition of the development of isolated, skilled joint movement or selective voluntary motor control (SVMC) (Staudt et al., 2003; Bax, Tydeman and Flodmark, 2006; Fowler et al., 2009).

1.3 Corticospinal Tracts

The CSTs are a WM motor tract in the brain and in typical development (TD), they control the directionality and force production of voluntary movements (Evarts, 1968). They originate in the primary motor cortex (PMC) and traverse through the superior corona radiata (SCR), posterior limb of the internal capsule (PLIC) and cerebral peduncle (CerPed) before crossing to the opposite side of the spinal cord at the level of pyramidal decussation (Natali, Reddy and Bordoni, 2021). They are responsible for selective motor control (SMC) and are particularly vulnerable to damage in spastic CP with PVL due to their anatomical location. Compromised CSTs due to a developmental disorder may present itself as entirely absent, hypoplastic or malformed (Natali, Reddy and Bordoni, 2021).

1.4 Selective Motor Control

While multiple impairments such as spasticity and decreased range of motion contribute to motor function deficits in CP, impaired SMC is a direct result of damage to the CST in the periventricular WM that is PVL. Impaired SMC clinically presents as a lack of isolated joint movement with undesired movements at other joints including flexor/extensor synergy patterns and/or mirror movement (Fowler et al., 2009). The control of force, speed and timing may also be reduced (Kennedy, 1990).

With underdeveloped SMC, independent coordination between the joints involving the LE is poor and, thus, SMC is an essential area of research in CP. Children with impaired SMC in

spastic CP tend to couple joint movements about the hip, knee and ankle, whereas more skilled and complex movements tend to uncouple joint movements (Fowler and Goldberg, 2009). While dependent coupling of hip, knee and ankle movements is present in infancy, they begin to dissociate at one month of age in TD (Fetters et al., 2004). When this coupling persists in spastic CP, the individual relies on alternative movements including synergistic motor patterns. Evidence suggests that SMC, as opposed to spasticity and strength, may have a more profound influence on the gait characteristics of those with spastic CP (Fowler and Goldberg, 2009; Fowler et al., 2009). The role of SMC should be explored as a factor affecting all aspects of spastic CP research including brain imaging, biomechanics and PT interventions.

1.5 The Selective Control Assessment of the Lower Extremity

Prior to 2009, a standardized clinical assessment tool to measure SMC in spastic CP was lacking and not reported despite its growing relevance in literature. As a result, a team of clinicians at the Center for CP at UCLA/Orthopedic Institute for Children developed the Selective Control Assessment of the Lower Extremity (SCALE) (Fowler et al., 2009). SCALE was developed as a means to universally quantify SVMC, or SMC upon request, using a valid, reliable assessment tool in CP. The development, utility, validation and interrater reliability of SCALE were established and content validity was reviewed by 14 experienced clinicians with a mean agreement of 91.9% (range 71.4 – 100%) for statements about content, administration and grading (Fowler et al., 2009). Additionally, 6 clinicians rated 20 participants with spastic CP and achieved a high level of interrater reliability demonstrated by intraclass correlation coefficients ranging from 0.88 to 0.91 ($p < 0.0001$) (Fowler et al., 2009).

When measuring SCALE, a participant is asked to selectively move their LE joint including the hip, knee, ankle, subtalar and toe joints. Each joint receives a score between 0 and 2 for a max score of 10 points per limb. A SCALE score of 2 indicates normal SVMC. A SCALE score of 1 could be given, for example, if a participant does some of the isolated movement but involuntary movement of the contralateral limb, such as mirroring, occurs. A SCALE score of 0 indicates absent SVMC, meaning the participant is unable to move the particular joint with very limited range of motion or requires mass flexor and extensor patterns to achieve small movements (Fowler et al., 2009).

1.6 Other Clinical Measures in CP

Two of the most commonly used clinical measures in spastic CP are the Gross Motor Function Classification System (GFMCS) (Palisano et al., 2008) and the Gross Motor Function Measure (Russell et al., 2004). GMFCS was developed to provide a simple method for classifying children with CP based on functional abilities and limitations. It is a categoric descriptor of mobility rather than a numerical quantification and GMFCS scores range from I to V. Level I includes walking at home and in the community, and running and jumping with limited speed, balance and coordination, whereas Level V indicates being transported in a manual wheelchair in all settings with greater limitations necessitating physical assistance and powered mobility (Palisano et al., 2008). GMFM is a numerical measure that was designed to evaluate gross motor function changes over time. The GMFM-66 is scored out of a total of 66 points and testing spans the spectrum of gross motor activities that include standing, walking, running and jumping.

SCALE is distinct from these other clinical measurements in that it is a numerical score focused solely on the underlying problem of selective voluntary motor control.

1.7 Diffusion-Weighted Imaging

Most people are accustomed to viewing T1-weighted or T2-weighted images. A T1-weighted image is shown in Figure 1-1. These types of imaging can give us information about structural or anatomical information about the brain such as the differences between grey matter and WM. However, they give us no information about the connectivity between different regions within the brain.

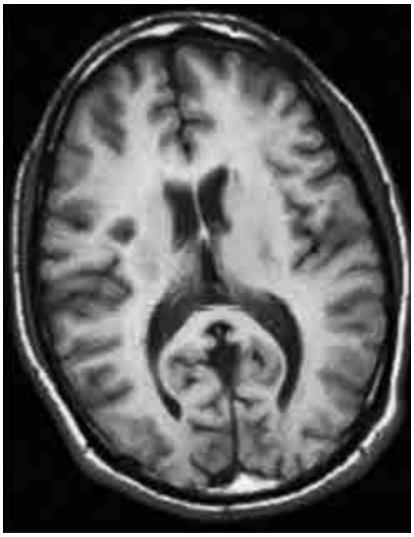

Figure 1-1: T1-weighted image from an axial view. Bright areas of the brain indicate WM and dark areas represent grey matter.

Diffusion-weighted imaging (DWI) has been widely adapted to study cerebral WM in spastic CP. It is an advanced functional MRI tool that uses signal contrast generation based on the translation displacement or differences in magnitude of the diffusion of water molecules in the brain (Basser and Jones, 2002; Alexander et al., 2007; Assaf and Pasternak, 2008; Huisman, 2010). Diffusion represents the random thermal movement of molecules known as Brownian motion and is determined by factors such as physiological environment (e.g. temperature) and microenvironmental architecture. DWI can provide valuable insight by tracing the restricted and unrestricted diffusion of water molecules to model WM connectivity between different regions within the brain. There are multiple ways to acquire and model DWI and diffusion tensor imaging (DTI) is one popular model (Basser and Jones, 2002; Alexander et al., 2007; Assaf and Pasternak, 2008; Huisman, 2010).

1.8 Diffusion Tensor Imaging

In a sentence, DTI can show us the direction in which water molecules diffuse in the brain by estimating the anisotropy of water molecules using tensors, the three-dimensional shape of diffusion (Basser and Jones, 2002; Alexander et al., 2007; Assaf and Pasternak, 2008; Huisman, 2010). An example of isotropic diffusion is in unrestricted areas of the brain such as the cerebrospinal fluid where water molecules have the ability to diffuse freely in all directions. Comparatively, anisotropic diffusion occurs in the bundles of axons wrapped in myelin sheaths organized throughout the brain where water encounters physical and environmental barriers restricting diffusion and preventing flow in certain directions. Figure 1-2 gives an example of tensors modelling isotropic vs. anisotropic diffusion (Karlsgodt et al., 2012).

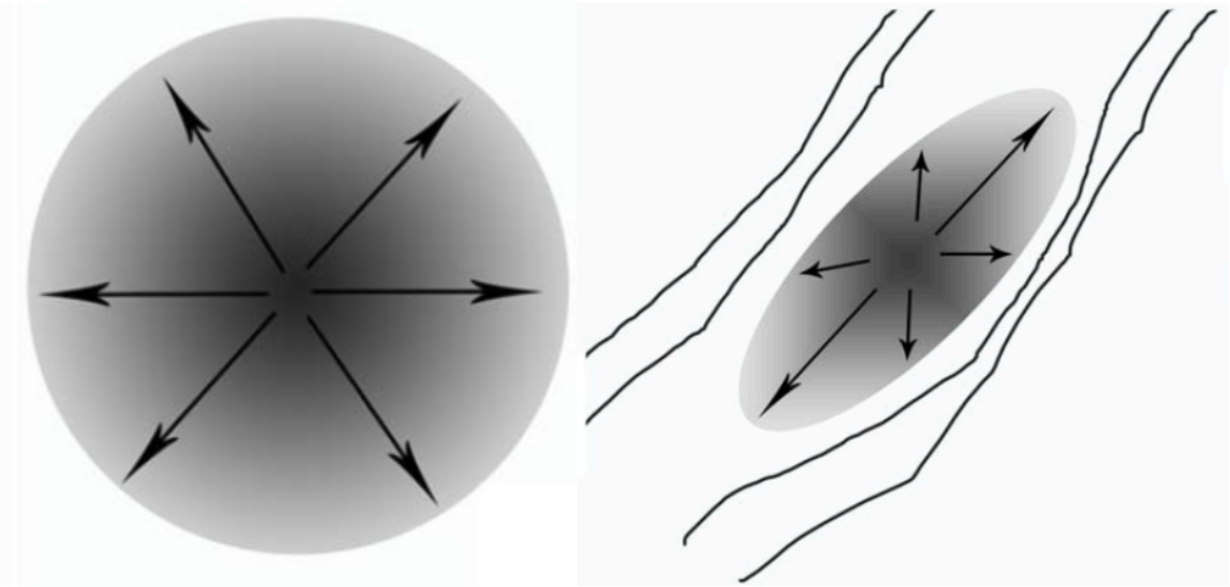

Figure 1-2: Tensor examples of isotropic diffusion (left) vs. anisotropic diffusion (right). Source: (Karlsgodt et al., 2012).

Different types of diffusion affect the shape of the tensor that is characterized by three principle diffusivities: eigenvalues λ1, λ2 and λ3. The sets of equations with respects to the eigenvalues in Figure 1-3 are used to calculate DTI measures that detail different types of diffusion (Basser and Jones, 2002; Alexander et al., 2007; Assaf and Pasternak, 2008; Huisman, 2010).

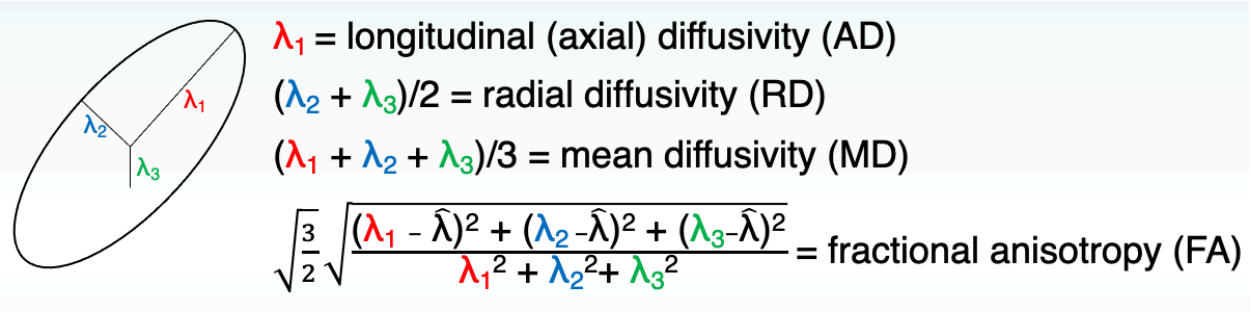

Figure 1-3: Equations for each DTI measure. Axial diffusivity (AD) is parallel to the axon. Radial diffusivity (RD) is perpendicular to the axon. Mean diffusivity (MD) provides an average of all 3 eigenvalues. Fractional anisotropy (FA) calculates the variation of each eigenvalue relative to the mean eigenvalue, $\hat{\lambda}$.

When plotting the value of each diffusivity measure in every voxel (or volume element; 3-D analog of a pixel), scalar maps of the quantification of the local tensors that display the spatial distribution of the diffusion rate within the brain are obtained. These multiple DTI measures FA, RD, AD and MD provide details about tissue alterations associated with WM damage in spastic CP. For FA, each voxel in generated maps is assigned a value between zero (implying complete isotropic diffusion in which diffusion theoretically occurs equally in all directions) to one (the hypothetical case of complete anisotropic or directionally dependent diffusion). In clinical populations and relative to normative values, lower FA has been interpreted as a local marker of the disruption of local tissue microstructural anisotropy or directionality, higher RD has corresponded with damaged myelination, lower AD has reflected axonal injury and higher MD has indicated greater overall diffusivity within a region (Basser and Jones, 2002; Song *et al.*, 2002; Alexander *et al.*, 2007; Assaf and Pasternak, 2008; Huisman, 2010; Vos *et al.*, 2012; Winklewski

et al., 2018). Together, these DTI outcomes reveal a holistic picture of microstructural differences in cerebral WM.

1.9 Significance of the Study

Damage to the CSTs and impaired SMC are primary features of children with spastic bilateral CP and PVL born premature. Studies have shown that SMC is a crucial factor impacting overall functional mobility. The relationship between SMC and the microstructural properties of the CSTs using DTI, however, has received little attention. To assess the relationship between these measures, we first established the WM differences between children with spastic bilateral CP and children with TD. The correlations between SCALE and FA, RD, AD and MD were then evaluated and SCALE correlations were compared to GMFM to examine its efficacy in predicting DTI outcomes. Furthermore, the efficacy of a novel intervention focused on intensive practicing of skilled LE SMC movements, Camp Leg Power, was investigated. To my knowledge, there is little to no research on the use of DTI to analyze neuroplasticity after a LE SMC intervention in spastic CP. The effect of Camp Leg Power on WM motor tracts and neuroplasticity was explored. Additionally, the relationship between SCALE and baseline motor outcomes was examined and changes in post-intervention motor outcomes were assessed. Lastly, the association between changes in DTI measures and changes in isokinetic knee joint torque after Camp Leg Power was analyzed to determine if WM changes in response to the intervention were directly related to biomechanical improvements. These studies were designed to evaluate SCALE as a clinical correlate of WM motor tracts including the CSTs and baseline motor outcomes, the efficacy of a

novel LE SMC intervention in promoting neuroplasticity and improving motor outcomes, and the correlation between post-intervention WM microstructural and motor outcome changes.

Chapter 2: Tractography of the Lower Extremity Corticospinal Tracts

2.1 Introduction

In children with spastic bilateral CP and PVL, the CSTs are particularly vulnerable to damage due to their anatomical location. The CSTs are responsible for controlling the directionality, force, speed and timing of voluntary movements (Evarts, 1968; Kennedy, 1990; Fowler et al., 2009). CST damage is a primary etiology of spastic bilateral CP and manifests physically as impaired SMC (Bax, Tydeman and Flodmark, 2006). The microstructural integrity of the CSTs is, therefore, most commonly studied as the culprit WM tract causing motor deficits in CP.

DTI has been used to assess the microstructural properties of the CSTs in children with spastic CP with tractography being a common method to study its pathology and reorganization (Scheck, Boyd and Rose, 2012). In tractography, a branch of DTI, the direction and magnitude of diffusion is used to reconstruct physical representations of WM tracts within the brain (Basser and Jones, 2002; Alexander et al., 2007; Assaf and Pasternak, 2008; Huisman, 2010). It allows for a detailed investigation of CST microstructure and connectivity as it isolates the CSTs from other WM regions of the brain. Tractography methodology makes the assumption that voxels with similar orientation of their principal anisotropic diffusion direction (or eigenvector) are part of the same tract. Under the additional assumption that the principal anisotropic diffusion direction is parallel to the local WM fascicles, fiber-tract trajectories can be followed. WM trajectories start at a specified seed region of interest (ROI), where the major direction of propagation is estimated. A

small distance is moved in that direction and then re-evaluated. This process is repeated until the tract terminates or tracts may also be constrained by using multiple ROIs (Basser and Jones, 2002; Alexander et al., 2007; Assaf and Pasternak, 2008; Huisman, 2010).

In a systematic review of 21 studies using DTI in CP, 13 out of the 21 studies used tractography, FA, and the CSTs were the most commonly analyzed (in 18 of the 21 studies) (Scheck, Boyd and Rose, 2012). While there has been some growing interest in the thalamocortical pathways, or ascending sensory pathways, having a greater influence on motor deficits (Hoon et al., 2009), motor function was measured using hand held dynamometry which is difficult to measure reliably in children with poor motor control (Shortland, 2011). Of the 13 studies using tractography, 12 analyzed FA of the CSTs and 8 assessed MD of the CSTs. In general, lower FA and higher MD were reported with no studies reporting higher FA nor lower MD in the CSTs of their cohorts (Scheck, Boyd and Rose, 2012). Several studies, not limited to tractography, reported positive correlations between FA of the CST and gross motor function as measured by GMFCS levels in spastic hemiplegia (Glenn et al., 2007), spastic diplegia (Lee et al., 2011) and spastic quadriplegia CP (Trivedi et al., 2010). While severity of motor impairment varied among these studies, they demonstrated a significant relationship between FA of the CSTs and gross motor function levels. The use of GMFCS in correlation analyses, however, have often been described as a limitation because it is a categorical descriptor of mobility rather than a continuous numerical value (Ceschin et al., 2015; Arrigoni et al., 2016; Vuong et al., 2021).

The correlations between DTI outcomes of the CSTs and SVMC as measured by SCALE have not been examined using tractography. As the CSTs are physiologically associated with SMC, SCALE could have a more profound relationship with tissue microstructure of the CSTs than other clinical motor function measures. Children with spastic bilateral CP, PVL and greater

SMC could have higher FA and lower RD, AD and MD of the CSTs as compared to those with less SMC. The purpose of this study was to use tractography in DTI to study the CSTs in the brains of children with spastic bilateral CP. Furthermore, it was to examine the relationship between DTI measures of the CSTs and SCALE score of the contralateral limb. We first had to establish the baseline microstructural diffusion properties of the CSTs. We hypothesized that the children with CP would have DTI measures in the CSTs exhibiting significant correlations with SCALE indicating less impairment for those with greater SVMC.

2.2 Methods

2.2.1 Study Cohort

Twelve participants with spastic bilateral CP were recruited for this MRI study. Inclusion criteria for all participants were the following: 1) between 5 and 18 years of age, 2) a history of prematurity, 3) a diagnosis of spastic bilateral CP and PVL as evidenced by MR imaging or sonography, 4) the ability to understand and follow verbal directions, 5) the ability to lie still and 6) the ability to walk with or without assistive devices.

Exclusion criteria for all participants were the presence of the following: 1) metal implants not verified as MR imaging-safe, 2) programmable implants including ventriculoperitoneal shunts and intrathecal baclofen pumps, 3) dental braces, 4) seizures not controlled by medication, 5) orthopedic surgery or neurosurgery within 1 year of starting the study and 6) BTX or casting within 3 months of starting the study.

This study was conducted in an outpatient clinical research setting (Center for CP at

UCLA/OIC and Ahmanson-Lovelace Brain Mapping Center). The institutional review board of the University of California Los Angeles provided ethics approval. Informed assent and consent for research were obtained from the children and their parents or guardians.

2.2.2 Selective Control Assessment of the Lower Extremity (SCALE)

SCALE was used to assess SVMC (Fowler et al., 2009). Participants were evaluated by one of three experienced physical therapists using a standardized protocol. Specific isolated movement patterns at the hip, knee, ankle, subtalar and toe joints were evaluated bilaterally. Left and right SCALE scores were evaluated separately ranging from 0 (absent SVMC) to 10 (normal SVMC) for each limb (Fowler et al., 2009).

2.2.3 MRI and Diffusion-Weighted Imaging Protocols

Prior to MRI sessions, children viewed a slide presentation describing procedures and practiced lying still while listening to recordings of scanner sounds. All T1-weighted and DWI scans were collected using a 32-channel coil on a 3T Siemens Magnetom Prisma MRI scanner (Siemens, Munich, Germany) without sedation. T1w MPRAGE images were obtained using TR = 2500 ms; TE = 1.8, 3.6, 5.39, and 7.18 ms; FOV = 256 × 256 mm^2; and isotropic voxel resolution = 0.8 × 0.8 × 0.8 mm^3. DWI scans were obtained using a single-shot, spin-echo, echo-planar acquisition with 6 reference images (b = 0 s/mm^2), 52 gradient directions (b = 1500 s/mm^2), TR = 3231 ms, TE = 89.6 ms, FOV = 210 × 210 mm^2, echo spacing = 0.69 ms, and isotropic voxel resolution = 1.5 × 1.5 × 1.5 mm^3.

2.2.4 Tractography of the Corticospinal Tracts

Tractography was carried out using BrainSuite, an imaging analysis program developed at UCLA's Brain Mapping Center (Shattuck and Leahy, 2002). The ROI method used to delineate the CSTs in this tractography study was refined over time and with more user experience.

In the first attempt to isolate the CSTs, spherical ROIs were placed in the PMC, PLIC and CerPed based on anatomy. The ROIs in the PMC and CerPed were relatively large and, therefore, although the ROIs were focused in the motor region of the brain, this method was not specific enough and likely captured a large number of WM tracts beyond the CSTs. Additionally, the CerPed spherical ROI captured the whole peduncle, including the peduncle in the left and right hemispheres (Figure 2-1).

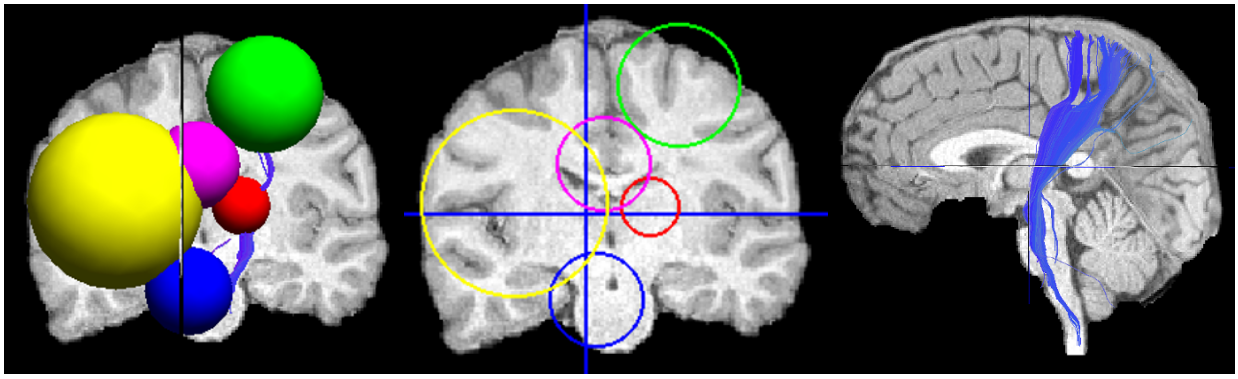

Figure 2-1: Initial tract-specific ROI method used to delineate the CSTs. The green, red and blue spheres are for the PMC, PLIC and CerPed, respectively. The yellow and purple spheres are "NOT ROIs" used to remove aberrant WM tracts. The image on the right is the resulting WM tract containing the CSTs.

As my knowledge on the neuroanatomy of the CSTs expanded, I transitioned from using large spherical ROIs to manually drawn ROIs. To isolate the CSTs, manually drawn ROIs were placed on axial slices (Wakana et al., 2007). The first ROI was drawn on the CerPed at the level of the decussation of the superior cerebellar peduncle (Figure 2-2 part (A)). After filtering whole brain tractography through this ROI, the central sulcus and tracts projecting into the motor cortex were identified. On the T1-weighted images, using an axial slice above the bifurcation of the motor and somatosensory tracts, a second ROI was drawn covering the entire PMC (Figure 2-2 part (B)) (Wakana et al., 2007). Any tracts crossing the midline, going into anatomical structures not relevant to the CSTs (i.e. the premotor cortex and somatosensory cortex) and not descending down the pons were removed using spherical "NOT ROIs" (Figure 2-2 parts (C-D)) (Wakana et al., 2007). The result thus far is the "full CST" containing both the LE and upper extremity (UE) CSTs as seen by the tracts displayed in Figure 2-2 part (E). LE CSTs were isolated from UE CSTs by placing a spherical "AND ROI" in the most medial gyrus of the PMC as seen from the coronal view (Figure 2-2 part (E)). This resulted in isolated leg or LE CSTs (Figure 2-2 part (F)).

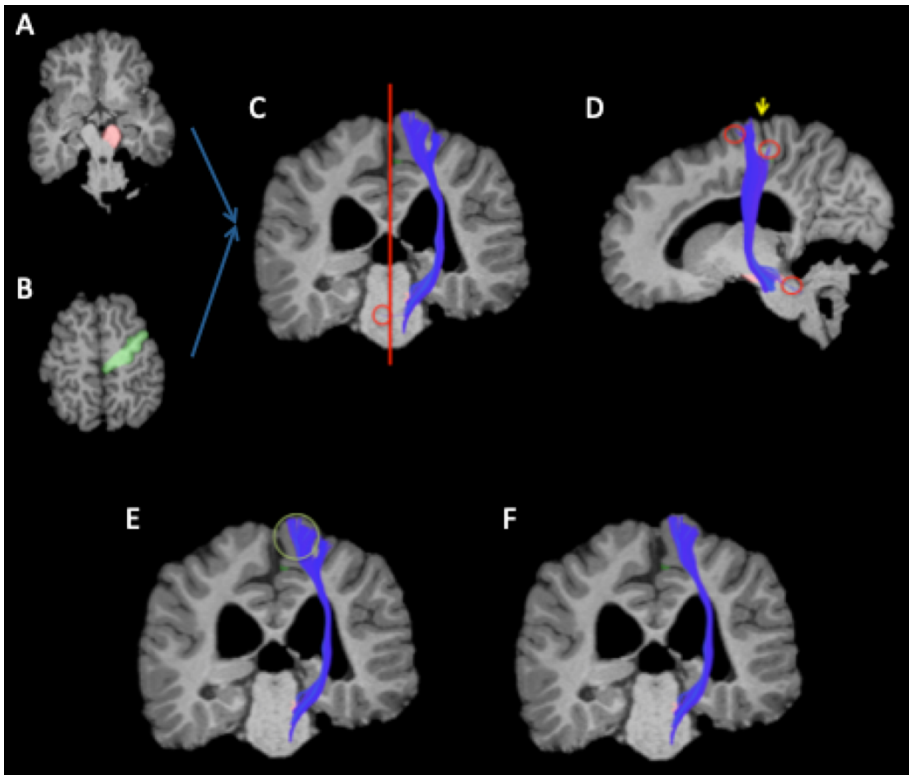

Figure 2-2: Tractography ROI method for isolating leg CSTs in exemplar subject with CP. Parts (A-F) are described in Methods Section 2.6. Red vertical line represents the midline. Red and green circles represent “NOT ROIs” and “AND ROIs” respectively.

The locations of the LE and UE CST ROIs is based on the anatomy of the CSTs. As seen in Figure 2-3, the LE tracts are closer to the ventricles and more medial in the PMC as seen from a coronal view (Aicardi and Bax, 1992; Fowler, Staudt and Greenberg, 2010). Example target ROIs in the PMC separating the LE CSTs (blue) from the UE CSTs (red) can be viewed in Figure 2-3 as well (Chang et al., 2012).

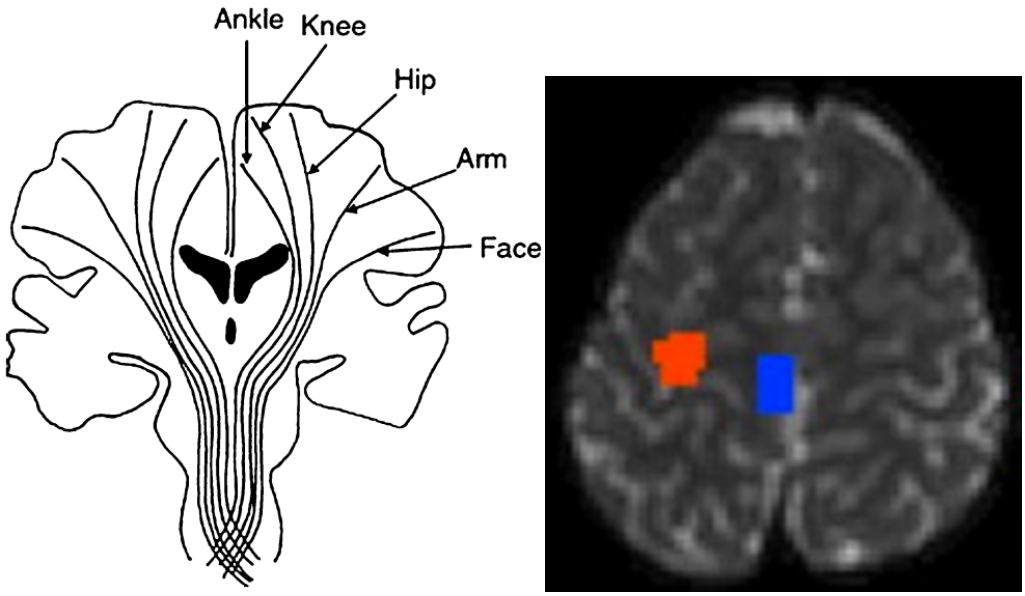

Figure 2-3: Anatomical location of the CSTs for the LE and UE as seen from a coronal view. Source: (Aicardi and Bax, 1992; Fowler, Staudt and Greenberg, 2010). Example target ROIs for the LE and UE in the PMC as seen from an axial view. Source: (Chang et al., 2012).

As the nature of this tractography ROI method grew more specific to the LE CSTs, it was discovered that the LE CSTs could not be visualized for all participants in the cohort. The "full CSTs" were, however, visible for all participants, containing either LE and UE CSTs or only the UE CSTs. In an attempt to use all participant data, the "full CSTs" were segmented vertically and DTI outcomes were averaged in regions within the PLIC and between the PLIC and CerPed (Figure 2-4).

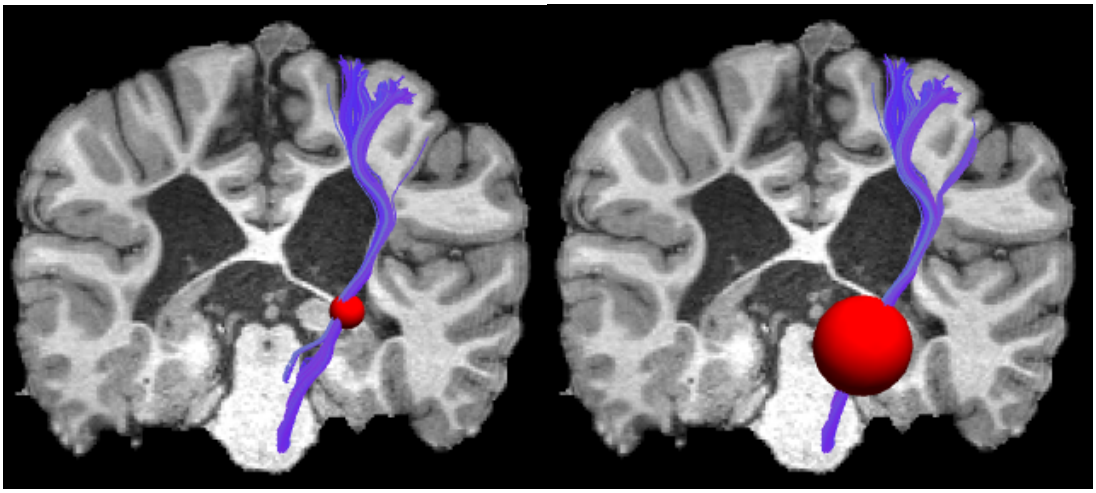

Figure 2-4: ROIs used to segment the "full CST" into regions with the PLIC (left) and between the PLIC and CerPed (right).

2.2.5 Statistical Analysis

Voxels containing the isolated CSTs were masked on structural scans. The masked structural images were then thresholded. Using DTI maps for FA, RD, AD and MD (processed via Human Connectome Project and Brain Diffusion Pipeline), DTI outcomes were then averaged for all voxels within the masked and thresholded CST voxels. To perform the segmented CST analyses, the PLIC and PLIC to CerPed ROIs were first masked using Python. The masked ROIs were then used to segment the isolated "full CST" tractography data using fslmaths. The "full CST" voxels contained within each segmented ROI were then averaged using fslstats. The relationships between DTI averages of the leg CSTs and segmented "full CSTs" and SCALE were assessed using simple linear regression in the BrainSuite Statistics Toolbox.

2.3 Results

Twelve children with spastic bilateral CP (2 females, 10 males; mean age, 11.5 ± 2.8 years; age range, 7.3-16.6 years) participated. GMFCS levels were: I (n=3), II (n=1), III (n=7) and IV (n=1) (Table 2-1). Unilateral SCALE scores ranged from 0 to 9 (Table 2-2).

		CP (n = 12)
Age (Years)	Mean (SD)	11.5 (2.8)
	Range	7.3-16.6
Sex	Male	10
	Female	2
GMFCS Level	I	3
	II	1
	III	7
	IV	1

Table 2-1: Demographics of participants with CP in the study.

*GMFCS describes a child's gross motor function ability from I (high) to IV (low) (Palisano et al., 2008).

When separating the "full CSTs" into UE and LE CSs, all participants had visible UE CSTs in both hemispheres of the brain; however, the LE CSTs were only visible for 5 participants in the left hemisphere of the brain and 8 participants in the right (Table 2-2).

Participant ID	Left SCALE	Right SCALE	Left LE CST	Right LE CST	Left UE CST	Right UE CST
1	8	8	X	O	O	O
2	3	4	O	O	O	O
3	2	5	X	O	O	O
4	9	9	O	O	O	O
5	5	5	X	X	O	O
6	2	2	O	O	O	O
7	0	1	X	X	O	O
8	8	8	X	O	O	O
9	4	3	X	X	O	O
10	7	6	O	O	O	O
11	4	4	O	O	O	O
12	2	2	X	X	O	O

Table 2-2: Bilateral SCALE scores of each participant and the presence of LE and UE CSTs in each hemisphere of the brain. O = present; X = absent.

Average DTI values for the entire LE CST were calculated for all participants with visible tracts. All mean DTI values were similar between both hemispheres of the brain (Table 2-3).

	Left hemisphere (n = 5)		Right hemisphere (n = 8)	
DTI Measure	Mean	SD	Mean	SD
FA	0.49	0.05	0.49	0.07
RD	7.7E-04	6.3E-05	8.0E-04	1.1E-04
AD	5.4E-04	6.9E-05	5.6E-04	1.2E-04
MD	1.2E-03	6.8E-05	1.3E-03	9.5E-05

Table 2-3: Average DTI values for LE CSTs for all participants with CP for whom LE CSTs could be reconstructed.

In the correlation analysis of DTI values of LE CSTs versus SCALE score of the contralateral limb, there was a significant positive correlation between FA and SCALE in the right hemisphere of the brain but not the left (Figure 2-5). RD correlated significantly and negatively with SCALE in both hemispheres of the brain (Figure 2-5). AD did not correlate with SCALE scores in either hemisphere (Figure 2-5). There was a significant negative correlation between MD and SCALE bilaterally (Figure 2-5).

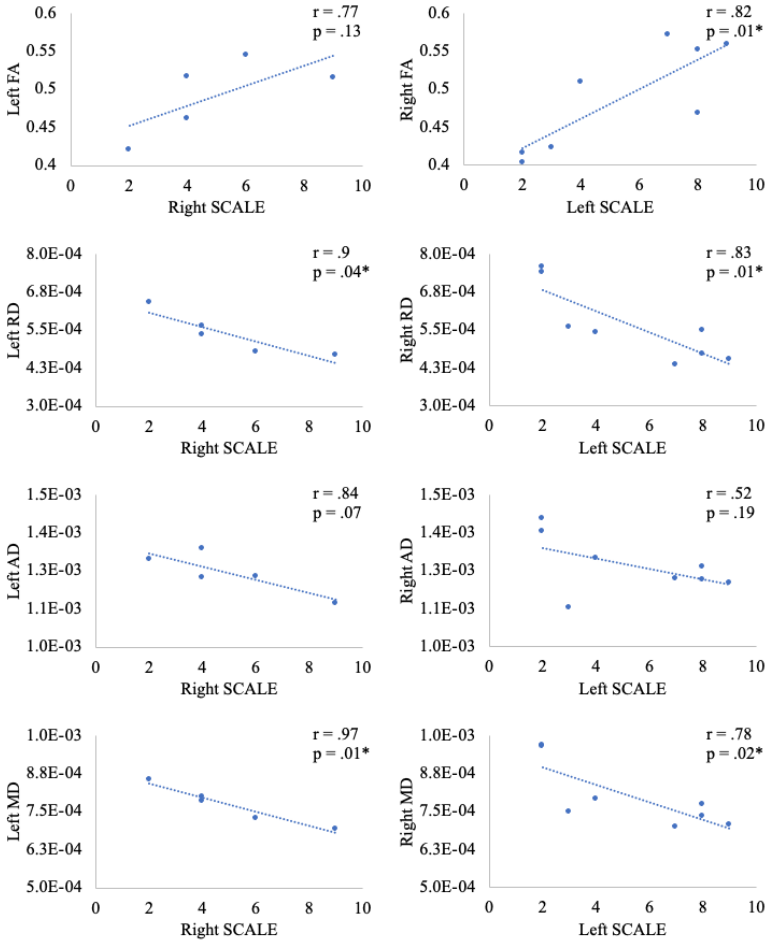

Figure 2-5: Correlation graphs for DTI outcomes of LE CSTs vs. contralateral SCALE score for subjects with CP whom LE CSTs could be visualized.

When calculating the mean DTI values within the PLIC of the "full CSTs," only minor differences were found between the left and right hemispheres of the brain (Table 2-4).

	Left hemisphere (n = 12)		Right hemisphere (n = 12)	
DTI Measure	Mean	SD	Mean	SD
FA	0.72	0.05	0.69	0.06
RD	3.3E-04	4.5E-05	3.5E-04	6.3E-05
AD	1.4E-03	1.0E-04	1.3E-03	6.6E-05
MD	6.9E-04	4.2E-05	6.8E-04	4.5E-05

Table 2-4: Average DTI values within the PLIC of the "full CSTs" for all participants with CP.

In the correlation analysis of mean DTI values within the PLIC of the "full CSTs" versus SCALE score of the contralateral limb, there was no significant correlation between FA and SCALE in the right hemisphere of the brain nor the left (Figure 2-6). RD correlated significantly and negatively with SCALE in the left hemisphere of the brain but not the right (Figure 2-6). AD did not correlate with SCALE scores in either hemisphere (Figure 2-6). There was a significant negative correlation between MD and SCALE in the left hemisphere but not the right (Figure 2-6).

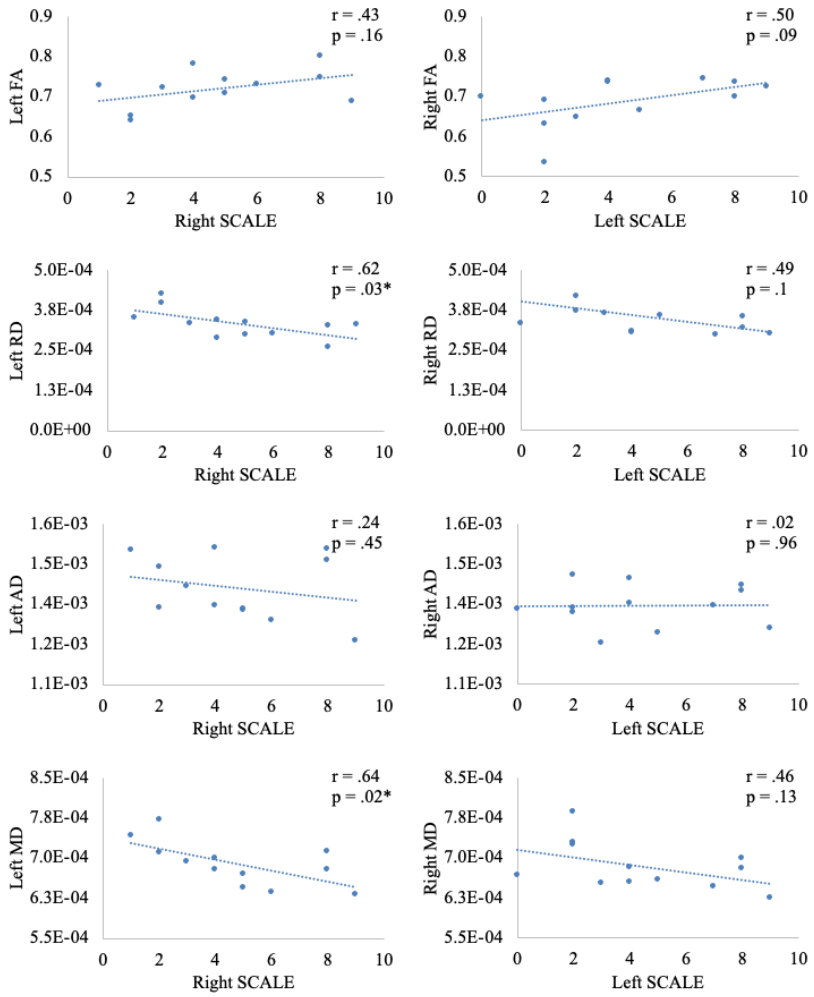

Figure 2-6: Correlation graphs for DTI outcomes within the PLIC of the "full CSTs" vs. contralateral SCALE score for all subjects with CP.

When calculating the mean DTI values between the PLIC and CerPed of the "full CSTs," only subtle differences were found between left and right hemispheres of the brain (Table 2-5).

	Left hemisphere (n = 12)		Right hemisphere (n = 12)	
DTI Measure	Mean	SD	Mean	SD
FA	0.62	0.06	0.64	0.06
RD	4.6E-04	6.8E-05	4.1E-04	6.4E-05
AD	1.4E-03	5.4E-05	1.4E-03	6.0E-05
MD	7.8E-04	4.6E-05	7.3E-04	4.4E-05

Table 2-5: Average DTI values between the PLIC and CerPed of the "full CSTs" for all participants with CP.

In the correlation analysis of mean DTI values between the PLIC and CerPed of the "full CSTs" versus contralateral SCALE scores, FA correlated significantly and positively in the right hemisphere of the brain but not the left (Figure 2-7). RD, AD and MD did not correlate significantly with SCALE in either hemisphere of the brain (Figure 2-7).

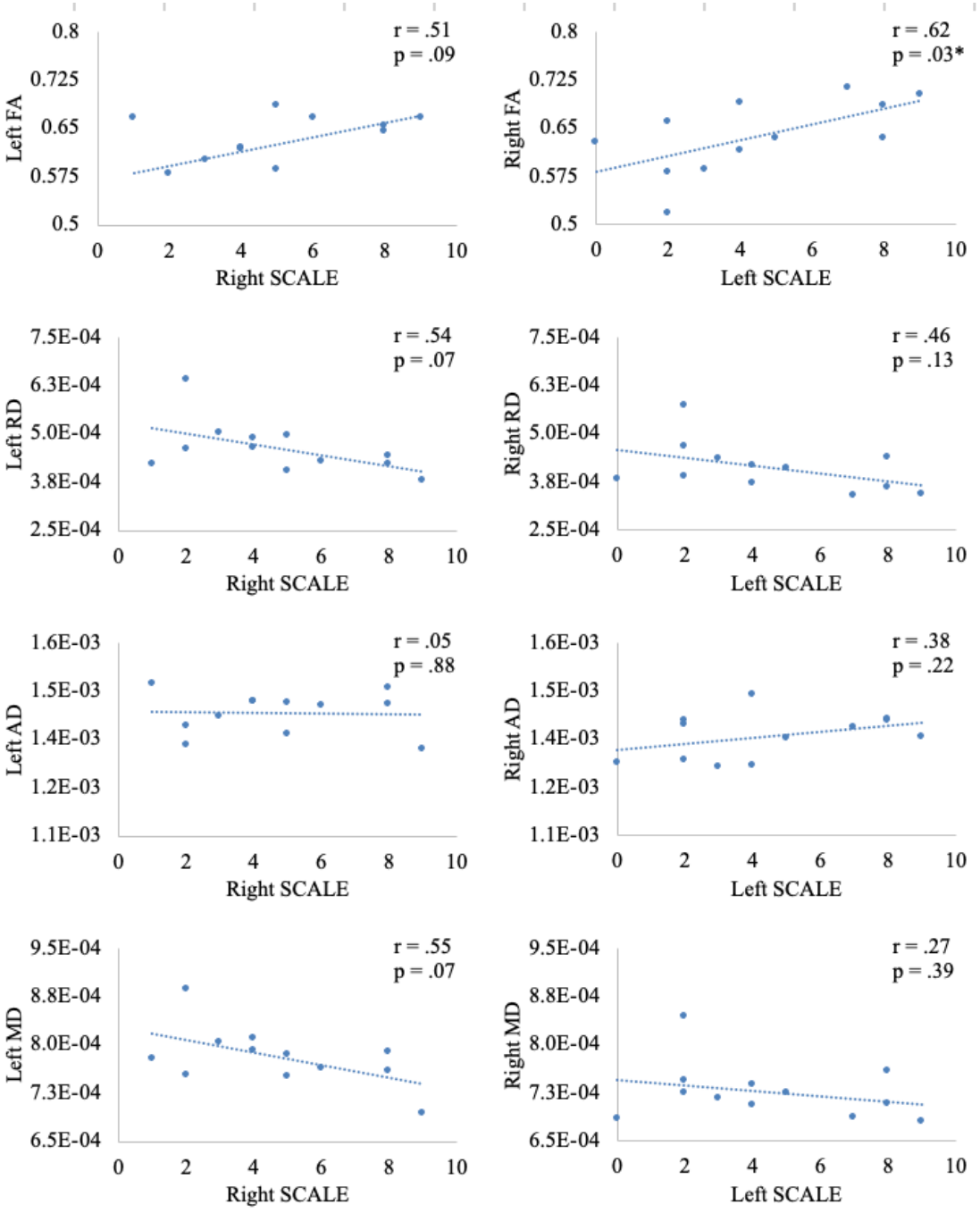

Figure 2-7: Correlation graphs for DTI outcomes between the PLIC and CerPed of the "full CSTs" vs. contralateral SCALE score for all subjects with CP.

2.4 Discussion

To my knowledge, this was the first study to establish SCALE, a sensitive measure of SVMC in spastic CP, as a clinical correlate of multiple DTI measures for the LE CSTs using tractography. We demonstrated that SCALE of the contralateral limb correlated with right FA, bilateral RD and bilateral MD. The positive correlation between FA and SCALE suggests that children with spastic bilateral CP and more SVMC have greater anisotropy and less impairment of their LE CSTs. The negative correlation between RD and SCALE suggests that those with more SVMC have greater myelination of their LE CSTs (Song et al., 2002; Winklewski et al., 2018; Lazari and Lipp, 2021). The negative correlation between MD and SCALE suggests that SVMC is connected to tissue complexity of the LE CSTs (Vos et al., 2012). These findings suggest that DTI outcomes of the LE CSTs are highly associated with SCALE score of the contralateral limb and, therefore, SVMC is sensitive to LE CST microstructural environment. This is important because SCALE was specifically designed to measure SVMC of the LE joints (Fowler et al., 2009).

Previous studies with cohorts of children with spastic bilateral CP have demonstrated a negative relationship between FA of the CSTs and GMFCS levels (Lee et al., 2011; Ceschin et al., 2015; Arrigoni et al., 2016). Lee et al. and Arrigoni et al., however, did not use tractography but rather voxel-based DTI methods for correlation analyses. While Arrigoni et al. found significant correlations between FA of the CSTs and GFMCS, the r values found in the present study using SCALE were greater ($0.77 > 0.51$ for the left hemisphere and $0.82 > 0.52$ for the right) suggesting SCALE to be a more sensitive clinical correlate of CST impairment. Additionally, Arrigoni et al. did not find significant correlations between GMFCS and RD nor MD of the CSTs while correlations for these measures were significant when using SCALE in the present study. While Ceschin et al. used tractography in their correlation analysis, they used principal component

analysis to determine the efficacy of FA variance along the CST in predicting motor deficiency, which differs from these methods. In all three studies, a limiting factor was the use of GMFCS because it is a categorical descriptor of mobility rather than a continuous numerical value (Scheck, Boyd and Rose, 2012; Ceschin et al., 2015; Arrigoni et al., 2016; Vuong et al., 2021). An additional limiting factor was that the LE CSTs were not differentiated from the UE CSTs. These correlations results are unique to this study and have not been presented in literature by other groups.

Correlations between DTI outcomes of the LE CSTs and SCALE using tractography support the conclusion that SCALE is a strong clinical correlate to cerebral WM damage in children with spastic bilateral CP and PVL. Since motor tracts decussate before reaching the spinal cord, right hemispheric LE CST data were correlated with left limb SCALE scores and vice versa (Natali, Reddy and Bordoni, 2021). Although the left LE CST FA versus right SCALE correlation was not significant, the data clearly demonstrate a positive relationship. The non-significance is likely due to a lack of power. As FA of the left LE CST only had 5 data points, the positive relationship could be significant when including more participants with visible LE CSTs. Since LE CSTs were not detectable in every participant with CP, there was a reduced sample size with left LE CSTs being reconstructed for only 5 subjects out of the possible 12 and right LE CSTs being reconstructed for 8 out of 12. With greater sample size of reconstructed LE CSTs, both hemispheres could potentially have statistically significant correlations between FA values and contralateral SCALE scores.

Difficulty in detecting CSTs using tractography is not exclusive to this study. Results published by Hodge et al. showed that only partial tracts were generated for some subjects with unilateral CP (Hodge et al., 2017). Partial tracts for their cohort were contained to segments between the PLIC and CerPed suggesting ventricular lesions may play a role in CST reconstruction

(Hodge et al., 2017). In addition, other studies have shown segmented or absent CSTs in unilateral CP (Kwon et al., 2014; Kim, Kwon and Son, 2015) and bilateral CP (Cho et al., 2013). Difficulty detecting the CSTs may be a result of the closer proximity of the LE CSTs to the periventricular damage (Fowler, Staudt and Greenberg, 2010). These findings suggested, however, that segmented ROI analysis from the CerPed to the PLIC may allow for the inclusion of more participants with partial CSTs.

When performing the segmented analyses on the PLIC and between the PLIC and CerPed of the "full CSTs" for all participants in our cohort (n = 12), the inclusion of additional potential motor tracts did not increase the strength of our findings. The strongest significant correlations were found when using the LE CSTs, even with the reduced number of participants with visible tracts. In a study published by Chang et al., it was discovered that lower extremity CSTs could be separated from upper extremity CSTs and that they also have inherently different FA values (Chang et al., 2012). Thus, it was imperative to isolate the two sets of tracts from one another, especially when considering that SCALE specifically measures SVMC of the LE.

Tractography in DTI is a powerful tool used for tract-specific analyses of WM diffusion properties and correlations of those diffusion properties to motor ability. It enables visualization and localization of specific tract injury within an individual. Initially, volumetric spherical ROIs were used for the participants with CP. As a result, both the lower and upper extremity CSTs, in addition to fibers originating from the premotor and somatosensory cortices, were included. It became clear from examining these tracts that this first method was overly inclusive. Therefore, a different approach using subject-specific, manually drawn ROIs was implemented, covering both the entire CerPed and PMC on axial slices (Figure 2-2).

There are several limitations to using tractography to analyze DTI data. While tractography provides discrete values for diffusion properties of delineated WM tracts within subject space, disruption of tracts depending on the cohort can greatly reduce sample size and power of a statistical analysis. Additionally, tract-specific methods may unintentionally limit the scope of analysis. Despite these limitations, results from the present study warrant further investigation of DTI outcomes of the LE CSTs in children with spastic bilateral CP and PVL. Future work should include LE CST analysis of a control group of children with TD using the same DWI acquisition protocol. Although we performed segmented tract analysis, an along-tract analysis on an axial slice-by-slice basis would be beneficial and provide greater insight into the regional vulnerability of the LE CSTs. While other studies have been able to perform some of the future work suggested for this project (Chang *et al.*, 2012; Ceschin *et al.*, 2015), we ultimately sought to pursue other statistical techniques in DTI where all WM voxels including LE CSTs could be analyzed for all participants.

Chapter 3: Selective Motor Control is a Clinical Correlate of Brain Motor Tract Impairment in Children with Spastic Bilateral Cerebral Palsy

3.1 Introduction

Children with spastic bilateral CP and PVL have a wide range of clinical outcomes and LE function varies between individuals. The microstructural properties of cerebral WM and the neuronal organization associated with the range of motor impairments in spastic CP are not well understood (Lee *et al.*, 2011; Ceschin *et al.*, 2015).

Spastic CP is associated with damage to the CSTs and other motor pathways that are responsible for SVMC, which reflects the ability to perform isolated, skilled and precise movements of a joint or limb with control of force and speed upon request (Fowler *et al.*, 2009). Impaired SVMC affects coordination between LE joints resulting in coupling of the hip, knee and ankle to varying degrees (Fowler and Goldberg, 2009). SVMC has been shown to have a strong influence on the gait and mobility characteristics of children with spastic CP (Noble, Gough and Shortland, 2019; MacWilliams *et al.*, 2022). In addition, it has been used as a prognostic factor for hamstring surgery (Goldberg, Fowler and Oppenheim, 2012) and selective posterior rhizotomy (Staudt and Peacock, 1989). SVMC, as measured by SCALE (Fowler *et al.*, 2009), had a larger causal effect on gross motor function when compared to dynamic motor control (based on gait electromyography), strength, spasticity, contractures and bony deformities (MacWilliams *et al.*, 2022). It is therefore imperative to examine SCALE and SMC as predictive factors for motor and whole brain WM impairment.

DTI has previously been used to assess microstructural WM differences in children with spastic bilateral CP (Lee *et al.*, 2011; Ceschin *et al.*, 2015; Arrigoni *et al.*, 2016; Mailleux *et al.*, 2020). Lower FA has been interpreted as a local marker for disruption of local tissue microstructural anisotropy or directionality, higher RD has corresponded with damaged myelination, lower AD has reflected axonal injury and higher MD has indicated greater overall diffusivity within a region (Basser and Jones, 2002; Song *et al.*, 2002; Alexander *et al.*, 2007; Assaf and Pasternak, 2008; Huisman, 2010; Vos *et al.*, 2012; Winklewski *et al.*, 2018).

WM differences between children with spastic bilateral CP and children with TD have been found using DTI in other studies (Lee *et al.*, 2011; Arrigoni *et al.*, 2016; Mailleux *et al.*, 2020). Motor function in children with spastic bilateral CP involve multiple regions of the brain beyond the CSTs and motor regions including commissural and association tracts, and the visual, limbic and sensory regions (Englander *et al.*, 2013; Ceschin *et al.*, 2015). Therefore, methods and approaches that focus on a set of a priori regions ultimately limit the scope of analysis and may underestimate the global extent of WM differences (Assaf and Pasternak, 2008). In contrast, Tract-Based Spatial Statistics (TBSS), a whole brain voxel-based approach, is a comprehensive method to assess WM (Smith *et al.*, 2006).

TBSS was developed to align DTI maps from multiple subjects in a standardized way for voxel-by-voxel comparisons. This technique involves non-linear registration followed by projection onto an alignment invariant tract representation or mean WM skeleton. It improved the sensitivity of voxel-wise analyses and improved the objectivity and interpretability of results (Smith *et al.*, 2006).

The following Figure 3-1 depicts the TBSS pipeline. After collecting raw T1-weighted and DWI scans, we used FSL's toolbox library to perform diffusion metric estimation and generate

DTI maps. In the first step of TBSS, every participant image was registered to the FMRIB58 atlas, bringing all DTI maps from their native space to a standard space to allow cross-subject, subject-to-subject comparisons. The second step was skeletonization where each subject's aligned DTI data was projected onto the mean WM skeleton (green) representing all WM tracts common to the atlas. The skeletonized DTI maps were then fed into *randomise*, a permutation-based testing tool, to perform voxel-wise statistics. In the final output as seen in Figure 3-1, voxels with significant findings were highlighted in red.

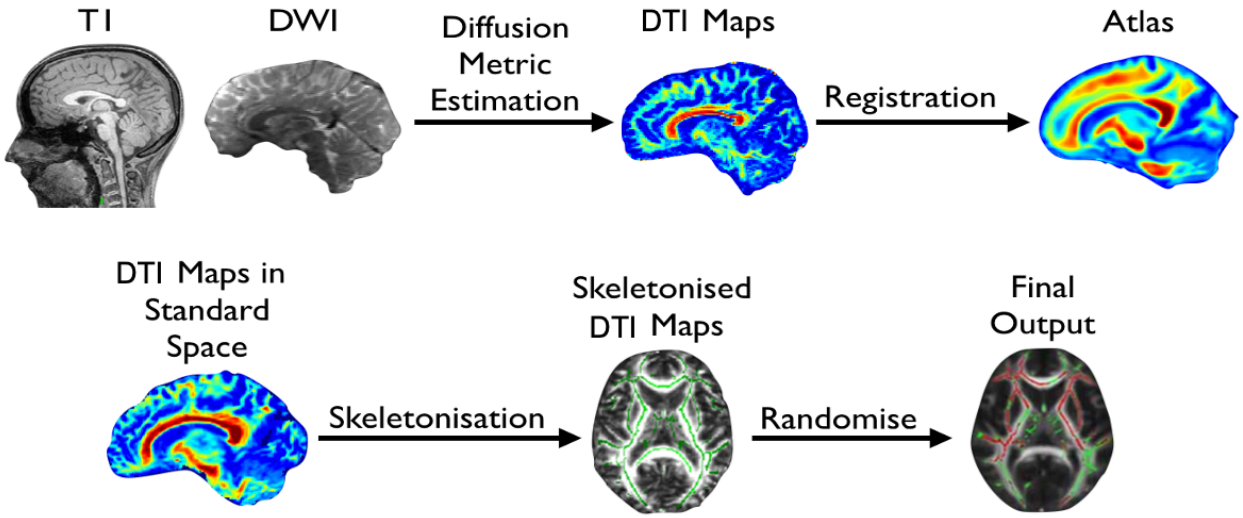

Figure 3-1: Steps involved in the TBSS pipeline, from left to right.

Altered WM in spastic bilateral CP relative to controls has been found using voxel-based approaches, including TBSS (Lee *et al.*, 2011; Ceschin *et al.*, 2015; Arrigoni *et al.*, 2016). In addition, correlations between DTI outcomes and GMFCS (Palisano *et al.*, 2008), a categorical score, have been reported (Lee *et al.*, 2011; Arrigoni *et al.*, 2016). While prior DTI correlation

analyses have used this mobility classification system to assess CP severity, none have used a motor performance measurement that includes SVMC, specifically LE SVMC.

To our knowledge, this is the first study to evaluate relationships between a clinical measure of SVMC in spastic CP and DTI outcomes for WM motor regions and the whole brain using TBSS. SVMC was assessed using SCALE (Fowler *et al.*, 2009). Our primary hypothesis was that 1) SCALE would exhibit a significant correlation with DTI outcomes in motor tracts, particularly the CSTs, and 2) SCALE would be more sensitive to WM impairment than the Gross Motor Function Measure (GMFM) (Russell *et al.*, 2004), a measure of gross motor function in spastic CP. Our secondary hypothesis was that significantly different DTI outcomes would be found for children with CP as compared to a control group of children with TD.

3.2 Materials and Methods

3.2.1 Participants

This study was conducted in an outpatient clinical research center (Center for CP at UCLA/OIC and Ahmanson-Lovelace Brain Mapping Center). The UCLA Institutional Review Board provided ethical approval. Informed consents and assents for research were obtained from the children and their parent(s) or guardian(s).

Inclusion criteria for all participants were (1) age between 5 and 18 years old, (2) ability to understand and follow verbal directions and (3) ability to lie still. Additional inclusion criteria for the CP group were (1) history of prematurity, (2) diagnosis of spastic bilateral CP and PVL as evidenced by MRI or ultrasound and (3) ability to walk with or without assistive devices.

Exclusion criteria for all participants were presence of (1) metal implants not verified as MRI safe, (2) programmable implants including VP shunts and intrathecal baclofen pumps, and (3) dental braces. Additional exclusion criteria for children with CP were (1) seizures not controlled by medication, (2) orthopedic or neurosurgery within one year of starting the study, and (3) BTX injections or casting within three months of starting the study. Additional exclusion criteria for the TD group were (1) morbidities such as neurodevelopmental, neuromuscular or neuropsychiatric diagnoses and (2) visible abnormalities as observed on T1-weighted structural scans and confirmed by a radiologist or practicing physician.

3.2.2 Clinical Assessments

The CP group was evaluated by experienced physical therapists using standardized protocols. GMFM dimensions D (standing) and E (walking, running and jumping) were assessed (Russell *et al.*, 2004). The GMFM-66 Gross Motor Ability Estimator program was used to compute final scores. SCALE was used to assess SVMC (Fowler *et al.*, 2009). Specific isolated movement patterns at the hip, knee, ankle, subtalar and toe joints were evaluated bilaterally. SCALE scores for each limb ranged from 0 (absent SVMC) to 10 (normal SVMC) (Fowler *et al.*, 2009). Left and right limb scores were summed for a total SCALE score with a maximum value of 20.

3.2.3 MRI Protocols

Prior to MRI sessions, children viewed a slide presentation describing MRI procedures and practiced lying still for 10 minutes while listening to recordings of MRI sounds. Movies were

provided during MRI acquisition for children to view upon request. All T1WI and DWI scans were acquired using a 32-channel coil on a 3.0 Tesla Prisma MRI Scanner (Siemens, Munich, Germany). T1-weighted MPRAGE images were obtained using TR = 2500 ms, TE = 1.8, 3.6, 5.39 and 7.18 ms, FOV = 256 x 256 mm^2, and isotropic voxel resolution = 0.8 x 0.8 x 0.8 mm^3. DWI scans were obtained using single-shot spin-echo, echo-planar acquisition with 6 reference images (b = 0 s/mm^2), 52 gradient directions (b = 1500 s/mm^2), TR = 3231 ms, TE = 89.6 ms, FOV = 210 x 210 mm^2, echo-spacing = 0.69 ms, and isotropic voxel resolution = 1.5 x 1.5 x 1.5 mm^3.

3.2.4 Statistical Analysis

TBSS, a whole brain voxel-based approach, was used to assess: 1) differences in DTI outcomes between the CP and TD groups and 2) correlations between DTI outcomes and SCALE and GMFM in the CP group. Whole brain analyses of DTI outcomes FA, RD, AD and MD were performed with TBSS using the FMRIB Diffusion Toolbox implemented in FMRIB's software library (FSL) (Smith *et al.*, 2006). The mean WM skeleton used in this analysis was derived from and overlaid on FMRIB58 standard-space FA template. Results were obtained after 5000 permutation-based randomized tests and corrected for multiple comparisons ($p < 0.05$) using the threshold-free cluster enhancement procedure (Smith and Nichols, 2009). Voxels with significant differences and correlations were projected separately onto the mean WM skeleton.

ROI analyses were performed to quantify voxels with significant findings within specific regions of the brain. Using Johns Hopkins University (JHU) ICBM-DTI-81 WM atlas labels (Mori *et al.*, 2008), ROIs were transferred to all images produced in the TBSS pipeline after nonlinear warping to the standard MNI52 space and skeletonization. ROIs located along the descending

pathways of the CSTs were parcellated bilaterally (Figure 1a): 1) area inferior to the cerebral peduncle (sub-CerPed), 2) CerPed, 3) PLIC and 4) SCR. The sub-CerPed ROIs are labeled as "CST" in the JHU WM atlas labels. ROIs for the corpus callosum (CC) were the genu, body and splenium.

To further compare the CP and TD groups, means for FA, RD, AD, and MD in each ROI were calculated. Data were tested for normal distribution using the Shapiro-Wilk test (Shapiro and Wilk, 1965). Between-group differences were analyzed using t-tests assuming unequal variance (JMP Pro 14, SAS Institute Inc., Cary, NC). Corrections for multiple comparisons were made using the Benjamini-Hochberg false discovery rate (Benjamini and Hochberg, 1995).

Means of each DTI measure within each motor ROI were correlated with SCALE and GMFM using simple linear regressions (JMP Pro 14, SAS Institute Inc., Cary, NC). Corrections for multiple comparisons were made using the Benjamini-Hochberg false discovery rate (Benjamini and Hochberg, 1995). Significant correlations between DTI outcomes and clinical measures (SCALE and GMFM) within each ROI were quantified for the CP group by performing voxel counts in FSL. The percentages of significant voxels in relation to the total number of voxels within ROIs were calculated.

3.3 Results

Twelve children with spastic bilateral CP (2 females, 10 males; mean age, 11.5 ± 2.8 years; age range, 7.3-16.6 years) participated. GMFCS levels were: I (n=3), II (n=1), III (n=7) and IV (n=1). Total SCALE scores ranged from 1 to 18. Twelve participants were recruited for the TD group (12 males; mean age, 10.3 ± 1.5 years; age range, 7.5-12.8 years).

		CP (n = 12)	TD (n = 12)
Age (Years)	Mean (SD)	11.5 (2.8)	10.3 (1.5)
	Range	7.3-16.6	7.5-12.8
Sex	Male	10	12
	Female	2	0
GMFCS Level	I	3	-
	II	1	-
	III	7	-
	IV	1	-

Table 3-1: Demographics of the CP and TD groups in this study.

3.3.1 Group Differences

The mean WM skeleton used for statistical comparisons of whole brain WM voxels is shown in Figure 3-2 (a). The CP group exhibited significantly lower FA values throughout the whole brain compared to the TD group (Figure 3-2 (b)). These areas included the CSTs, somatosensory cortex, parietal lobe, optic radiation, anterior limb of the internal capsule, external capsule, and CC. Within the CSTs, FA was significantly lower in the CerPed, PLIC, and motor cortex but no significant differences were found in the SCR. RD was higher for the CP group throughout the brain but fewer differences were found at the level of the CerPed compared to other regions (Figure 3-2 (c)). Bidirectional results were seen for AD (Figure 3-2 (d)), which was lower for the CP group at the level of the CerPed and cortex (coronal view) but higher for the CP group in the posterior end of the PLIC (axial view) and SCR bilaterally (coronal view). Fewer differences in AD were seen at the level of the cortex compared to other regions. MD was higher for the CP group within the CC, right CerPed, and bilateral PLIC and SCR (Figure 3-2 (e)).

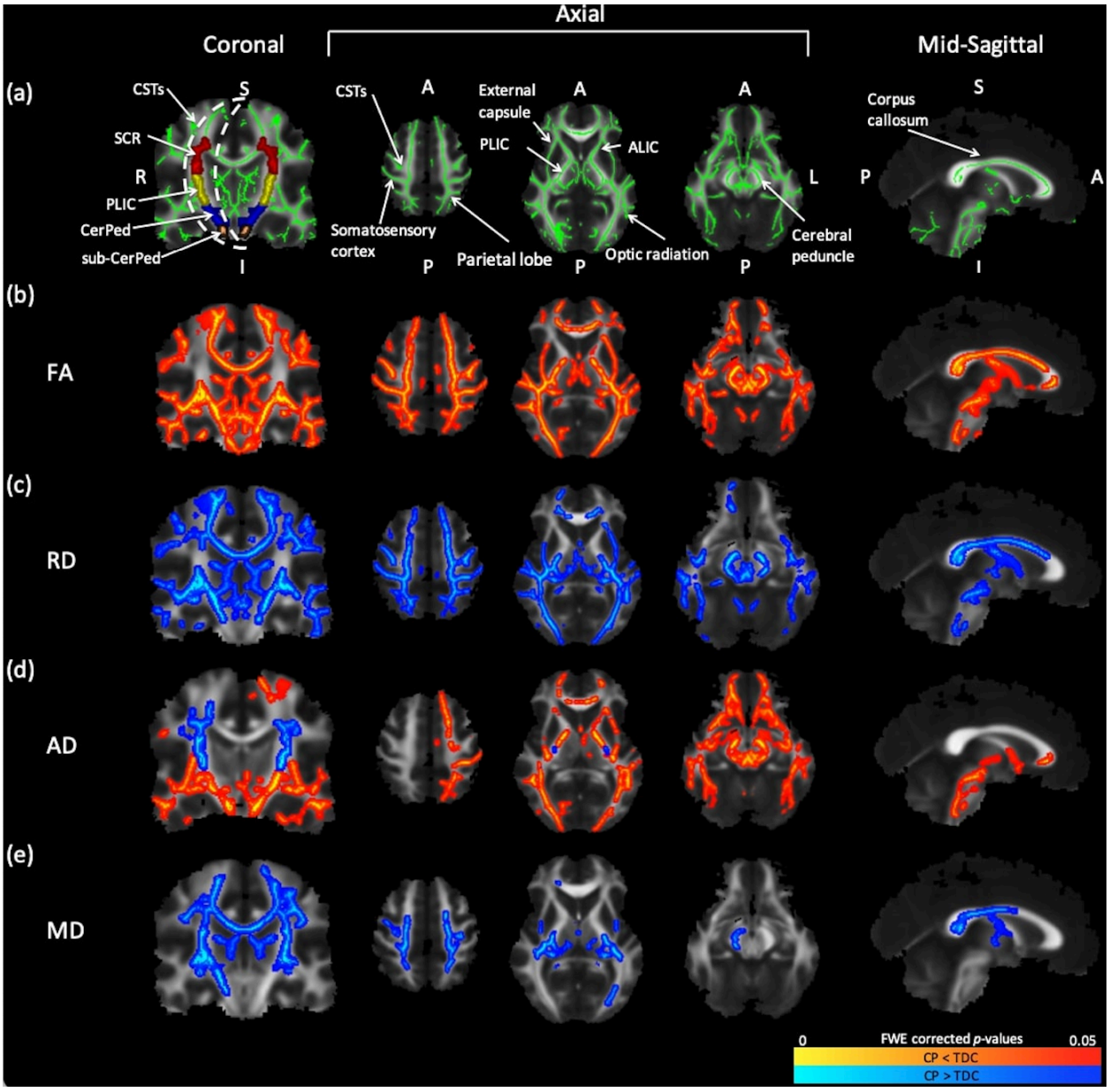

Figure 3-2: TBSS results display significant differences ($P < .05$) in DTI measures between the CP and TD groups. Coronal slices were selected at the level of the corticospinal tracts (CSTs). From left to right, axial slices were selected at the level of the motor cortex, posterior limb of the internal capsule (PLIC), and cerebral peduncle (CerPed), respectively. Mid-sagittal slices were selected at the level of the corpus callosum. (a) The WM skeleton is shown in green with arrows

labeling the CSTs, somatosensory cortex, parietal lobe, external capsule, anterior limb of the internal capsule (ALIC) and corpus callosum. In the coronal view, ROIs for the superior corona radiata (SCR; red), PLIC (yellow), CerPed (blue), and sub-CerPed (orange) are shown. Significant differences between the CP and TD groups are shown for: (b) fractional anisotropy (FA), (c) radial diffusivity (RD), (d) axial diffusivity (AD), and (e) mean diffusivity (MD). The hot colormaps denote whether a DTI measure for the CP group was less than (red-yellow) or greater than (blue-light blue) the TD group. A indicates anterior; FWE, family-wise error; I, inferior; L, left; P, posterior; R, right; S, superior.

ROI analysis revealed significant differences between mean DTI outcomes of the CP and TD groups within specific ROIs located along the CSTs and CC (Figure 3-3). Significantly lower FA values in the right sub-CerPed, CerPed bilaterally, and CC body and splenium were found for the CP group. In contrast, RD was significantly higher for the CP group in the CerPed bilaterally and CC body and splenium. AD was significantly lower for the CP group in the left CerPed and higher in the SCR bilaterally. MD was significantly higher for the CP group in the SCR bilaterally and CC body and splenium.

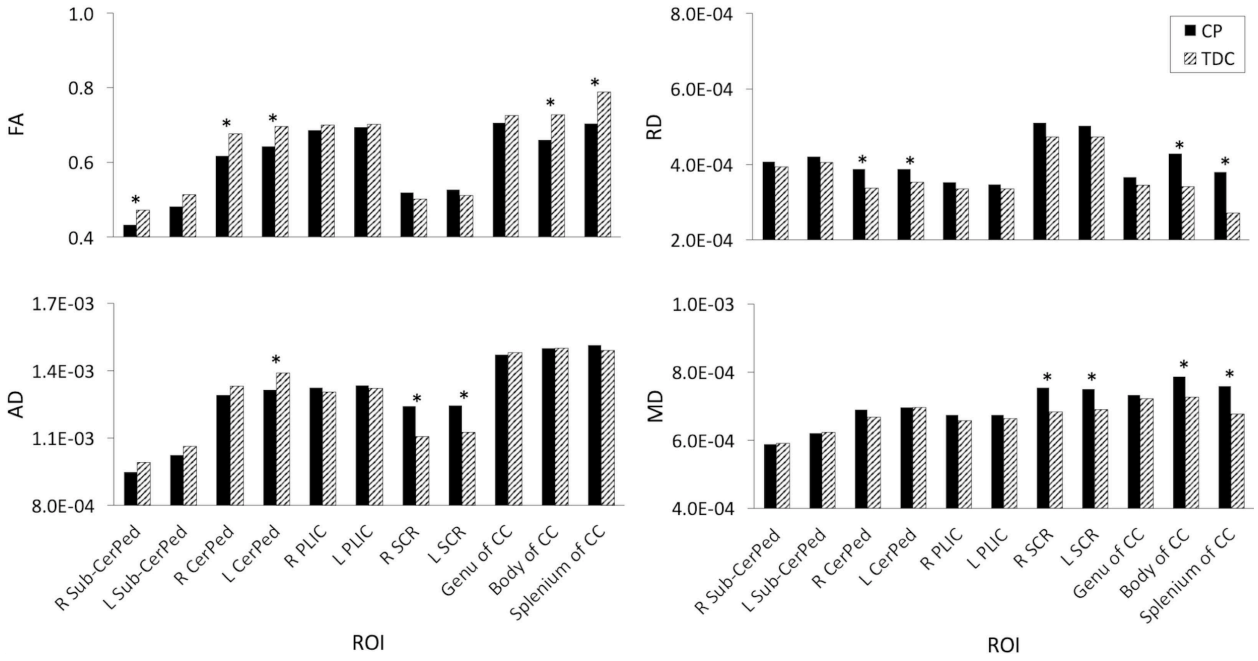

Figure 3-3: Mean differences in DTI measures between the CP and TD groups within ROIs for the corticospinal tracts and corpus callosum (CC). * indicates significant differences ($P < .05$). AD indicates axial diffusivity; CerPed, cerebral peduncle; FA, fractional anisotropy; L, left; MD, mean diffusivity; PLIC, posterior limb of the internal capsule; RD, radial diffusivity; R, right; SCR, superior corona radiata.

3.3.2 Correlation Analyses

In the whole brain correlation analyses for the CP group, significant correlations were found for FA and RD but not AD and MD (Figure 3-4). Significant positive correlations were found between FA and SCALE for all slices shown in Figure 3-4 (a). These correlations were associated with motor function regions including the CSTs at the level of the CerPed (right > left), PLIC (right > left), and motor cortex (left < right), and the CC. Fewer voxels within these motor regions exhibited significant positive correlations between FA and GMFM (Figure 3-4 (b)). In the

motor cortex, FA correlated with both SCALE and GMFM for bilateral lower extremity CSTs and left upper extremity CSTs as seen from the coronal views. More voxels showed significant correlations with SCALE than GMFM in these regions. RD exhibited significant negative correlations with SCALE in the CC (Figure 3-4 (c)) but significant correlations with GMFM were not found (Figure 3-4 (d)).

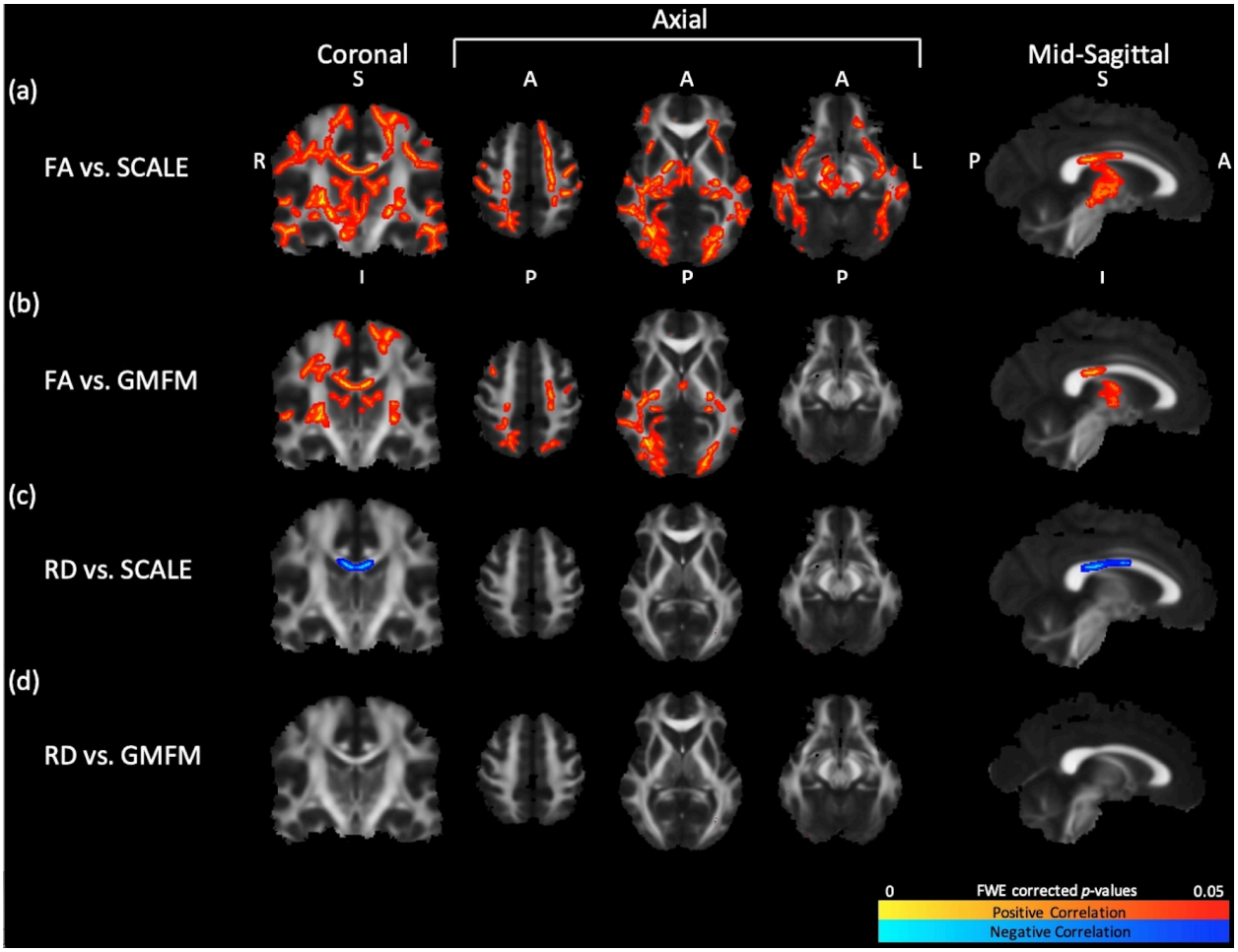

Figure 3-4: TBSS results display significant correlations ($P < .05$) between DTI measures and clinical measures for the CP group. Coronal slices were selected at the level of the corticospinal tracts. From left to right, axial slices were selected at the level of the motor cortex, posterior limb of the internal capsule. and cerebral peduncle, respectively. Mid-sagittal slices were selected at the

level of the corpus callosum. Significant correlations are shown for: (a) fractional anisotropy (FA) vs. SCALE, (b) FA vs. GMFM, (c) radial diffusivity (RD) vs. SCALE, and (d) RD vs. GMFM. The hot colormaps denote whether the correlations were positive (red-yellow) or negative (blue-light blue). A indicates anterior; FWE, family-wise error; GMFM, Gross Motor Function Measure; I, inferior; L, left; P, posterior; R, right; S, superior; SCALE, Selective Control Assessment of the Lower Extremity.

Pearson correlation coefficients for correlations between DTI measures and clinical measures within CST and CC ROIs are shown in Table 3-2. Significant correlations between average DTI measures within motor ROIs and SCALE were found for RD in the left and right PLIC and AD in the left CerPed. Significant correlations between average DTI measures within motor ROIs and GMFM were found for FA in the left and right PLIC and RD in the left and right PLIC.

Table 3-2: Correlations between clinical measures and averaged DTI outcomes within ROIs

	R Sub-CerPed		L Sub-CerPed		R CerPed		L CerPed		R PLIC		L PLIC		R SCR		L SCR		Genu of CC		Body of CC		Splenium of CC	
Correlations	r	*p* -value	r	*p* -value	r	*p* -value	r	*p* -value	r	*p* -value	r	*p* -value	r	*p* -value	r	*p* -value	r	*p* -value	r	*p* -value	r	*p* -value
FA vs. SCALE	0.38	0.35	0.41	0.26	0.63	0.10	0.57	0.10	0.68	0.10	0.60	0.10	0.53	0.11	0.23	0.41	0.59	0.10	0.60	0.10	0.35	0.32
FA vs. GMFM	0.36	0.31	0.50	0.18	0.59	0.12	0.62	0.12	0.74*	0.03	0.75*	0.03	0.31	0.14	0.29	0.37	0.43	0.24	0.42	0.24	0.29	0.37
RD vs. SCALE	0.40	0.32	0.33	0.28	0.58	0.20	0.40	0.20	0.77*	0.05	0.68*	0.05	0.58	0.11	0.39	0.28	0.22	0.20	0.61	0.09	0.40	0.28
RD vs. GMFM	0.31	0.34	0.41	0.28	0.51	0.24	0.47	0.27	0.79*	0.02	0.77*	0.02	0.61	0.13	0.39	0.28	0.06	0.34	0.41	0.27	0.37	0.34
AD vs. SCALE	0.28	0.65	0.47	0.36	0.48	0.36	0.61*	0.01	0.12	0.77	0.10	0.77	0.49	0.36	0.47	0.36	0.47	0.36	0.65	0.77	0.37	0.77
AD vs. GMFM	0.35	0.42	0.58	0.26	0.51	0.27	0.59	0.26	0.02	0.99	0.06	0.99	0.50	0.36	0.40	0.27	0.30	0.36	0.45	0.86	0.31	0.99
MD vs. SCALE	0.26	0.71	0.00	0.91	0.39	0.56	0.05	0.96	0.75	0.10	0.52	0.16	0.57	0.16	0.44	0.35	0.40	0.69	0.19	0.16	0.10	0.35
MD vs. GMFM	0.13	0.95	0.00	0.99	0.29	0.55	0.04	0.99	0.68	0.17	0.46	0.42	0.59	0.23	0.42	0.42	0.43	0.99	0.16	0.42	0.00	0.43

CSTs, corticospinal tracts; FA, fractional anisotropy; RD, radial diffusivity; AD, axial diffusivity; MD, mean diffusivity; SCALE, Selective Control Assessment of the Lower Extremity; GMFM, Gross Motor Function Measure; CerPed, cerebral peduncle; PLIC, posterior limb of the internal capsule; SCR, superior corona radiata; CC, corpus callosum. *p<.05

Voxel counts of significant correlations between DTI outcomes and clinical measures within CST and CC ROIs are shown in Table 3-3. FA correlated positively with SCALE within the right sub-CerPed, CerPed (right > left), PLIC (right > left), SCR (right > left), and CC body and splenium. Compared to SCALE, fewer voxels showed significant positive correlations between FA and GMFM within the PLIC, SCR, CC body and splenium, and throughout the whole brain (30.4% versus 14.4%, respectively). No voxels showed significant correlations between FA and GMFM within the CerPed and sub-CerPed ROIs. RD correlated negatively with SCALE for voxels within all CC ROIs but not CST ROIs. No significant correlations between RD and GMFM were found in voxels for the CST and CC ROIs.

Table 3-3: ROI correlation analyses comparing motor and whole brain WM regions

Regions	Voxel Count	Voxels with significant correlations			
		FA vs. SCALE (%)	FA vs. GMFM (%)	RD vs. SCALE (%)	RD vs. GMFM (%)
CSTs					
Sub-CerPed R	375	23 (6.1)	0 (0)	0 (0)	0 (0)
Sub-CerPed L	395	0 (0)	0 (0)	0 (0)	0 (0)
CerPed R	598	266 (44.5)	0 (0)	0 (0)	0 (0)
CerPed L	624	74 (11.9)	0 (0)	0 (0)	0 (0)
PLIC R	845	198 (23.4)	74 (8.8)	0 (0)	0 (0)
PLIC L	858	20 (2.3)	18 (2.1)	0 (0)	0 (0)
SCR R	1294	451 (34.9)	387 (29.9)	0 (0)	0 (0)
SCR L	1279	94 (7.3)	25 (2.0)	0 (0)	0 (0)
CC					
Genu	1758	0 (0)	0 (0)	54 (3.1)	0 (0)
Body	3138	1177 (37.5)	692 (22.1)	874 (27.9)	0 (0)
Splenium	2298	904 (39.3)	615 (26.8)	686 (29.9)	0 (0)
Whole brain	126000	38251 (30.4)	18136 (14.4)	2779 (2.2)	0 (0)

Note: CC indicates corpus callosum; CerPed, cerebral peduncle; CSTs, corticospinal tracts; FA, fractional anisotropy; GMFM, Gross Motor Function Measure; L, left; PLIC, posterior limb of the internal capsule; R, right; RD, radial diffusivity; SCALE, Selective Control Assessment of the Lower Extremity; SCR, superior corona radiata.

3.4 Discussion

This was the first study to associate SCALE, a sensitive measure of SVMC, with DTI outcomes for the CSTs and other WM tracts in children with spastic bilateral CP using TBSS. We demonstrated that FA correlated with SCALE in key regions of the CSTs. A previous DTI study had reported that sensory, but not motor tracts, correlated with motor function using visual assessment of tract impairment (Hoon *et al.*, 2009). Motor function in that study, however, was measured using hand-held dynamometry, which is difficult to measure reliably in children with poor motor control (Shortland, 2011). Additionally, motor skill/ambulatory level was not well defined. In our analysis, both SCALE and GMFM, which are valid clinical measures for spastic CP, were associated with CST impairment. SCALE emerged as the stronger clinical correlate using TBSS. To quantify the spatial group differences, we performed voxel counts in 3D motor ROIs. In comparison to GMFM, the number of voxels with significant correlations between SCALE and FA was greater, establishing SCALE as the more sensitive clinical correlate. Previous studies demonstrating a positive relationship between CST FA and functional ability were limited by their use of the GMFCS rating scale, which is a categorical descriptor of mobility (Lee *et al.*, 2011; Arrigoni *et al.*, 2016). In contrast, SCALE and GMFM employed in the present study are numerical measures of motor function.

Correlations of FA and RD with SCALE in the CC showed similar trends as Arrigoni et al. (2016), who reported correlations of FA and RD with GMFCS in the body of CC (Arrigoni *et al.*, 2016). The significant negative correlations between RD and SCALE in the present study suggest that callosal fibers serving interhemispheric sensorimotor communication are better myelinated

for children with greater SVMC. These findings may reflect one component of SCALE scoring procedures, the presence of mirroring, which lowers the score. Mirroring occurs when an intentional joint movement on one side of the body is accompanied by an obligatory synkinetic movement on the contralateral side (Fowler *et al.*, 2009). There are known associations between myelination of the CC and inhibition of mirroring (Nass, 1985; Mayston, Harrison and Stephens, 1999; Beaulé, Tremblay and Théoret, 2012). Additionally, transcallosal motor fibers located in the CC body are believed to play an important role in motor control and inhibition of unwanted mirror movements (Wahl *et al.*, 2007) and lower FA in transcallosal motor fibers has been associated with mirroring in the hands of children with bilateral spastic CP and PVL (Koerte *et al.*, 2011). The same mechanism likely occurs in LE mirroring but has not been studied to our knowledge.

Widespread correlations between SCALE and FA beyond the motor regions were found. In Figure 3-4, FA correlations with SCALE but not GMFM were seen in the brainstem, visual association pathways, and temporal lobes, suggesting that the integrity of these association pathways was more important for skilled, precise movements than for gross motor activities. Although a direct link between these regions and the ability to execute precise lower extremity movements is difficult to ascertain, such extensive correlations support prior studies demonstrating a relationship between motor function in spastic CP and long range network connectivity disruption of various non-motor networks including WM regions comprising the visual, limbic and sensory systems (Englander *et al.*, 2013; Ceschin *et al.*, 2015). Additionally, lower SCALE scores may be associated with the overall severity of CP including comorbidities of visual and cognitive impairments.

Consistent with previous studies, children with spastic CP exhibited lower FA, higher RD and higher MD in key regions of the CSTs, specifically the CerPed, PLIC and motor cortex,

compared to children with TD (Lee *et al.*, 2011; Arrigoni *et al.*, 2016). While PVL is a hallmark of spastic CP, no significant between-group differences in FA were found in the periventricular WM. FA values in this region are affected by an abundance of crossing fibers beyond the CSTs including corticopontine, corticobulbar and thalamocortical tracts causing more variability in FA. This factor leads to overall reduced measurements of FA in this region and may contribute to the statistically nonsignificant group differences (Ceschin *et al.*, 2015). In spastic CP, WM pathology extends beyond the periventricular WM (Lee *et al.*, 2011; Arrigoni *et al.*, 2016). Accordingly, we found widespread increases in RD for the CP group in the somatosensory cortex, parietal lobe, optic radiation, anterior limb of the internal capsule, external capsule, and CC. These increases in RD within the CSTs and throughout the whole brain are consistent with a lack of mature myelinated fibers and secondary Wallerian degeneration (Volpe, 2009).

Little is known about the relevance of AD differences between spastic CP and TD groups. In this analysis, mixed results were found for AD. Unexpectedly AD was higher in the periventricular WM including the SCR for the CP cohort (Figure 3-2 (d) and Figure 3-3). This finding may be associated with the radial diffusion of crossing fibers running perpendicular to the ascending/descending tracts in this region (Counsell *et al.*, 2006). The interpretation of this result is not straightforward as the utility of AD as a putative marker of axonal degeneration or a precise descriptor of tissue microstructure is still under investigation (Song *et al.*, 2002; Wheeler-Kingshott and Cercignani, 2009).

Statistically significant group differences and correlations observed in TBSS were not always reflected in ROI analyses (Figure 3-2, 3-3, 3-4 and Table 3-2). For example, significant correlations in the ROI analyses were seen for RD versus SCALE in the PLIC bilaterally and AD versus SCALE in the left CerPed. FA versus GMFM and RD versus GMFM correlations were

found in the PLIC bilaterally as well. These significant correlations were not found when using *randomise* in TBSS. This can be attributed to the fact that ROI analysis smoothed data over large areas, reducing noise and the number of multiple comparisons. The purpose of performing the voxel counts for the TBSS correlation analysis was, therefore, to quantify the spatial differences found when using SCALE and GMFM so that it can clearly be seen how SCALE is a more sensitive clinical correlate than GMFM on a voxel-by-voxel basis.

Notably, group difference and correlation analyses in TBSS revealed brain-wide effects in the CP group suggesting widespread microstructural tissue disruptions and associations with SCALE. Although motor tracts are deemed the region of injury in CP, WM pathways implicated in vision, hearing, sensation, proprioception and cognition may be impacted (Shang *et al.*, 2015). These findings are consistent with common comorbidities of spastic CP and may also suggest a global adaptation and neuroplasticity owing to recruitment of different brain regions post-damage. While it has been primarily understood that the function of the CSTs is directly related to SMC, it is plausible that recruitment of adjacent or surrounding tracts are involved in control of precise, skilled movements.

Correlations between SCALE and FA were found in the following regions in addition to the LE CSTs: the external capsule (EC), anterior limb of the internal capsule (ALIC), optic radiation and parietal lobe. These structures are potentially important for children with spastic bilateral CP and PVL and may be related to SMC to a certain extent. The inferior portion of the EC is packed with cholinergic fibers related to cognition and the superior portion contains association tracts connecting anterior and posterior parts of each hemisphere linking expression and language (Nolze-Charron *et al.*, 2020). The ALIC contains fibers passing through the thalamus and brainstem to the prefrontal cortical regions and are associated with emotion, motivation,

cognition processing and decision-making (Safadi *et al.*, 2018). The optic radiation is important in children with spastic CP and PVL as motor impairment can often be accompanied by visual deficits (Bax *et al.*, 2005; Shang *et al.*, 2015). Damage to the parietal lobe is important because it affects proprioception, or control in relation to one's external space, which can have secondary motor effects such as control of force and posture (Freund, 2003).

The global widespread group differences can also be understood in terms of network connectivity disruptions in the CP group. Englander et al. have shown changes to both short- and long-range brain network connectivity not limited to the sensorimotor network in severe versus moderate CP, although they did not include a healthy control sample (Englander *et al.*, 2013). While we did not have sufficient sample size to differentiate between severe and moderate cases of CP, our global voxel-wise findings implicated similar WM regions in the CP group including the visual, auditory, and cognitive systems. Ceschin et al. found widespread voxel-wise reductions in FA in CP and also showed disruption in network connectivity in CP based on global topological connectivity measures throughout the whole brain (Ceschin *et al.*, 2015). Furthermore, they found alterations in frontal–striatal and fronto-limbic nodes suggesting compensatory reorganization involving these frontal lobe pathways. Jiang et al. used diffusion imaging to show reduced global and nodal network efficiency and increased shortest path length using the fiber count metric in infants diagnosed with periventricular WM injury and spastic CP (Jiang *et al.*, 2019, 2021). Their study defined nodes as anatomical regions on the cortical gray matter and implicated impairment to the frontal, visual, and cingulate cortices in addition to the supplementary motor area causing visual spatial or visual perception deficits (Jiang *et al.*, 2021).

Therefore, while our hypotheses targeted the CSTs and WM motor tracts in general, our brain-wide WM group differences and brain-wide SCALE correlations suggest both a network-

structure disruption effect and a network-region recruitment effort by long-range brain fibers that may serve in a compensatory capacity in response to PVL injury. This warrants development of new network-driven hypotheses targeting brain connectivity and compensatory mechanisms in response to perinatal brain injury.

In contrast to Chapter 2, we were able to visualize WM differences and correlations in the LE CSTs within the PMC for all participants when using TBSS (Figure 3-2 and Figure 3-4), which was not possible for our cohort when using tractography. A limitation of TBSS, however, was registration using the adult FMRIB58 standard-space FA template for a cohort of children. Studies for an atlas to model the younger brains of children and adolescents should be developed. Additionally, TBSS resulting slice images are primarily qualitative with only voxels highlighting areas which areas contain significant group differences and correlations. To quantify effect sizes and the strength of correlations, additional analyses such as ROI analysis and voxel counts need to be performed. Future work should include developing methods to quantify the group difference effect sizes and correlations in TBSS on a voxel-by-voxel basis.

The study was limited by a small sample size as we could only include participants who could cooperate with MRI imaging without sedation. ROI analyses at the level of the primary motor cortex could not be performed as this region was not included in predefined segmentations of the JHU WM atlas labels.

3.5 Conclusions

This study establishes SCALE as a clinical correlate of multiple DTI measures more sensitive than gross motor function. SCALE was sensitive to WM impairment within the CSTs,

CC and throughout the whole brain. This study supports FA and RD as strong indicators of WM motor injury. It confirmed that children with spastic bilateral CP have altered WM diffusion properties throughout the whole brain, including the CSTs. Responsiveness to intervention using DTI measures is an important area for future research in CP.

Chapter 4: Improved Myelination Following Camp Leg Power, a Selective Motor Control Intervention for Children with Spastic Bilateral Cerebral Palsy: a Diffusion Tensor MRI Study

4.1 Introduction

Chapter 3 discussed how DTI has been used to assess cerebral WM damage in children with spastic bilateral CP (Lee *et al.*, 2011; Ceschin *et al.*, 2015; Arrigoni *et al.*, 2016; Vuong *et al.*, 2021) using measures FA, RD, AD and MD to characterize WM microstructure. Relative to normative data, reduced FA has been interpreted as a marker of disruption of local tissue structural anisotropy or directionality, higher RD as decreased myelination, lower AD as axonal injury and higher MD as greater overall diffusion within a region (Basser and Jones, 2002; Assaf and Pasternak, 2008; Winklewski *et al.*, 2018).

In summary, lower FA (Lee *et al.*, 2011; Ceschin *et al.*, 2015; Arrigoni *et al.*, 2016; Vuong *et al.*, 2021), higher RD and MD (Arrigoni *et al.*, 2016; Vuong *et al.*, 2021) and bidirectional results for AD (Arrigoni *et al.*, 2016; Vuong *et al.*, 2021) have been reported for children with spastic bilateral CP compared to children with TD. In children with spastic bilateral CP, significant correlations between DTI measures and GMFCS levels (Lee *et al.*, 2011; Arrigoni *et al.*, 2016), Gross Motor Function Measure (GMFM) (Vuong *et al.*, 2021) and SCALE scores (Vuong *et al.*, 2021) have been found. In addition, SCALE scores were found to correlate positively with FA and negatively with RD in more motor regions of the brain compared to GMFM (Vuong *et al.*, 2021).

Neuroplasticity as evidenced by changes in microstructural properties of WM motor tracts in spastic CP is still not well-understood. Studies of DTI measures in response to exercise

interventions are limited and improvements have yet to be clearly demonstrated. Most studies have focused on UE therapy in children with unilateral CP and contrasting results have been reported (Rickards *et al.*, 2014; Kim, Kwon and Son, 2015; Nemanich, Mueller and Gillick, 2019). No significant changes were found in any DTI measure in cohorts of children and young adults with unilateral CP (age 2-21 years) following constraint-induced therapy (Rickards *et al.*, 2014) and constraint-induced therapy preceded by transcranial direct current stimulation (Nemanich, Mueller and Gillick, 2019). In contrast, Kim et al. found increased FA following a task-specific UE exercise intervention in infants with CP who were <12 months of age at baseline (Kim, Kwon and Son, 2015) suggesting that microstructural changes may be more likely in younger children who have greater plasticity.

DTI changes of brain motor regions in children with spastic CP in response to a LE exercise intervention have received little attention. Two studies conducted in India used tractography to examine the effect of an intensive 6-month rehabilitation program on FA of motor and sensory tracts in conjunction with LE BTX injection for children who were full-term with spastic bilateral CP, age 2-8 years (Trivedi *et al.*, 2008; Chaturvedi *et al.*, 2013). Participants were reported as having GMFCS levels ranging from I to IV at baseline. PT including strengthening, gait training and stretching (30 minutes of each) was performed daily for 24 weeks. BTX injections targeted culprit muscles that were identified using gait video recordings and spasticity assessments and were followed by 6-weeks of casting. In the first study (n = 8) (Trivedi *et al.*, 2008), all children had BTX and casting in addition to PT. A significant increase in FA of the CSTs at the level of the PLIC was reported. Additionally, improvements in GMFCS levels were reported. This unexpected finding (Palisano *et al.*, 2007) may be related to the young age of the participants and potentially limited access to medical treatment prior to intensive rehabilitation. In the second study (n = 36)

(Chaturvedi *et al.*, 2013), the same PT program was implemented but participants were randomized to either BTX or no BTX groups and the motor outcome was GMFM. Significant increases in FA of motor and sensory bundles and GMFM were found in both groups regardless of BTX assignment. Overall, these studies support the efficacy of intensive LE PT with no additional benefit of BTX. FA improvements found in these two studies have not been seen in other studies of LE motor intervention in spastic CP. One reason may be the high PT dosage, which is not feasible in most settings and may place a considerable burden on a child and their family. In a third study by Jain et al. (n = 10), neither FA nor the apparent diffusion coefficient increased after 6 months of physiotherapy with BTX injection for a cohort of children with spastic bilateral CP, age 3-12 years (Jain *et al.*, 2014). The ROIs, however, were defined differently (based on WM perfusion). Most studies of LE interventions in spastic CP to date have not included RD, which is a marker of myelination (Song *et al.*, 2002; Lazari and Lipp, 2021), or MD, which measures overall diffusion (Vos *et al.*, 2012) in their analyses.

While previous CP studies used DTI to observe specific and isolated WM motor tracts, full tract reconstruction can be difficult in cohorts with impaired WM leading to exclusion of participants (Kwon *et al.*, 2014; Kim, Kwon and Son, 2015; Hodge *et al.*, 2017), especially for the LE CSTs as seen in Chapter 2. Additionally, focusing on a set of a-priori WM tracts may limit the scope of analysis and underestimate the global extent of WM neuroplasticity. TBSS, a whole-brain voxel-based approach, can be used to observe the intervention effect on all WM tracts including the WM motor regions of the brain (Smith *et al.*, 2006) and circumvents these issues.

To our knowledge, the effect of an intensive LE SMC intervention on WM motor tract microstructure has not been studied in children with spastic bilateral CP born premature with PVL. We hypothesized that: 1) WM DTI measures (FA, RD, AD and MD) would improve following

intensive task-specific SMC intervention and 2) participants with greater baseline SCALE scores would exhibit greater improvements.

4.2 Materials and Methods

In this report, we used DTI and TBSS to analyze changes in whole brain and motor region WM microstructure after an intervention targeting isolated, skilled LE SMC movements in children with spastic bilateral CP. We aimed to determine whether practicing skilled isolated joint movements could elicit neuroplasticity of brain motor regions and whether changes in DTI outcomes would correlate with SCALE.

This study was conducted in an outpatient clinical research setting (Center for CP at UCLA/OIC and Ahmanson-Lovelace Brain Mapping Center). The institutional review board of the University of California Los Angeles provided ethics approval. Informed assent and consent for research were obtained from the children and their parents or guardians.

4.2.1 Participants

Twelve participants with spastic bilateral CP were recruited for this intervention DTI study. Inclusion criteria for all participants were the following: 1) between 5 and 18 years of age, 2) a history of prematurity, 3) a diagnosis of spastic bilateral CP and PVL as evidenced by MR imaging or sonography, 4) the ability to understand and follow verbal directions, 5) the ability to lie still and 6) the ability to walk with or without assistive devices.

Exclusion criteria for all participants were the presence of the following: 1) metal implants not verified as MR imaging-safe, 2) programmable implants including ventriculoperitoneal shunts and intrathecal baclofen pumps, 3) dental braces, 4) seizures not controlled by medication, 5) orthopedic surgery or neurosurgery within 1 year of starting the study and 6) BTX injection or casting within 3 months of starting the study.

4.2.2 Functional Outcome Measures

Children with CP were evaluated by experienced physical therapists using standardized protocols. SCALE was used to assess SVMC (Fowler *et al.*, 2009). Specific isolated movement patterns at the hip, knee, ankle, subtalar and toe joints were evaluated bilaterally. SCALE scores for each limb range from 0 (absent SVMC) to 10 (normal SVMC). Left and right limb scores were summed for a total possible SCALE score of 20 points.

4.2.3 Lower Extremity Selective Motor Control Intervention (Camp Leg Power)

The Camp Leg Power LE SMC intervention included practice of skilled, isolated LE joint movements, isokinetic knee exercises at variable speeds, ankle-controlled video gaming, gait and functional training and LE sensory enrichment using a summer camp format. Under the supervision of experienced physical therapists, each participant had 15 camp sessions for 3 hours/day over a 1-month period. Skilled, isolated movements of the hip, knee, ankle, subtalar and toe joints were practiced. Using a Biodex System 4 Pro dynamometer (Biodex Medical Systems, Shirley, NY), isokinetic knee extension (KE) and knee flexion (KF) exercises were performed

bilaterally for a minimum of 10 sessions. Each participant was trained at speeds up to 300 deg/s depending on their initial ability to produce torque and progressed as able during each session. Participants operated video games using ankle dorsiflexion and plantar flexion movements on a robotic device (Wu *et al.*, 2011) for at least 5 minutes per limb for a minimum of 10 sessions. Gait and functional training in activities that emphasized intra- and inter-limb control were practiced. These included kicking, navigating obstacles, stair climbing and treadmill/overground walking encouraging maximal step length. Barefoot sensory enrichment activities were performed such as walking on different surfaces.

4.2.4 Image Acquisition Protocol

Prior to MRI sessions, children viewed a slide presentation describing procedures and practiced lying still while listening to recordings of scanner sounds. All T1-weighted and diffusion-weighted imaging (DWI) scans were acquired using a 32-channel coil on a 3T Siemens Magnetom Prisma MRI scanner without sedation. T1w MPRAGE images were obtained using TR = 2500 ms; TE = 1.8, 3.6, 5.39, and 7.18 ms; FOV = 256 × 256 mm^2; and isotropic voxel resolution = 0.8 × 0.8 × 0.8 mm^3. DWI scans were obtained using a single-shot, spin-echo, echo-planar acquisition with 6 reference images (b = 0 s/mm^2), 52 gradient directions (b = 1500 s/mm^2), TR = 3231 ms, TE = 89.6 ms, FOV = 210 × 210 mm^2, echo spacing = 0.69 ms, and isotropic voxel resolution = 1.5 × 1.5 × 1.5 mm^3.

4.2.5 Statistical Analysis

TBSS, a whole-brain voxel-based approach, was used to assess pre-post differences in DTI outcomes FA, RD, AD and MD (Smith *et al.*, 2006). The mean WM skeleton used in this analysis was derived from and overlaid on the FMRIB58 standard-space FA template (https://fsl.fmrib.ox.ac.uk/fsl/fslwiki/FMRIB58_FA). Statistical analysis was performed using paired t-tests (5000 permutations). In addition, correlation analyses between pre-post DTI differences within each voxel and total SCALE score were performed. All results were corrected for multiple comparisons ($p < 0.05$) using the threshold-free cluster enhancement procedure implemented in *randomise* (Smith and Nichols, 2009). Voxels with significant post-intervention differences and correlations were displayed on the mean WM skeleton.

4.2.6 Region of Interest Parcellation

ROI analyses were performed to quantify voxels with significant post-intervention differences. Using the Johns Hopkins University ICBM-DTI-81 WM atlas labels (http://neuro.debian.net/pkgs/fsl-jhu-dti-whitematter-atlas.html) (Mori *et al.*, 2008), we transferred ROIs to all images produced in the TBSS pipeline after nonlinear warping to the standard Montreal Neurological Institute 152 space and skeletonization. Mean differences for RD and MD within motor ROIs showing significant post-intervention decreases with TBSS were calculated using paired t-tests (JMP Pro 14, SAS Institute Inc., Cary, NC). Corrections for multiple comparisons were made using the Benjamini-Hochberg false discovery rate (Benjamini and Hochberg, 1995). Significant pre-post differences within ROIs using TBSS were further quantified by performing voxel counts in FSL (http://www.fmrib.ox.ac.uk/fsl). ROIs located along the

descending pathways of the CSTs were parcellated bilaterally to analyze the primary WM motor regions (Fig. 4-1 (a)): 1) sub-CerPed, 2) CerPed), 3) PLIC and 4) SCR. Secondary ROIs were the ALIC, EC, anterior corona radiata (ACR) and the CC genu and body. The percentages of significant voxels in relation to the total number of voxels within ROIs were calculated.

4.3 Results

Twelve children with spastic bilateral CP and PVL (age mean ± SD: 11.5 ± 2.8 years; range: 7.3–16.6 years) participated in this intervention study (see Table 2-1). They were born preterm ranging from 24 to 33 weeks gestational age. GMFCS levels were: I (n = 3), II (n = 1), III (n = 7), and IV (n = 1). Total SCALE scores ranged from 1 to 18.

The mean WM skeleton used for all TBSS whole-brain voxel-based comparisons is shown in Figure 4-1 (a). Significant post-intervention decreases in RD were found throughout major WM tracts including the CSTs, ALIC, EC, ACR and CC (Figure 4-1 (b)). Within the CSTs, RD decreased significantly in the bilateral PLIC and left SCR as seen in the coronal and axial views. In the superior axial slice, decreased RD can be viewed in the left motor and somatosensory cortices. Significant post-intervention decreases in MD were found in similar WM regions of the brain (Figure 4-1 (c)): the CSTs (bilateral PLIC and left SCR, ALIC, EC, ACR and CC). In addition, decreased MD is apparent in both frontal lobes. No significant post-intervention increases in RD or MD were found and no significant post-intervention changes in either direction for FA or AD were found. Significant correlations were not found between changes in FA, RD, AD and MD and total SCALE score.

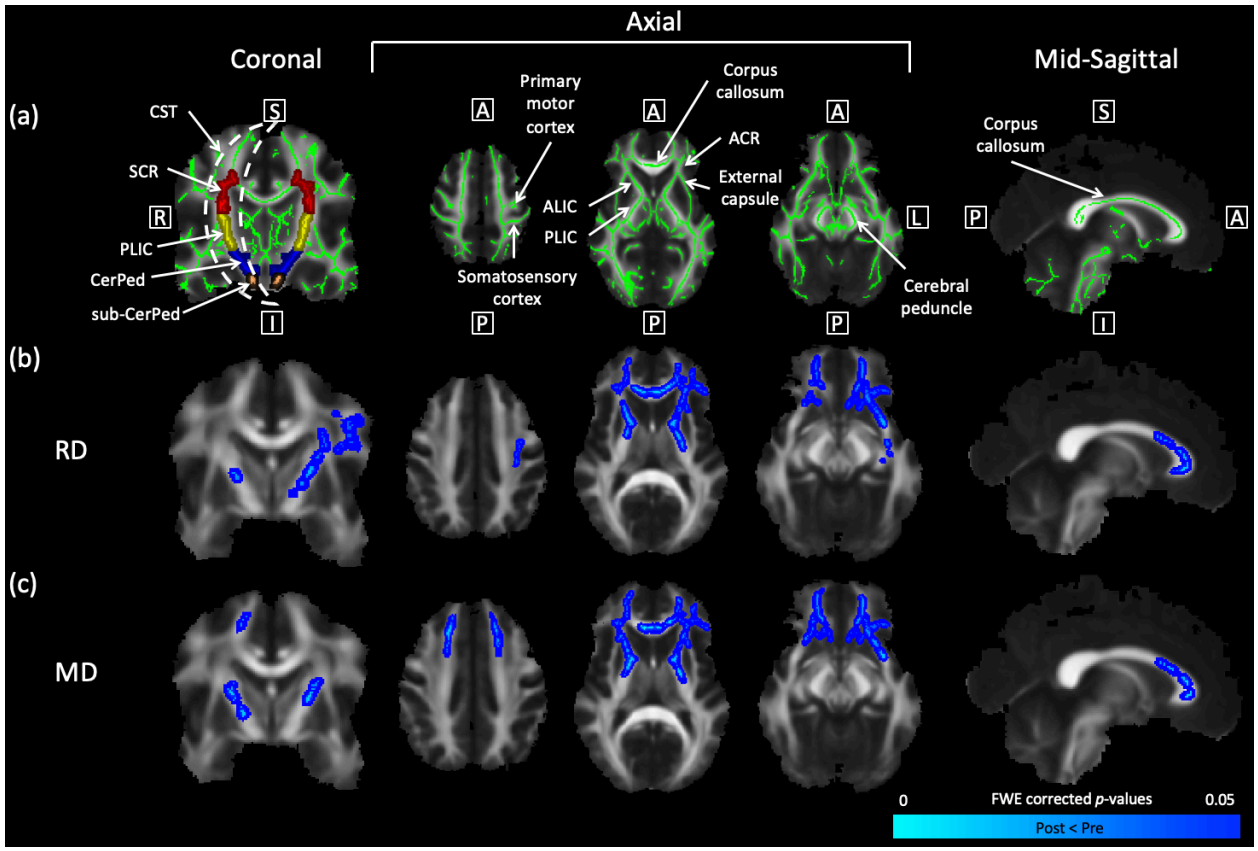

Figure 4-1. TBSS results show significant reductions in RD and MD ($p < 0.05$) after LE intervention. Coronal slices were selected at the level of the CSTs. From left to right, axial slices were selected at the level of the primary motor cortex, PLIC and CerPed, respectively. Mid-sagittal slices were selected at the level of the corpus callosum. (a) The WM skeleton is shown in green with additional arrows labeling the somatosensory cortex, anterior limb of the internal capsule (ALIC), anterior corona radiata (ACR) and external capsule. In the coronal view, ROIs for the SCR (red), PLIC (yellow), CerPed (blue) and sub-CerPed (orange) are shown. Significant pre-post differences for the CP group are shown for (b) RD and (c) MD. The colormap (blue-light blue) denotes a significant decrease in the DTI measure. R – right, S – superior, I – inferior, A – anterior, P – posterior, L – left, FWE – family-wise error.

Results for average DTI decreases within WM ROIs showing prior significant pre-post changes using TBSS is shown in Table 4-1. RD decreased significantly in ROIs for the right ALIC, left ACR and CC genu. MD decreased significantly in ROIs for the right ALIC, ACR bilaterally and CC genu. While significant decreases for only RD were found in the left fornix, left retrolenticular part of the internal capsule and left superior fronto-occipital fasciculus using TBSS, these differences were not significant when calculating mean differences within ROIs.

Table 4-1
Average DTI Decreases within WM ROIs.

ROI	RD				MD			
	Pre	Post	Difference	P-value	Pre	Post	Difference	P-value
R ALIC	4.30E-04	4.20E-04	-1.01E-05	0.03*	6.97E-04	6.86E-04	-1.10E-05	0.04*
L ALIC	4.41E-04	4.32E-04	-9.24E-06	0.05	6.99E-04	6.92E-04	-6.91E-06	0.17
R PLIC	3.54E-04	3.52E-04	-1.58E-06	0.71	6.80E-04	6.76E-04	-3.64E-06	0.23
L PLIC	3.52E-04	3.46E-04	-5.99E-06	0.24	6.79E-04	6.76E-04	-3.45E-06	0.40
R EC	5.57E-04	5.53E-04	-3.99E-06	0.29	7.53E-04	7.49E-04	-3.31E-06	0.23
L EC	5.61E-04	5.54E-04	-6.64E-06	0.11	7.55E-04	7.50E-04	-4.41E-06	0.22
R ACR	5.27E-04	5.19E-04	-8.10E-06	0.05	7.46E-04	7.37E-04	-9.10E-06	0.04*
L ACR	5.36E-04	5.22E-04	-1.39E-05	0.01*	7.52E-04	7.41E-04	-1.09E-05	0.03*
L SCR	5.12E-04	5.03E-04	-9.14E-06	0.05	7.56E-04	7.51E-04	-5.29E-06	0.17
Genu of CC	3.80E-04	3.65E-04	-1.46E-05	0.03*	7.45E-04	7.34E-04	-1.09E-05	0.04*
Body of CC	4.35E-04	4.29E-04	-5.91E-06	0.24	7.93E-04	7.86E-04	-6.24E-06	0.18
L Fornix	5.28E-04	5.24E-04	-4.58E-06	0.38	-	-	-	-
L RPIC	4.95E-04	4.88E-04	-7.80E-06	0.07	-	-	-	-
L SFOF	5.10E-04	5.04E-04	-5.54E-06	0.05	-	-	-	-

ALIC - anterior limb of the internal capsule, PLIC - posterior limb of the internal capsule, EC - external capsule, ACR - anterior corona radiata, SCR - superior corona radiata, CC - corpus callosum, RPIC - retrolenticular part of the IC, SFOF - superior fronto-occipital fasciculus.

The number of voxels with significant pre-post changes in RD and MD within motor and non-motor WM ROIs is shown in Table 4-2. RD and MD decreased significantly within ROIs for the bilateral ALIC, bilateral PLIC, bilateral EC, bilateral ACR, left SCR and CC genu and body. In all regions with bilateral ROIs, a greater percentage of changes was seen in the left hemisphere of the brain as compared to the right for both RD and MD, with the exception of MD in the bilateral ALIC (right > left). In addition to these regions, significant decreases for only RD were found in the left fornix, left retrolenticular part of the internal capsule and left superior fronto-occipital fasciculus (Table 4-2).

Table 4-2

Voxel counts of WM ROIs.

ROI	Voxel Count	Voxels with Significant Pre-Post Decreases	
		RD (%)	MD (%)
R ALIC	792	278 (35.1)	400 (50.5)
L ALIC	819	341 (41.6)	205 (25.0)
R PLIC	845	30 (3.6)	98 (11.6)
L PLIC	858	244 (28.4)	114 (13.3)
R EC	1331	19 (1.4)	41 (3.1)
L EC	1431	320 (22.4)	164 (11.5)
R ACR	1619	365 (22.5)	569 (35.1)
L ACR	1613	897 (55.6)	802 (49.7)
L SCR	1279	180 (14.1)	84 (6.6)
Genu of CC	1758	914 (52.0)	710 (40.4)
Body of CC	3138	201 (6.4)	256 (8.2)
L Fornix	401	25 (6.2)	-
L RPIC	753	49 (6.5)	-
L SFOF	1388	165 (11.9)	-

ALIC - anterior limb of the internal capsule, PLIC - posterior limb of the internal capsule, EC - external capsule, ACR - anterior corona radiata, SCR - superior corona radiata, CC - corpus callosum, RPIC - retrolentricular part of the IC, SFOF - superior fronto-occipital fasciculus.

4.4 Discussion

To our knowledge, this is the first study to show significantly decreased RD and MD in brain WM motor regions after an intensive LE SMC intervention in children with spastic bilateral CP. No significant post-intervention increases in RD nor MD were found. Few studies of children with spastic CP have analyzed post-intervention DTI changes beyond FA. Following our intervention, RD and MD decreased significantly in key regions of the CSTs including the bilateral PLIC, left SCR and left primary motor cortex. Decreased RD of WM tracts is suggestive of improved myelination (Song *et al.*, 2002; Lazari and Lipp, 2021), whereas a decrease in MD may suggest intervention guided neuroplastic changes related to alterations in microstructural tissue complexity (Thomas *et al.*, 2005; Scheck, Boyd and Rose, 2012; Vos *et al.*, 2012; Scheck *et al.*, 2015). In children with TD, myelination is rapidly developed during infancy (Poduslo and Jang, 1984) and is dynamically regulated throughout adolescence (Corrigan *et al.*, 2021) but deficits have been widely reported for children with spastic CP and PVL (Kinney, 2005; Billiards *et al.*, 2008; Volpe, 2009; Vuong *et al.*, 2021). It has been theorized that task-based interventions focused on practicing new complex motor skills, as performed in this study, promote myelination (Baraban, Mensch and Lyons, 2016; Lakhani *et al.*, 2016; de Faria Jr. *et al.*, 2019; Bloom, Orthmann-Murphy and Grinspan, 2022). Others reported improved CST myelination (using DTI tract-based quantitative susceptibility mapping) in children with spastic CP following cord blood stem-cell therapy and usual rehabilitation therapy (Englander *et al.*, 2015; Sun *et al.*, 2017; Zhang *et al.*, 2021) precluding direct comparisons.

Our current findings of improved myelination in the CC genu and body are consistent with potential neuroplastic changes in response to SMC-focused therapy activities. In a study of rats trained in a spatial learning and memory task, WM changes in the CC as evidenced by changes in

DTI indices FA and apparent diffusion coefficient were accompanied by increased myelin basic protein expression (Blumenfeld-Katzir *et al.*, 2011). These findings support the association between acquisition of new complex motor skills and increased CC myelination. The CC is an important large WM structure that is believed to play a role in bilateral coordination (Wahl *et al.*, 2007), especially inhibition of physiologic mirroring that normally diminishes with age during early childhood (Mayston, Harrison and Stephens, 1999). Loss of transcallosal inhibition is one proposed cause of acquired obligatory mirror movements in patients with upper motor neuron lesions (Nass, 1985; Beaulé, Tremblay and Théoret, 2012; Riddell *et al.*, 2019). These abnormal mirror movements in CP contribute to SMC deficits and lower SCALE scores (Fowler *et al.*, 2009). Lower FA in transcallosal fibers in the body of the CC has been associated with UE mirroring in children with spastic CP and PVL (Koerte *et al.*, 2011). We previously demonstrated a correlation between SCALE scores and DTI parameters in the CC in a cross-sectional analysis of this cohort (Vuong *et al.*, 2021).

Significant post-intervention decreases in RD and MD in other WM regions such as the ALIC, ACR, EC, sensorimotor cortex and frontal lobes suggest recruitment of neighboring WM tracts directly adjacent or within close proximity to the CSTs. Prior studies of adults recovering from stroke have demonstrated significant changes in functional connectivity between the primary motor cortices (Liu *et al.*, 2015; Li *et al.*, 2016), as well as post-intervention (repetitive transcranial magnetic stimulation and occupational therapy) changes in similar WM regions (Ueda *et al.*, 2021). The regions of the brain where we see RD and MD changes are areas of the brain that contain rich interconnections between the cortex, thalamus and association regions (Chayer and Freedman, 2001; Karababa *et al.*, 2015; Safadi *et al.*, 2018; Zhao *et al.*, 2019; Nolze-Charron *et al.*, 2020). Although motor improvement in children with spastic CP is made more complex by

ongoing processes in the developing brain, similar patterns and principles of neuroplasticity likely apply. It is therefore plausible that coactivation and improved myelination of these adjacent or additional WM tracts are necessary in regulating neuroplasticity of the motor regions of the brain.

LE interventions aimed specifically at developing and improving SMC in CP are limited and primarily focused on the ankle joint (Wu *et al.*, 2010, 2011). Imaging data following more generalized LE rehabilitation has been focused on FA. Two studies that focused on general LE exercise and BTX (6 months) in children with CP (age 2-8 years) reported increased FA in the PLIC of the CST (Trivedi *et al.*, 2008) and in motor fiber bundles (Chaturvedi *et al.*, 2013); regions where we found decreased RD and MD. Additionally, increased FA was found in 2 motor tracts (CST and PLIC) and 5 association tracts (CC, inferior and superior longitudinal fasciculus, uncinate and cingulum) following intensive voice treatment (14 weeks) in children with CP (7-16 years) and secondary dysarthria (Reed *et al.*, 2017). While the DTI measures analyzed did not include RD, these findings support the ideas in the present study that recruitment and activation of the CSTs play a critical role in responsiveness to: 1) intense LE intervention and 2) practicing new complex motor skills. It is possible that improved myelination preceded or accompanied improvements in FA in these previous studies but RD was not assessed. A longer intervention duration and a younger CP cohort may be required to promote significant changes in FA.

Statistically significant post-intervention differences found for RD and MD using TBSS were not always reflected in ROI analyses (Figure 4-1 and Table 4-2). Significant pre-post findings for RD and MD using TBSS and ROI analyses, however, were in agreement for the right ALIC, left ACR, right ACR (for only MD) and CC genu. These differences can be attributed to the fact that ROI analysis smoothed data over large areas, reducing noise and the number of multiple comparisons. More regions with significant post-intervention findings were found for arguably the

more statistically strict voxel-by-voxel TBSS analysis (compared to using average DTI values within ROIs). The purpose of performing the voxel counts for the TBSS correlation analysis was, therefore, to quantify the spatial differences so that it can clearly be seen which regions of the brain exhibited post-intervention changes on a voxel-by-voxel basis.

Significant post-intervention decreases in RD and MD were not associated with SCALE scores in this analysis despite the significant correlation between RD and SCALE at baseline (Vuong *et al.*, 2021). Isolated, skilled movements require good CST function; therefore, we hypothesized that children with higher SCALE scores would have greater capacity to learn and perform skilled movements resulting in greater myelination. One explanation may be that children with lower SCALE scores are more likely to move in synergistic patterns, have lower levels of physical activity and experience ankle and foot constraint due to greater dependence on orthotics. The Camp Leg Power intervention was therefore more novel for these participants and greater motor learning may have occurred than was expected.

This study was limited by a relatively small sample size due to MRI exclusion criteria. Children with spastic CP commonly have shunts, baclofen pumps and may undergo orthopedic surgery requiring metal implants (Thompson *et al.*, 2020). In addition, involuntary movements are common and sometimes exaggerated by noise further limiting good MRI acquisition. The inclusion of a control group of children with spastic bilateral CP who did not undergo the Camp Leg Power intervention would strengthen these findings. The study by Trivedi *et al*. (2008) included a control group of children with TD and did not find significant within-group differences in FA nor MD over a much longer time period. A randomized controlled trial with a larger cohort is needed to confirm our results. An additional limitation was that ROI analysis of the CSTs at the level of the primary motor cortex was not performed as it is not included in the Johns Hopkins

University WM atlas labels. Younger children with greater potential for plasticity (Mundkur, 2005) may be more likely to show improvement but are more difficult to scan without sedation. Efforts are currently underway to adapt SCALE and develop a SMC LE intervention for infants and toddlers.

In summary, intensive practice of skilled LE SMC movements by children with spastic bilateral CP and PVL born prematurely was associated with increased myelination in WM motor tracts, including the CSTs and the CC. Improved myelination of adjacent and nearby WM tracts suggest additional neuroplasticity associated with skilled LE SMC learning. A longer intervention duration at earlier ages may optimize WM neuroplasticity.

Chapter 5: Selective Motor Control is a Clinical Correlate of Baseline Motor Outcomes and Motor Outcome Changes Following Camp Leg Power

5.1 Introduction

Camp Leg Power is a novel intervention in spastic CP focused on the development and practice of skilled, isolated LE movements. Only a limited number of studies have examined LE interventions aimed specifically at improving SMC in CP. Previous studies focused primarily on the ankle joint, demonstrating improved ankle motion and ankle SMC using a robotic device (Wu *et al.*, 2010, 2011). Camp Leg Power was additionally developed as a task-oriented, intense (implying high dosage) intervention. A study by Salem and Godwin demonstrated significant improvements for dimensions D and E of the GMFM after a 5 week training period, supporting task-oriented strength training as an efficacious method in improving functional mobility in CP (Salem and Godwin, 2009). Several studies involving intensive constraint induced UE PT in a camp model successfully improved hand function in children with unilateral CP (Bonnier, Eliasson and Krumlinde-Sundholm, 2006; Sakzewski, Ziviani and Boyd, 2011). During Camp Leg Power, therapy was administered with minimal use of braces to promote full awareness of active movement. The participants were fully engaged with activities designed to promote sensory and motor improvement including isolated, skilled motor tasks, isokinetic knee exercises with the use of a dynamometer, robotic gaming using the ankle and gait training. The effect of a LE SMC intervention in children with spastic CP has not been studied.

In SCALE assessment, SVMC is measured for 5 major bilateral LE joints: hip, knee, ankle, subtalar and toe. Several factors are considered including selectivity, involuntary and obligatory movements, range of motion, the ability to reciprocate movement, speed and force (Fowler *et al.*, 2009). These selective movements are different from habitual movement patterns during functional tasks such as walking, running or climbing stairs. In response to Camp Leg Power, it was not expected for SCALE scores to change or improve, which is difficult to achieve, as SCALE is more of a fine motor measure of SMC at individual joints. On the other hand, an example of a more discrete measure of SMC is induced KE acceleration during the swing phase of gait (Goldberg, Requejo and Fowler, 2011). While SCALE scores were not expected to change, they have nonetheless been found to correlate with intralimb coordination (Fowler and Goldberg, 2009) and have a larger causal effect on gross motor function when compared to strength, spasticity, contractures and bony deformities (MacWilliams *et al.*, 2022). SCALE is also a strong prognostic factor for hamstring surgery (Goldberg, Fowler and Oppenheim, 2012) and selective posterior rhizotomy (Staudt and Peacock, 1989).

As SCALE measures CST function (see Chapters 2 and 3) and CST function relates to the force, speed and timing of joint movement (Kennedy, 1990), we aimed to examine the efficacy of SCALE at predicting other motor performance measures collected during Camp Leg Power such as the 10-meter walk/run test (10mWRT), 6-minute walk test (6MWT), GMFM scores, ankle robot dosing, isokinetic KE and KF torques, step length and stride length. We aimed to collect motor outcome measures for which good quality data could be reliably gathered across time. In particular, knee joint torque is a strong proxy for SMC and correlation analysis with SCALE as most children with spastic CP can produce some amount of torque at the knee. It does not have the greatest distal impairment in spastic CP as does the ankle (Fowler, Staudt and Greenberg, 2010) and it has

previously been examined, for example, in a stationary cycling intervention for this population (Fowler *et al.*, 2010). Furthermore, we aimed to examine the efficacy of Camp Leg Power at improving these functional motor outcome measures. We hypothesized that each motor outcome measure for the participants with spastic CP would: (1) correlate with SCALE scores indicating those with greater SVMC have more functional ability at baseline and (2) exhibit post-intervention improvements and good long-term maintenance after LE SMC PT.

5.2 Methods

5.2.1 Participants

Twenty-three participants with spastic CP were recruited for this LE SMC intervention study. Inclusion criteria for all participants were the following: 1) between 5 and 18 years of age, 2) a diagnosis of spastic CP, 3) the ability to understand and follow verbal directions and 4) the ability to walk with or without assistive devices such a cane, walker or crutch.

Exclusion criteria for all participants were the presence of the following: 1) seizures not controlled by medication, 2) orthopedic surgery or neurosurgery within 1 year of starting the study, 3) BTX injection or casting within 3 months of starting the study, (4) severe medical problems restricting the ability to exercise and (5) participation is other PT more than 2 hours/week during the study period.

This study was conducted in an outpatient clinical research setting (Center for CP at UCLA/OIC and Ahmanson-Lovelace Brain Mapping Center). The institutional review board of

the University of California Los Angeles provided ethics approval. Informed assent and consent for research were obtained from the children and their parents or guardians.

5.2.2 Clinical Assessments

The CP group was evaluated by experienced physical therapists using standardized protocols. GMFM dimensions D (standing) and E (walking, running and jumping) were assessed (Russell *et al.*, 2004). The GMFM-66 Gross Motor Ability Estimator program was used to compute final scores. SCALE was used to assess SVMC (Fowler *et al.*, 2009). Specific isolated movement patterns at the hip, knee, ankle, subtalar and toe joints were evaluated bilaterally. SCALE scores for each limb ranged from 0 (absent SVMC) to 10 (normal SVMC) (Fowler *et al.*, 2009). Left and right limb scores were summed for a total SCALE score with a maximum value of 20.

5.2.3 Lower Extremity Selective Motor Control Intervention (Camp Leg Power)

The Camp Leg Power LE SMC intervention included practice of skilled, isolated LE joint movements, isokinetic knee exercises at variable speeds, ankle-controlled video gaming, gait and functional training and LE sensory enrichment using a summer camp format. Under the supervision of experienced physical therapists, each participant had 15 camp sessions for 3 hours/day over a 1-month period. Skilled, isolated movements of the hip, knee, ankle, subtalar and toe joints were practiced. Biomechanics data from Camp Leg Power were collected at pre, post and 6 months follow-up (FU).

Using a Biodex System 4 Pro dynamometer (Biodex Medical Systems, Shirley, NY), isokinetic KE and KF exercises were performed bilaterally for a minimum of 10 sessions. Each participant was trained at a range of speeds 0, 30, 60, 90, 120, 180, 240 and 300 deg/s depending on their initial ability to produce torque and progressed as able during each training session. The trunk recline was 15 deg relative to vertical with the torso, pelvis and thigh firmly secured to the chair using straps to maintain testing position. Corrections were made for limb weight-assisted torque due to gravity. At evaluation time points (pre, post and 6 months FU), three repetitions of KE and KF were performed at each testing speed with a 60 sec rest between each set. Ten repetitions were performed for each exercise and speed during the training sessions between pre and post time points. Isometric testing (0 deg/s) was performed with the knee positioned at 60 deg for extension and 45 deg for flexion. Isometric contractions were sustained for 5 sec per rep and 20 seconds between each rep. Speeds 0 and 30 deg/s were not trained and data for these speeds were collected only during evaluation time points. Testing was performed bilaterally for participants with bilateral CP and only the involved limb for participants with unilateral CP.

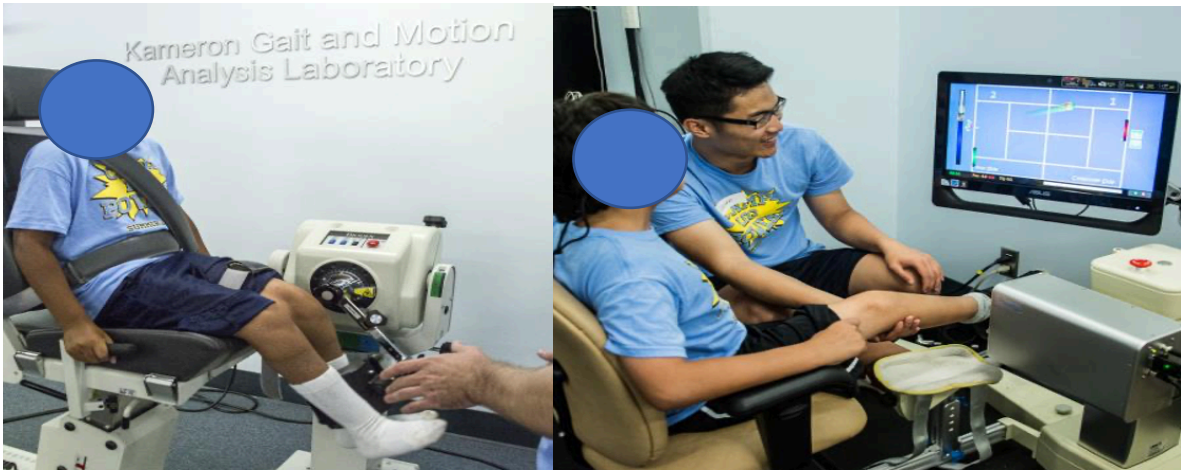

Figure 5-1: Camp Leg Power participants on the Biodex System 4 Pro dynamometer (Biodex Medical Systems, Shirley, NY) and robotic-gaming ankle device (Wu *et al.*, 2011).

Participants operated video games using ankle dorsiflexion and plantar flexion movements on a robotic device (Wu *et al.*, 2011) for at least 5 minutes per limb for a minimum of 10 sessions. Gait and functional training in activities that emphasized intra- and inter-limb control were practiced. These included kicking, navigating obstacles, stair climbing and treadmill/overground walking encouraging maximal step length. Barefoot sensory enrichment activities were performed such as walking on different surfaces.

5.2.4 Motor Outcome Measures

Motor outcome measures were collected at baseline (pre), immediately after Camp Leg Power (post) and 6-months FU. Motor outcome exams were administered and recorded by experienced physical therapists or a trained gait and motion analysis laboratory engineer for the 10mWRT, 6MWT, ankle robot dosing (reps/session), peak isokinetic KE and KF torque performed at various speeds, and step length and stride length during gait evaluation at preferred speeds.

5.2.5 Gait Analysis

An Eagle eight-camera system setup (Motion Analysis Corporation, Santa Rosa, CA) sampling at 60Hz was used to collect gait data. Participants wore 18 reflective markers using a modified Helen Hayes marker set and walked barefoot with handheld assistance for balance, if required, at their preferred, self-selected walking pace across a 25-foot path. Gait analysis data with typical equipment were collected if available and brought to the assessment by the participant. Spatial-temporal data (step and stride lengths) were calculated using Cortex and OrthoTrak

processing software (Motion Analysis Corporation, Santa Rosa, CA). All steps used for spatial-temporal averages were checked for consistency and aberrant trials were discarded. Step and stride length were normalized to body height (Beck *et al.*, 1981).

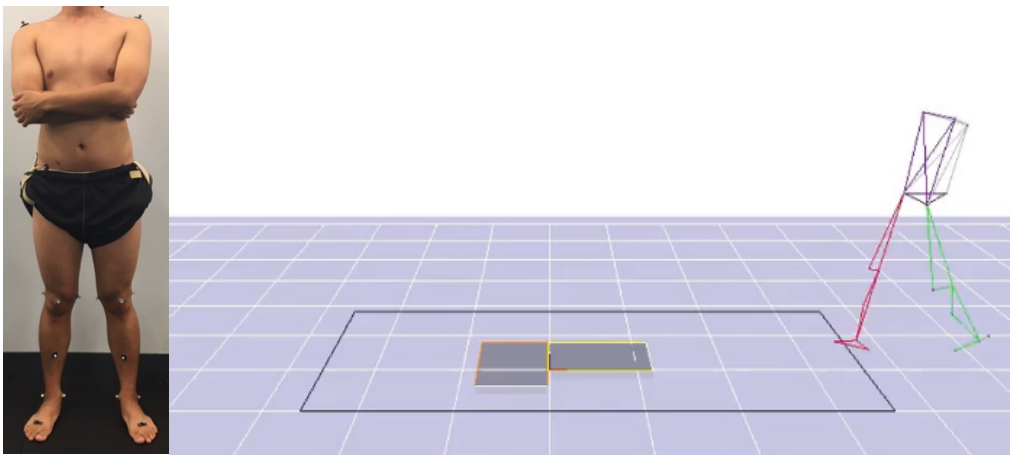

Figure 5-2: The modified Helen Hayes marker set (left) and 3-D rendering of the model walking along the laboratory pathway in Cortex (Motion Analysis Corporation, Santa Rosa, CA) used for gait analysis evaluation (right).

5.2.6 Statistical Analysis

Data were tested for normal distribution using the Shapiro-Wilk test (Shapiro and Wilk, 1965). Simple linear regressions were performed for all correlation analyses using Pearson correlation coefficients (JMP Pro 14, SAS Institute Inc., Cary, NC). Parametric paired t-tests were used for post-intervention and FU analyses of motor outcome measures. Otherwise nonparametric testing was used for data not normally distributed. Statistical significance was set at $p < 0.05$.

Isokinetic knee joint torque data were separated into high (SCALE score > 4) and low (SCALE score ≤ 4) groups for analysis. Post peak torque values were recorded from one of the

last 5 sessions of Camp Leg Power to examine each participant's maximum capacity to produce torque. Mean peak KE and KF torque values were compared across time points using a repeated measure analysis of variance model ($p < 0.05$). Normal quantile plots of the residual errors were examined in this analysis to verify that the residual errors had a normal distribution, justifying the use of a parametric model. Some torque observations below a threshold of detection were observed as "zero," meaning they were left censored if they fell below the unobserved threshold of detection. To adjust for this, the repeated measure model was expanded into a tobit repeated measure model (Tobin, 1958). Calculations were carried out using R 4.0.5.

5.3 Results

Twenty-three children with spastic CP (6 females, 17 males; mean age, 10.1 ± 2.8 years; age range, 5.3-16.6 years) participated in Camp Leg Power. Three children were diagnosed with unilateral CP and twenty children with bilateral CP. GMFCS levels were: I (n=5), II (n=4), III (n=12) and IV (n=2). Total SCALE scores ranged from 1 to 18.

	Spastic CP
N	23
Mean Age ± SD	10.1 ± 2.8 y
Age Range	5.6 - 16.6 y
CP Diagnosis	3 hemiplegia 20 diplegia
GMFCS Levels	I (n=5) II (n=4) III (n=12) IV (n=2)

Table 5-1: Demographics of all participants with spastic CP in Camp Leg Power.

5.3.1 Baseline Motor Outcome Correlations with SCALE

In the baseline correlation between 10mWRT time and total SCALE score, the data exhibited a negative relationship ($r = 0.40$ and $p = 0.06$). With the removal of the single outlier in the 10mWRT data, the negative correlation was significant with $r = 0.62$ and $p = 0.003$. A significant positive correlation was found between 6MWT distance and total SCALE score with $r = 0.66$ and $p = 0.02$. Total SCALE score correlated significantly and positively with GMFM with $r = 0.87$ and $p < 0.001$. Ankle plantar and dorsiflexion reps/session for each limb on the ankle robot gaming device had significant positive correlations with ipsilateral SCALE scores bilaterally ($r = 0.68$ with $p = 0.01$ and $r = 0.69$ with $p = 0.01$ for the left and right ankle, respectively).

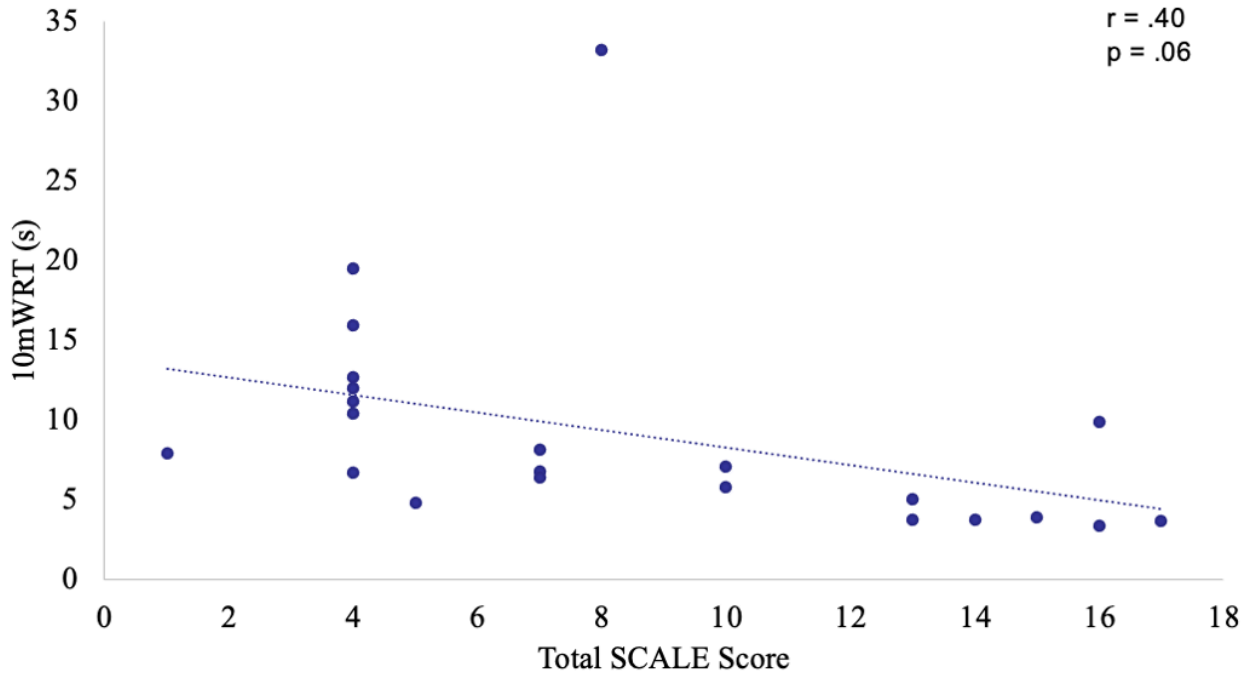

Figure 5-3: Baseline correlation between 10mWRT times and total SCALE score (n = 22).

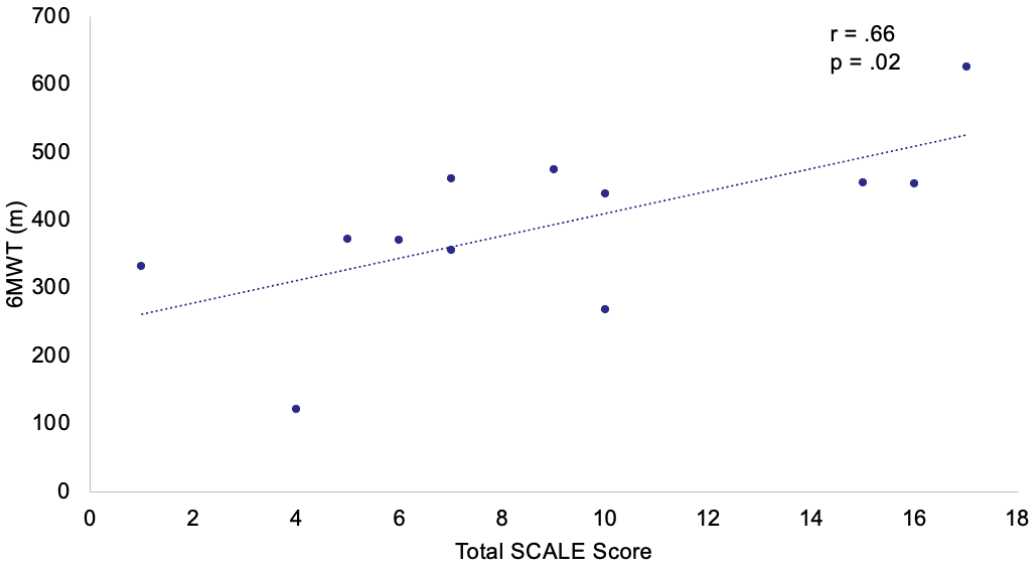

Figure 5-4: Baseline correlation between 6MWT distances and total SCALE score (n = 12).

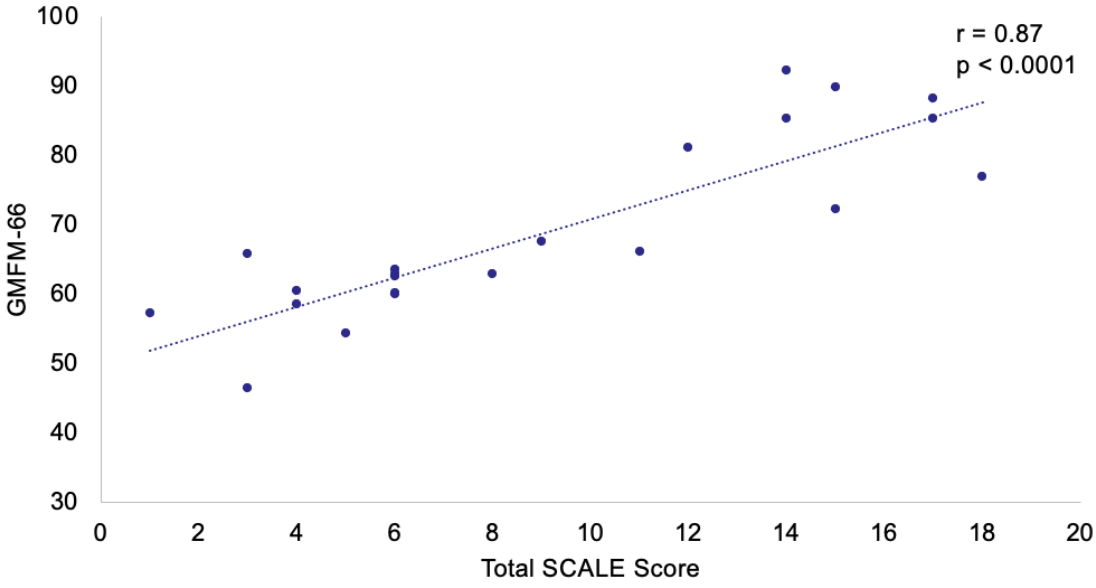

Figure 5-5: Baseline correlation between GMFM and total SCALE score (n = 22).

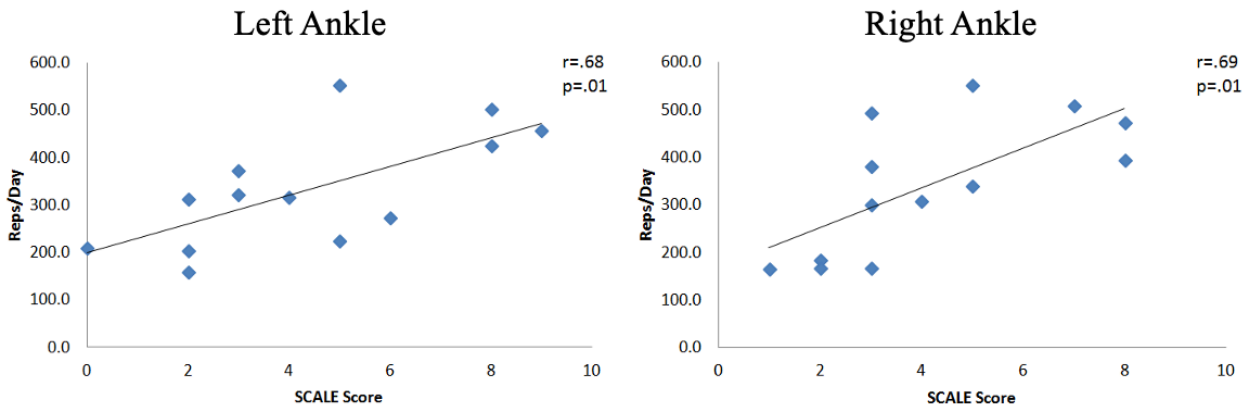

Figure 5-6: Baseline correlations between ankle plantar and dorsiflexion reps/session for each limb on the ankle robot gaming device versus ipsilateral SCALE score.

Left and right KE and KF peak torque values correlated significantly and positively with ipsilateral SCALE scores across a range of speeds as displayed in Figures 5-7 and 5-8. Joints with zero torque were not included in these regression analyses. A greater number of participants had torque values equal to zero as speeds increased for KE and KF. More participants in the high SCALE score group could produce torque at high speeds than the low SCALE score group.

(A)

KE Torque	Total # of T = 0	High n T = 0/8	Low n T = 0/13	r	p
0	0	0	0	.70	.0004
30	0	0	0	.61	.003
60	0	0	0	.59	.005
90	1	0	1	.64	.002
120	2	0	2	.56	.01
180	4	1	3	.74	.0007
240	8	1	7	.77	.002
300	10	1	9	.68	.02

(B)

KE Torque	# of T = 0	High n T = 0/9	Low n T = 0/13	r	p
0	0	0	0	.75	<.0001
30	0	0	0	.59	.004
60	0	0	0	.63	.002
90	1	0	1	.63	.002
120	3	1	2	.61	.006
180	4	1	3	.57	.01
240	7	1	6	.22	.42
300	12	2	10	.59	.07

Figure 5-7: (A) Left (n = 21) and (B) right (n = 22) KE torque correlations versus ipsilateral SCALE score across speeds.

(A)

KF Torque	# of T = 0	High n T = 0/8	Low n T = 0/13	R	p
0	1	0	1	.82	<.0001
30	6	0	6	.62	.01
60	5	0	5	.83	<.0001
90	6	0	6	.79	.0005
120	8	1	7	.75	.003
180	10	1	9	.63	.04
240	13	2	11	.53	.18
300	15	3	12	.46	.35

(B)

KF Torque	# of T = 0	High n T = 0/9	Low n T = 0/13	r	p
0	2	0	2	.83	<.0001
30	7	0	7	.67	.006
60	7	1	6	.79	.0005
90	4	0	4	.69	.001
120	8	1	7	.80	.0006
180	11	1	10	.53	.09
240	13	2	11	.45	.23
300	16	4	12	.35	.50

Figure 5-8: (A) Left (n = 21) and (B) right (n = 22) KF torque correlations versus ispilateral SCALE score across speeds.

Left and right normalized step lengths had significant positive correlations with ipsilateral SCALE scores with $r = 0.74$ and $p < 0.001$ for the left limb and $r = 0.68$ and $p < 0.001$ for the right (Figure 5-9). Normalized stride length had a significant positive correlation with total SCALE score as well with $r = 0.78$ and $p < 0.001$ (Figure 5-10).

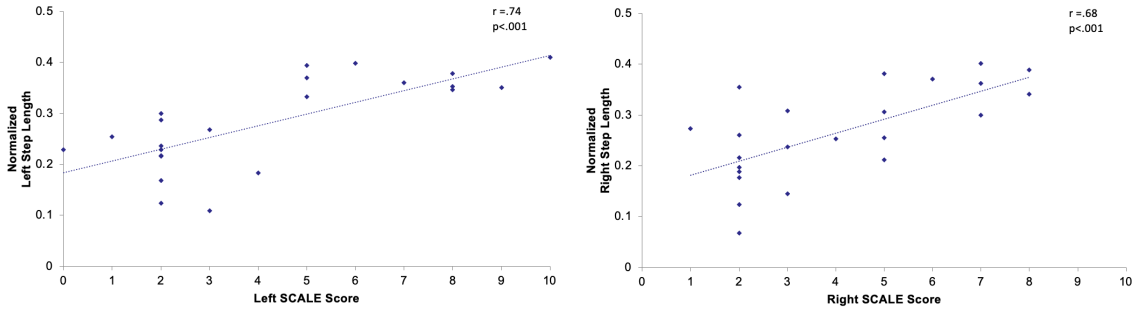

Figure 5-9: Left and right normalized step lengths versus ipsilateral SCALE score (n = 23).

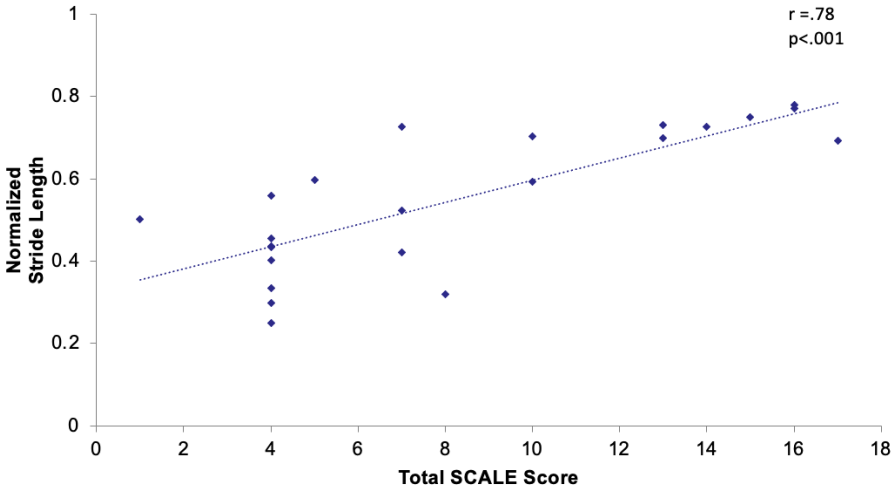

Figure 5-10: Normalized stride length versus total SCALE score (n = 23).

5.3.2 Post-Camp Leg Power Motor Outcome Changes

Following Camp Leg Power, 10mWRT times did not improve at post or FU time points (Figure 5-11). The 6MWT distances, however, increased significantly from pre to post ($p = 0.001$) and although the pre-FU change was not significant, the ability to walk longer distances was maintained as evidenced by the increased distance (Figure 5-12). GMFM improved significantly from pre-post and pre-FU (Figure 5-13).

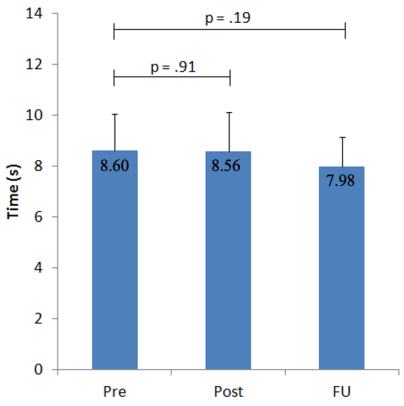

Figure 5-11: 10mWRT times at pre, post and FU (n = 21).

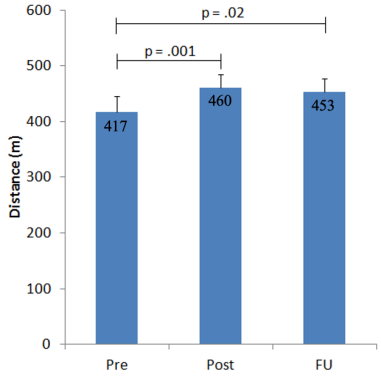

Figure 5-12: 6MWT distances at pre, post and FU (n = 11).

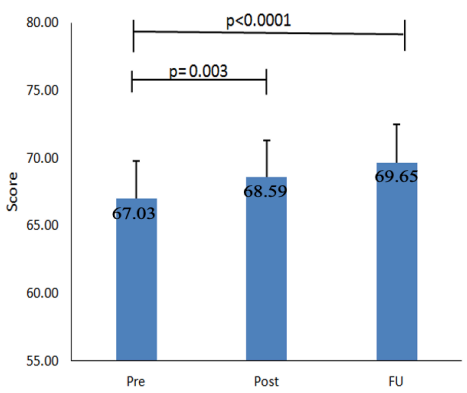

Figure 5-13: GMFM scores at pre, post and FU (n = 18).

Within high and low SCALE score groups, the percentages of participants able to generate any amount of knee joint torque were calculated across speeds (Figure 5-14). At higher speeds, less participants could produce torque in general with the low SCALE score group having more participants with torque equal to zero than the high SCALE score group. This disparity between high and low SCALE score groups was greater for KF torque than KE torque at higher speeds. Immediately after Camp Leg Power, both groups showed improved ability to produce torque across higher speeds (Figure 5-14).

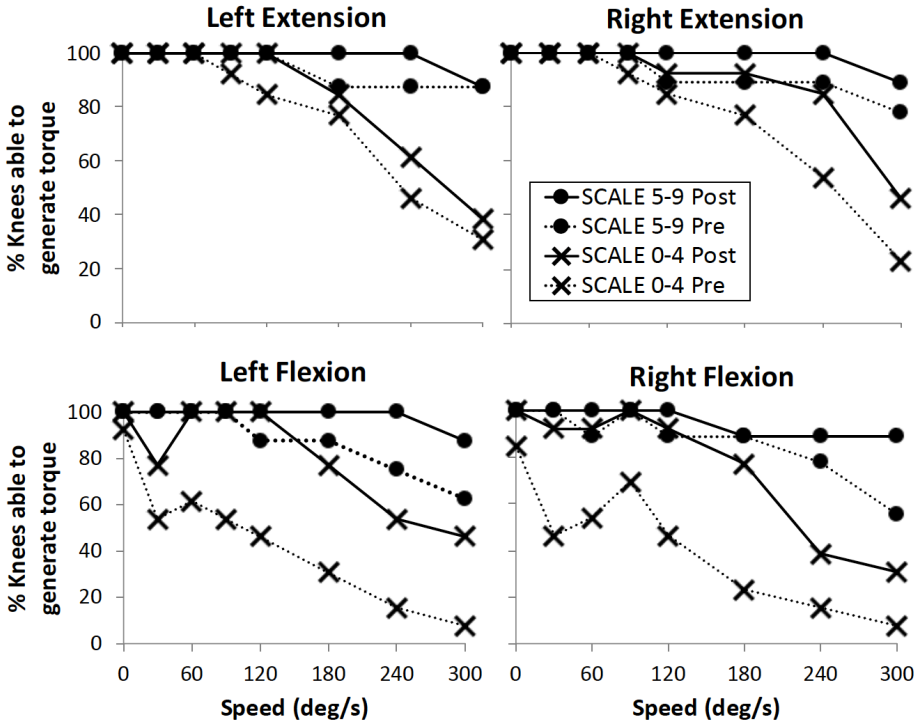

Figure 5-14: Percent knees able to generate KE and KF torque across speeds.

Left KE and KF mean peak torques and right KE and KF mean peak torques within high and low SCALE score groups compared across time points are shown in Figures 5-15 to 5-18. In general, torque generation became more difficult with increased speeds. Torque generation was much greater for the high SCALE score group than the low SCALE score group across all speeds. At almost all speeds, the high SCALE score group (red) showed significant pre-post improvements and considerable maintenance of improvement at FU for both peak KE and KF torque bilaterally. While the low SCALE score group (blue) improved from pre to post with some maintenance of improvement, they did so at a smaller range of speeds compared to the high SCALE score group. This disparity was even more evident when analyzing peak KF torque bilaterally.

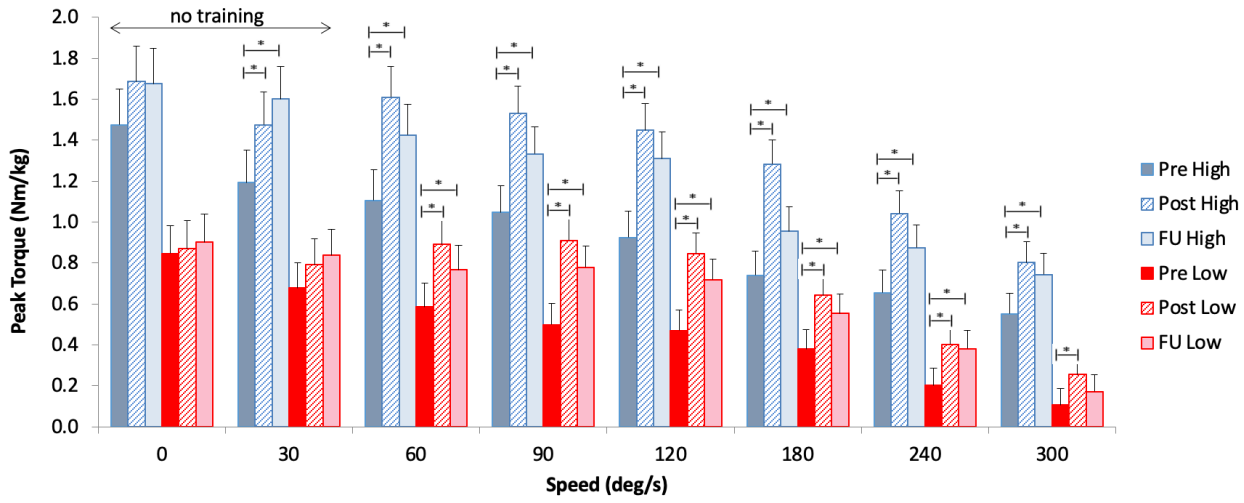

Figure 5-15: Left KE torque for high and low SCALE score groups across speeds at pre, post and FU (n = 22). *p < .05.

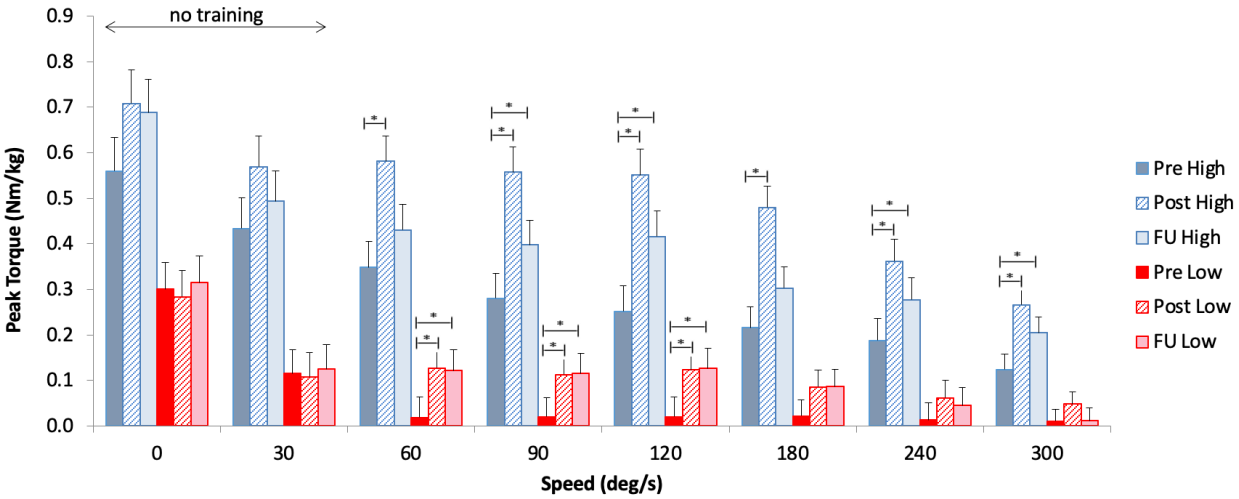

Figure 5-16: Left KF torque for high and low SCALE score groups across speeds at pre, post and FU (n = 22). *p < .05.

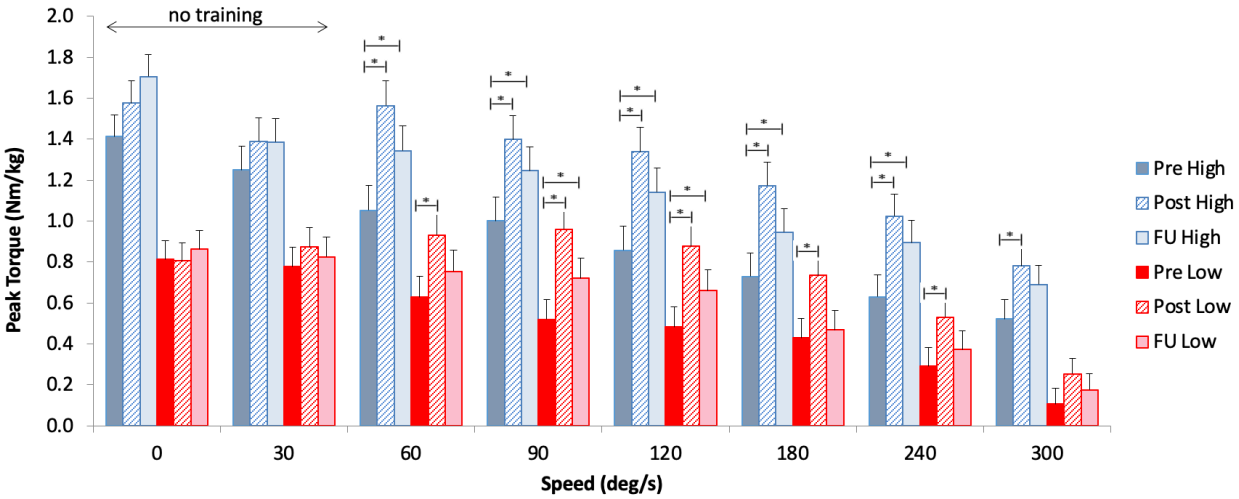

Figure 5-17: Right KE torque for high and low SCALE score groups across speeds at pre, post and FU (n = 21). *p < .05.

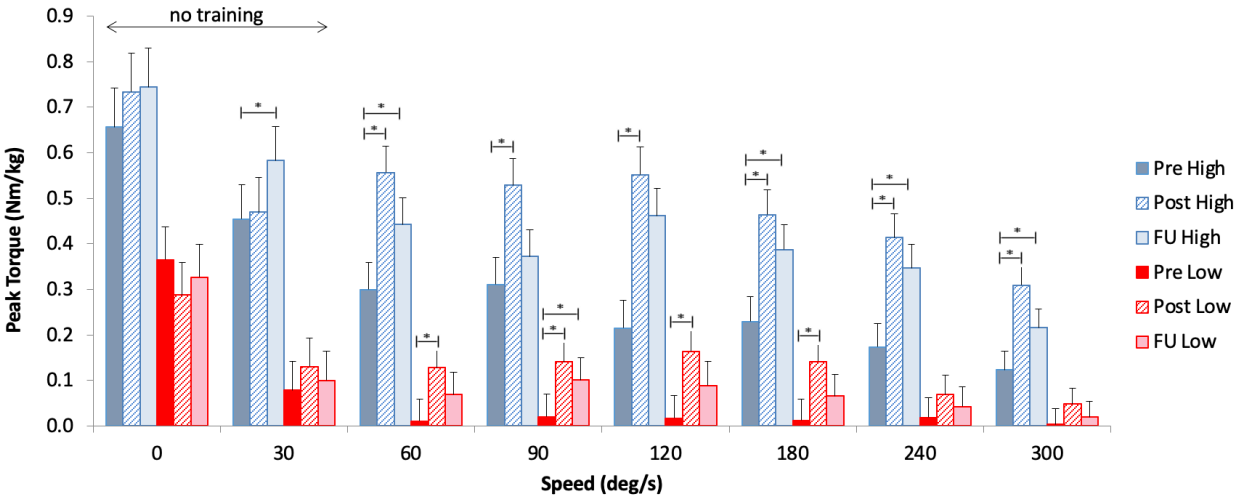

Figure 5-18: Right KF torque for high and low SCALE score groups across speeds at pre, post and FU (n = 21). *p < .05.

For participants whom we could collect gait data using their typical equipment across pre, post and FU time points (n = 12), mean normalized stride length values improved from 0.73 to 0.83 then 0.81, respectively (Figure 5-19). A significant change in normalized stride length was found from pre to post with p = 0.01. The increase in stride length was maintained at FU but the results were not significant.

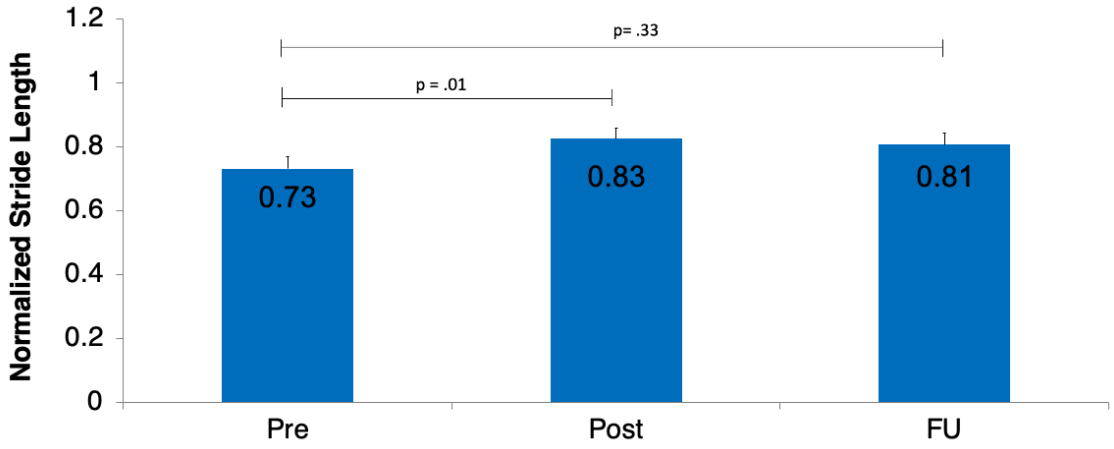

Figure 5-19: Normalized stride length for participants walking in their typical condition including assistive devices at pre, post and FU (n = 12).

5.4 Discussion

Camp Leg Power is a novel LE SMC intervention that improves upon several motor outcome measures typically evaluated in spastic CP. Physical therapy aimed at practicing LE SMC movements is an effective intervention method to improve KE and KF torque and stride length during gait. Both high and low SCALE score groups improved knee joint torque following intervention for multiple speeds. Children with greater SVMC showed improvement at more speeds and better maintenance of these measures suggesting those with higher SCALE scores are more likely to have a better response to a LE SMC intervention. Participants were also able to effectively increase their stride length at preferred walking speeds. These findings are significant because force production, movement speed and independent joint coordination are important features of SMC and optimal motor performance during walking.

Imbalances in strength were seen at the knee as peak KF torque values were lower than peak KE torque values across all speeds. This imbalance in CP antagonist muscles has been documented in a study using handheld dynamometry to measure isometric strength for several muscle groups relative to TD (Darras *et al.*, 2021). The study found that knee flexors had a greater strength deficit (53%) relative to controls compared to knee extensors (37%). A similar deficit pattern was found for the hip flexors (32%) and hip extensors (13%). Additionally, these findings verify the greater distal impairment of the knee relative to the hip in spastic CP (Fowler, Staudt and Greenberg, 2010).

Following Camp Leg Power, improvements in the 6MWT distances represent an increase in functional walking capacity/endurance (Fiss *et al.*, 2019) and improvements in GMFM scores indicate an increase in gross motor function (Russell *et al.*, 2004). While the 10mWRT times did not improve significantly after intervention, they still showed a decreasing trend where participants on average were able to decrease the amount of time they took to travel 10 meters. Significant findings may have been more difficult to find with this examination due to the shorter data collection times (relative to the 6MWT for example).

SCALE is a strong clinical correlate of various motor outcome measures in spastic CP. In the present study, SCALE scores correlated significantly with 6MWT times, GMFM scores, ankle plantar and dorsiflexion reps/session (ankle robot dosing), isometric and isokinetic KE and KF torque across a range of speeds, step length bilaterally and stride length. These findings suggest that SCALE is a strong predictor of baseline motor function prior to any intervention and verifies findings by several other studies. SCALE has been shown to correlate with strength using manual muscle testing (Balzer *et al.*, 2016), Fugl-Meyer (Balzer *et al.*, 2016), spasticity (Balzer *et al.*, 2016; Noble, Gough and Shortland, 2019) and muscle volume (Balzer *et al.*, 2016; Noble, Gough

and Shortland, 2019). SCALE scores have also been shown to correlate with GMFCS levels (Fowler *et al.*, 2009; Balzer *et al.*, 2016; Inoue and Yokoi, 2020), GMFM scores (Balzer *et al.*, 2016; Noble, Gough and Shortland, 2019; MacWilliams *et al.*, 2022), hip and knee joint coordination during the swing phase of gait (Fowler and Goldberg, 2009), knee joint acceleration during the swing phase of gait (Goldberg, Requejo and Fowler, 2011), gait profile score (Chruscikowski *et al.*, 2017), Edinburgh Visual Gait Score (Sardoğan *et al.*, 2021) and step length (Zhou *et al.*, 2019).

A limitation of this study was varying cohort sizes depending on the functional motor outcome measure. The reason for varying cohort sizes was due to outliers in the data sets, assessments not performed during certain years of Camp Leg Power, change of typical equipment used for gait throughout the intervention and one participant unable to return at FU. Additionally, three participants received the LE SMC intervention two years in a row, however, the data analyzed were from participation in their first year of Camp Leg Power.

In summary, intensive practice of skilled LE SMC movements by children with spastic CP born premature was associated with overall improved motor function. Children with greater SVMC showed more pre-post improvement and better long-term maintenance. Additionally, SCALE is a strong predictor of a plethora of functional motor outcome measures. A longer intervention duration at earlier ages may optimize motor function improvements.

Chapter 6: Post-Camp Leg Power Correlation Analyses Among Selective Motor Control, Brain Imaging and Biomechanics

6.1 The Relationship Between Selective Motor Control and Brain Imaging

Previously in Chapter 3, it was shown that SCALE scores correlated significantly with baseline FA and RD in several major WM tracts including the CST and CC using TBSS and ROI analysis. These findings suggested that SCALE is a good clinical correlate of brain motor tract impairment in spastic CP. TBSS was also used to examine post-Camp Leg Power changes in RD and MD versus total SCALE scores in Chapter 4. The absence of significant findings in this voxel-by-voxel analysis could have occurred due to greater motor learning by those with lower SVMC as several Camp Leg Power activities were performed barefoot and, therefore, not with their usual equipment.

Additional analyses not mentioned in the previous chapters include post-intervention changes in RD and MD versus total SCALE scores using ROI analysis. The average change in RD and MD was first calculated for each participant with CP in all WM ROIs where significant reductions occurred using TBSS (Table 4-2). These outcomes were then correlated with total SCALE scores using Pearson correlation coefficients. In this ROI analysis relating SMC and post-intervention DTI outcomes, changes in RD and MD in the right PLIC were negatively correlated with total SCALE score (Figure 6-1). Additionally, changes in RD in the left fornix were negatively correlated with total SCALE score (Figure 6-2). These statistics, however, were not corrected for multiple comparisons as reported in previous chapters. The negative trends, nonetheless, suggest the potential of SCALE in predicting which participants may be more likely

to have improved myelination (those with greater SVMC) following Camp Leg Power. It is important to note that these trends were found in the PLIC, a WM motor region of the CST. With respects to the fornix, it may play an important role in cognition and episodic memory recall (Senova *et al.*, 2020). The relationship between SMC and changes in brain imaging warrants further examination among all intervention studies in spastic CP.

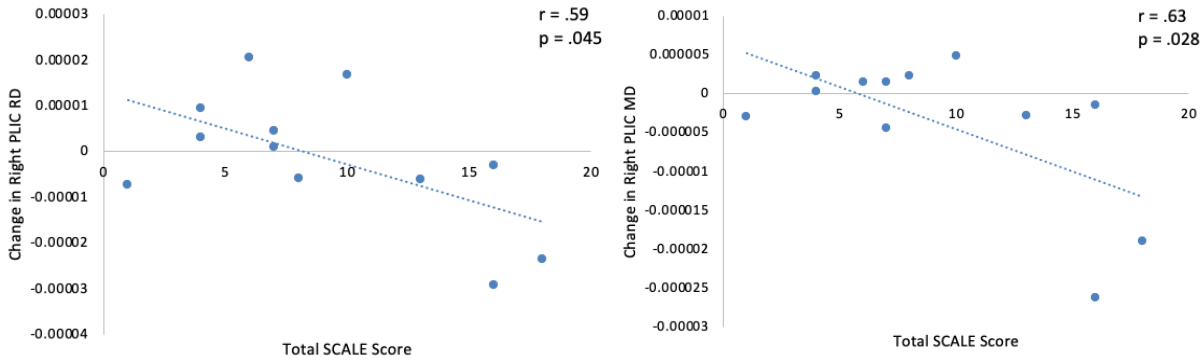

Figure 6-1: Right PLIC RD and MD changes versus total SCALE score.

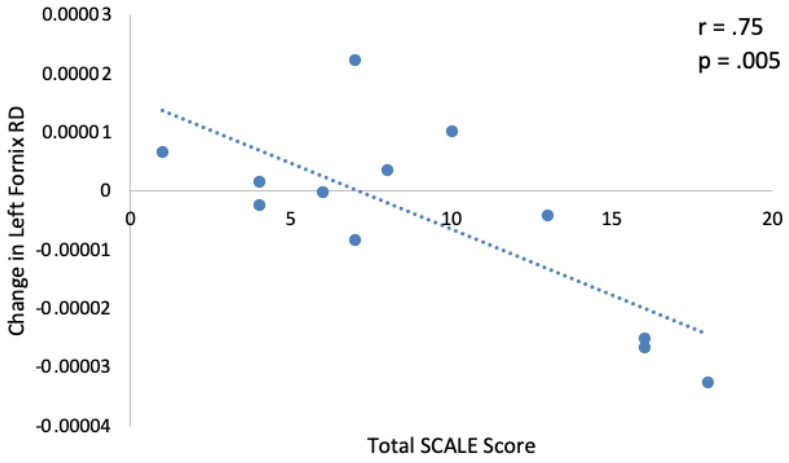

Figure 6-2: Left fornix RD changes versus total SCALE score.

6.2 The Relationship Between Selective Motor Control and Biomechanics

Previously in Chapter 5, it was shown that ipsilateral SCALE scores correlate with KE and KF torque generation across various speeds suggesting greater baseline knee joint torque generation for those with greater SVMC (Figures 5-7 and 5-8). Additional analyses performed sought to examine the relationship between ipsilateral SCALE scores and changes in KE and KF torque at 180 and 240 deg/s immediately following Camp Leg Power. These high speeds were selected because they were challenging speeds at which many participants learned how to produce torque after intervention (Figure 5-14). Pearson correlation coefficients were calculated and, while post-intervention KE torque changes did not correlate with SCALE, significant correlations were demonstrated between KF changes and ipsilateral SCALE scores (Figures 6-3 and 6-4). With the recommendation of a trained statistician, restricted cubic spline curves (as seen in red) were fit to the data to show that those with greater SCALE scores could produce more KF torque at 180 and 240 deg/s bilaterally post-intervention. These findings suggest SCALE is a good predictor of motor outcome measures following a LE SMC intervention. As KF is the more difficult task in CP (Darras *et al.*, 2021), it follows that those with greater SVMC were able to produce more KF torque after Camp Leg Power as they may have had greater motor learning ability and more initial capacity to improve. The restricted cubic spline curve may have overfit the data for the change in left KF torque at 240 deg/s versus SCALE score as a single outlier with low SCALE score of 0 made more improvement than expected.

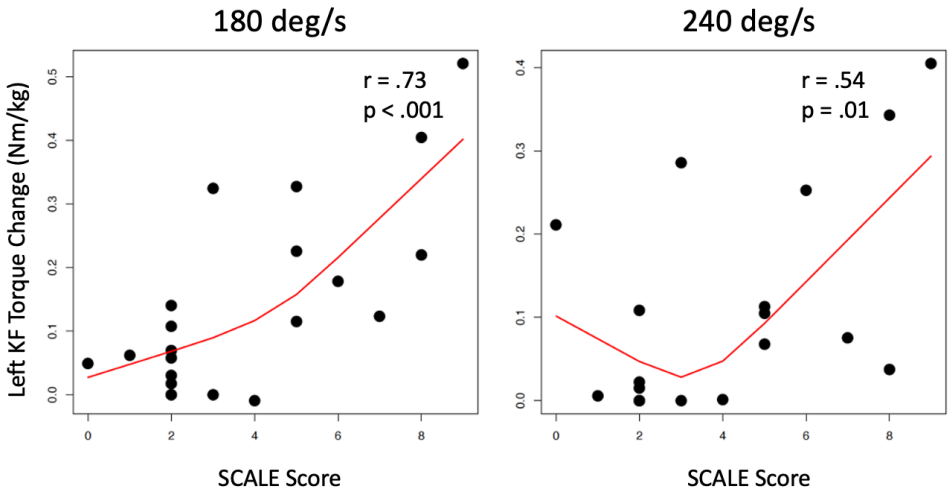

Figure 6-3: Left KF changes at 180 and 240 deg/s versus left SCALE score.

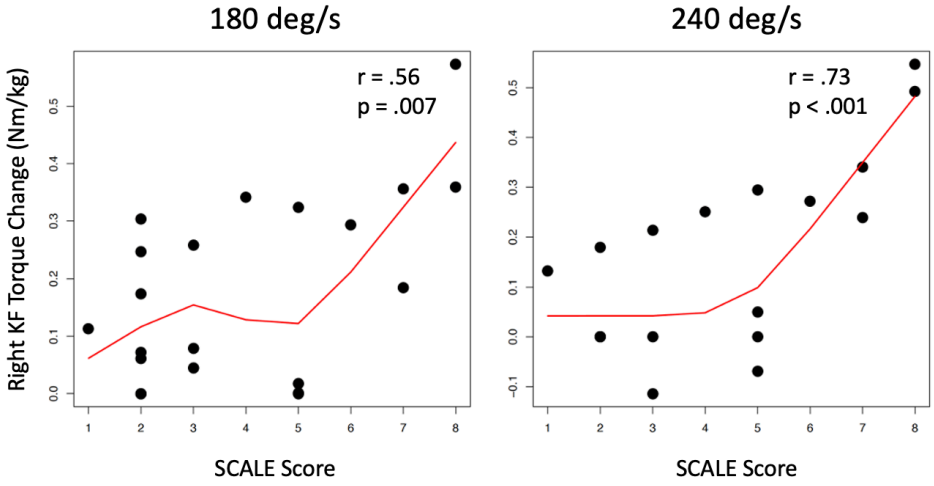

Figure 6-4: Right KF changes at 180 and 240 deg/s versus right SCALE score.

6.3 The Relationship Between Brain Imaging and Biomechanics

To my knowledge, few studies have related changes in DTI outcomes to changes in biomechanics measures. The significance of this analysis was to determine if there was a correlation between the brain DTI changes and changes in KE and KF torque after the novel LE

SMC intervention in spastic CP. TBSS was first used to analyze post-intervention changes in RD and MD versus changes in KE and KF torque at speeds 90 and 120 deg/s. Higher speeds of 90 and 120 deg/s were used for these correlation analyses because almost all participants were able to generate torque at these speeds at baseline (Figure 5-14). While improved myelination post-intervention undoubtedly coincided with increased peak knee joint torque generation following Camp Leg Power, this analysis sought to answer whether those participants who made the greatest changes in the brain also made the most knee biomechanics improvements. TBSS, however, did not show any significant findings between these measures on a voxel-by-voxel basis. We also examined whether: (1) baseline measures of RD and MD could predict KE and KF torque changes at 90 and 120 deg/s and (2) baseline measures of KE and KF torque at 90 and 120 deg/s could predict changes in RD and MD using TBSS. These analyses also did not produce any significant findings.

Lastly, to further examine the relationship between brain DTI changes and knee joint biomechanics changes after Camp Leg Power, ROI analyses were performed. Average change in RD and MD values within all ROIs with significant post-intervention reductions using TBSS were calculated for each participant with spastic bilateral CP. The change in left, right and average KE and KF torques at 90 and 120 deg/s were calculated for each participant as well. After performing correlation analyses using Pearson correlation coefficients, spurious results were found. While these statistics were not corrected for multiple comparisons as performed in previous chapters, the trends in the data suggest: (1) improved myelination in the CC genu was associated with increases in average KF torque at 120 deg/s (Figure 6-5), (2) increased overall diffusivity in the right ACR was associated with increases in right KF torque at 120 deg/s (Figure 6-6) and (3) increased overall diffusivity in the left SFOF was associated with increases in right KF torque at 120 deg/s (Figure

6-7). These mixed results suggest improved myelination of motor regions (CC genu) and increased overall diffusivity of nearby regions (right ACR and left SFOF) contributed to increases in KF torque at 120 deg/s post-Camp Leg Power. The implications of these results are not clear and the results warrant further analysis into the relationship between cerebral WM DTI changes and biomechanics changes after intervention.

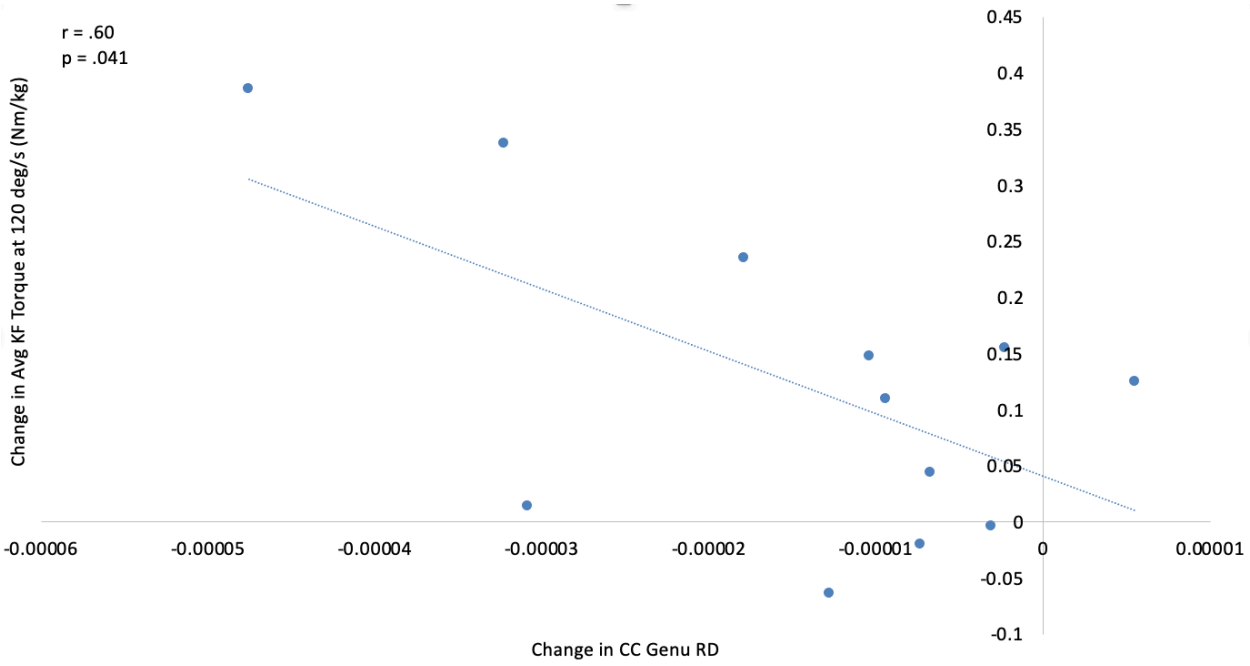

Figure 6-5: Change in average KF torque at 120 deg/s versus CC genu RD changes.

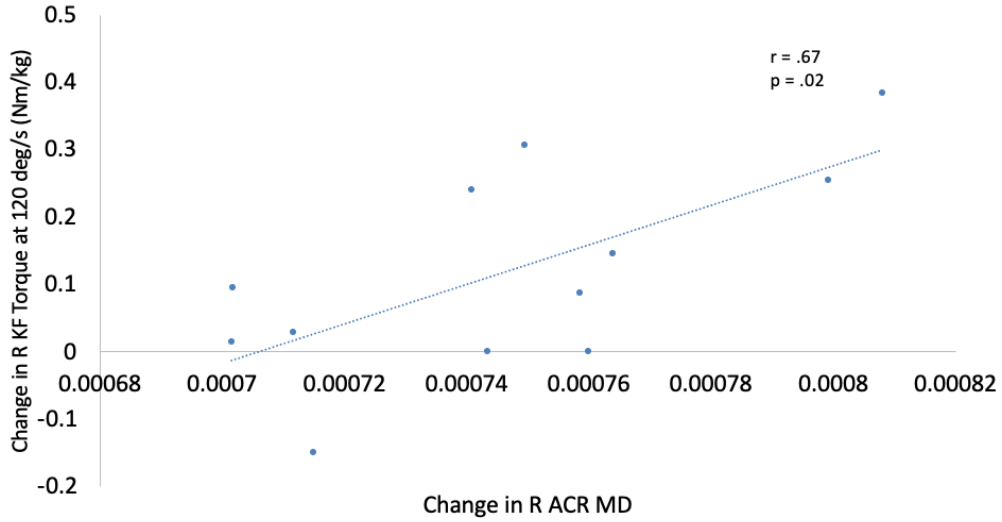

Figure 6-6: Change in right KF torque at 120 deg/s versus right ACR MD changes.

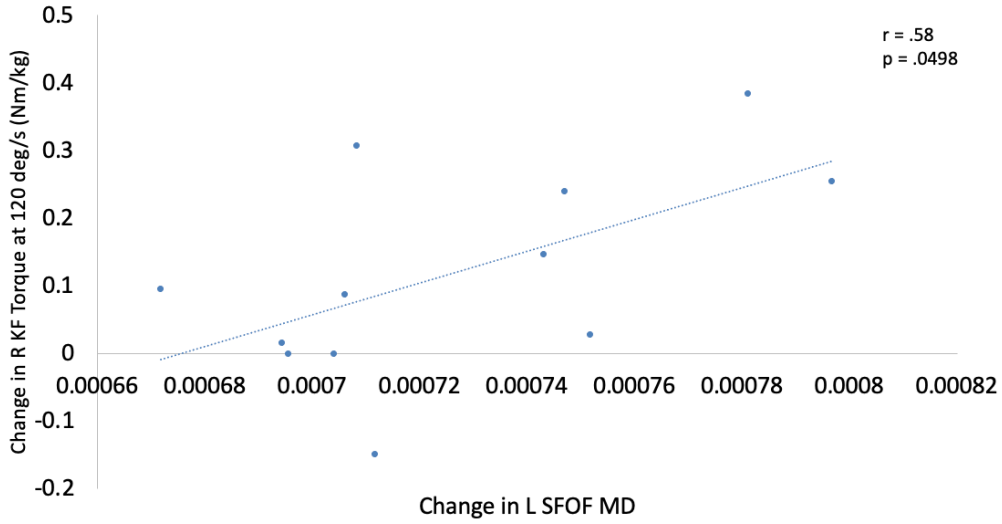

Figure 6-7: Change in right KF torque at 120 deg/s versus left SFOF MD changes.

Chapter 7: Summary and Future Directions

7.1 Summary

DWI and DTI are powerful MRI techniques to study WM differences, correlations and neuroplasticity in the brains of children with spastic bilateral CP and PVL. While the CST is known to be related to SMC function, an underlying impairment in CP, little is known about CST microstructural impairment, the relationship between CST impairment and clinical measures of motor function, and neuroplasticity in response to a novel intervention in spastic CP focused on intensive practice of LE SMC movements. As tract-specific visualization of the LE CSTs was difficult in this cohort, part of the work presented in this dissertation detailed WM differences between children with spastic bilateral CP and children with TD using TBSS, a whole brain voxel-by-voxel analysis. The children with spastic bilateral CP had wide-spread microstructural differences in WM motor regions including the CSTs and throughout the whole brain. This work established SCALE, a clinical measure of SVMC, as a strong correlate of brain WM motor impairment and several baseline motor function outcome measures. Furthermore, it introduced Camp Leg Power, a task-oriented, intensive exercise intervention targeting SMC improvement. The results showed that children with spastic CP and varied motor ability improved their motor function in response to the intervention coinciding with evidence of improved myelination in several WM tracts including motor regions of the brain. SCALE was a good prognostic factor in determining post-intervention motor outcomes, specifically knee joint biomechanics measures. This work contributes to the overall understanding of neuroimaging, clinical correlates of impaired WM and motor function, neuroplasticity and motor function changes in response to a novel intervention in spastic CP.

7.2 Future Directions

Future work following the results from this dissertation can take several directions. Tractography analysis (used in Chapter 2) can be expanded to examine other motor and non-motor WM tracts implicated in spastic CP as brain-wide differences relative to TD were found (as seen in TBSS results from Chapter 3). Ultimately, whole brain tractography can eventually be examined and tract-specific delineation methods can allow for regional vulnerability analysis of every major WM tract showing impairment in spastic CP. SCALE correlations with DTI measures (as seen in Chapter 3) can be compared to other clinical motor outcome measures beyond gross motor function. Additionally, other brain imaging measures such as grey matter volume and cortical thickness can be examined for this cohort relative to TD. A randomized controlled trial can be implemented to further validate the neuroplasticity findings in response to Camp Leg Power (Chapter 4). A group of children with spastic bilateral CP and PVL and a group of children with TD who do not receive the intervention can be recruited as control groups receiving DWI scans and motor function outcome evaluations at the same time points. The inclusion of these groups can strengthen the motor outcome findings following Camp Leg Power reported in Chapter 5 as well. In addition, the intervention can be adapted for younger children with spastic CP and for a longer period of time. With increased length of intervention, more WM DTI changes including FA and AD may be found. The relationships between SMC, brain imaging and biomechanics in spastic CP (reported in Chapter 6) can be further explored. KE and KF torque changes across all speeds can be examined in the correlation analyses performed in Chapter 6. Future work can also look at change in DTI outcomes versus the change in other motor function outcome measures reported including the 10mWRT times, 6MWT distances, GMFM scores, step lengths and stride lengths.

Bibliography

1. Aicardi, J. and Bax, M. (1992) 'Diseases of the nervous system in childhood', in *Clinics in Developmental Medicine*. London: Mac Keith Press, pp. IX–XVII.
2. Alexander, A. L. *et al.* (2007) 'Diffusion tensor imaging of the brain', *Neurotherapeutics: The Journal of the American Society for Experimental NeuroTherapeutics*, 4(3), pp. 316–329. doi: 10.1016/J.NURT.2007.05.011.
3. Arrigoni, F. *et al.* (2016) 'Whole-brain DTI assessment of white matter damage in children with bilateral cerebral palsy: Evidence of involvement beyond the primary target of the anoxic insult', *American Journal of Neuroradiology*, 37(7), pp. 1347–1353. doi: 10.3174/ajnr.A4717.
4. Assaf, Y. and Pasternak, O. (2008) 'Diffusion Tensor Imaging (DTI)-based White Matter Mapping in Brain Research: A Review', *Journal of Molecular Neuroscience*, 34(1), pp. 51–61. doi: 10.1007/s12031-007-0029-0.
5. Balzer, J. *et al.* (2016) 'Construct validity and reliability of the Selective Control Assessment of the Lower Extremity in children with cerebral palsy', *Developmental Medicine & Child Neurology*. John Wiley & Sons, Ltd, 58(2), pp. 167–172. doi: 10.1111/DMCN.12805.
6. Baraban, M., Mensch, S. and Lyons, D. A. (2016) 'Adaptive myelination from fish to man', *Brain Research*, 1641(Pt A), pp. 149–161. doi: 10.1016/j.brainres.2015.10.026.
7. Bass, N. (1999) 'Cerebral palsy and neurodegenerative disease', *Current Opinion in Pediatrics*, 11(6), pp. 504–507.
8. Basser, P. J. and Jones, D. K. (2002) 'Diffusion-tensor MRI: theory, experimental design and data analysis - a technical review', *NMR in Biomedicine*, 15(7–8), pp. 456–467. doi: 10.1002/nbm.783.

9. Bax, M. *et al.* (2005) ‘Proposed definition and classification of cerebral palsy’, *Developmental Medicine & Child Neurology*, 47(8), pp. 571–576.
10. Bax, M., Tydeman, C. and Flodmark, O. (2006) ‘Clinical and MRI Correlates of Cerebral Palsy - The European Cerebral Palsy Study’, *Journal of the American Medical Association*, 296(13), pp. 1602–1608. doi: 10.1001/jama.296.13.1602.
11. Beaulé, V., Tremblay, S. and Théoret, H. (2012) ‘Interhemispheric control of unilateral movement’, *Neural Plasticity*, 2012. doi: 10.1155/2012/627816.
12. Beck, R. J. *et al.* (1981) ‘Changes in the gait patterns of growing children’, *Journal of Bone and Joint Surgery*, 63(9), pp. 1452–1457. Available at: https://pubmed.ncbi.nlm.nih.gov/7320036/ (Accessed: 13 November 2022).
13. Benjamini, Y. and Hochberg, Y. (1995) ‘Controlling the False Discovery Rate: A Practical and Powerful Approach to Multiple Testing’, *Journal of the Royal Statistical Society: Series B (Methodological)*. John Wiley & Sons, Ltd, 57(1), pp. 289–300. doi: 10.1111/J.2517-6161.1995.TB02031.X.
14. Billiards, S. S. *et al.* (2008) ‘Myelin Abnormalities without Oligodendrocyte Loss in Periventricular Leukomalacia’, *Brain Pathology*, 18(2), pp. 153–163. doi: 10.1111/j.1750-3639.2007.00107.x.
15. Bloom, M. S., Orthmann-Murphy, J. and Grinspan, J. B. (2022) ‘Motor Learning and Physical Exercise in Adaptive Myelination and Remyelination’, *American Society for Neurochemistry*, 14. doi: 10.1177/17590914221097510.
16. Blumenfeld-Katzir, T. *et al.* (2011) ‘Diffusion MRI of Structural Brain Plasticity Induced by a Learning and Memory Task’, *PLoS ONE*, 6(6). doi: 10.1371/JOURNAL.PONE.0020678.
17. Bonnier, B., Eliasson, A.-C. and Krumlinde-Sundholm, L. (2006) ‘Effects of constraint-

induced movement therapy in adolescents with hemiplegic cerebral palsy: a day camp model', *Scandinavian Journal of Occupational Therapy*. Scand J Occup Ther, 13(1), pp. 13–22. doi: 10.1080/11038120510031833.

18. Ceschin, R. *et al.* (2015) 'Regional vulnerability of longitudinal cortical association connectivity: Associated with structural network topology alterations in preterm children with cerebral palsy', *NeuroImage: Clinical*, 9, pp. 322–337. doi: 10.1016/j.nicl.2015.08.021.
19. Chang, M. C. *et al.* (2012) 'Diffusion tensor imaging demonstrated radiologic differences between diplegic and quadriplegic cerebral palsy', *Neuroscience Letters*. Neurosci Lett, 512(1), pp. 53–58. doi: 10.1016/J.NEULET.2012.01.065.
20. Chaturvedi, S. K. *et al.* (2013) 'Comparative assessment of therapeutic response to physiotherapy with or without botulinum toxin injection using diffusion tensor tractography and clinical scores in term diplegic cerebral palsy children', *Brain & Development*, 35(7), pp. 647–653. doi: 10.1016/J.BRAINDEV.2012.10.012.
21. Chayer, C. and Freedman, M. (2001) 'Frontal Lobe Functions', *Current Neurology and Neuroscience Reports*, 1(6), pp. 547–552.
22. Cho, H. K. *et al.* (2013) 'Diffusion Tensor Imaging–Demonstrated Differences Between Hemiplegic and Diplegic Cerebral Palsy with Symmetric Periventricular Leukomalacia', *American Journal of Neuroradiology*. American Journal of Neuroradiology, 34(3), pp. 650–654. doi: 10.3174/AJNR.A3272.
23. Chruscikowski, E. *et al.* (2017) 'Selective motor control correlates with gait abnormality in children with cerebral palsy', *Gait & Posture*. Elsevier, 52, pp. 107–109. doi: 10.1016/J.GAITPOST.2016.11.031.
24. Corrigan, N. M. *et al.* (2021) 'Myelin development in cerebral gray and white matter during

adolescence and late childhood', *NeuroImage*, 227. doi: 10.1016/J.NEUROIMAGE.2020.117678.

25. Counsell, S. J. *et al.* (2006) 'Axial and radial diffusivity in preterm infants who have diffuse white matter changes on magnetic resonance imaging at term-equivalent age', *Pediatrics*, 117(2), pp. 376–86. doi: 10.1542/peds.2005-0820.
26. Darras, N. *et al.* (2021) 'Development of Lower Extremity Strength in Ambulatory Children With Bilateral Spastic Cerebral Palsy in Comparison With Typically Developing Controls Using Absolute and Normalized to Body Weight Force Values', *Frontiers in Neurology*. Front Neurol, 12. doi: 10.3389/FNEUR.2021.617971.
27. Englander, Z. A. *et al.* (2013) 'Diffuse reduction of white matter connectivity in cerebral palsy with specific vulnerability of long range fiber tracts', *NeuroImage: Clinical*. Neuroimage Clin, 2, pp. 440–447. doi: 10.1016/J.NICL.2013.03.006.
28. Englander, Z. A. *et al.* (2015) 'Brain structural connectivity increases concurrent with functional improvement: Evidence from diffusion tensor MRI in children with cerebral palsy during therapy', *NeuroImage: Clinical*, 7, pp. 315–324. doi: 10.1016/j.nicl.2015.01.002.
29. Evarts, E. V. (1968) 'Relation of pyramidal tract activity to force exerted during voluntary movement', *Journal of Neurophysiology*, 31(1), pp. 14–27. doi: 10.1152/JN.1968.31.1.14.
30. de Faria Jr., O. *et al.* (2019) 'Activity-dependent central nervous system myelination throughout life', *Journal of Neurochemistry*, 148(4), pp. 447–461. doi: 10.1111/jnc.14592.
31. Fetters, L. *et al.* (2004) 'Kicking coordination captures differences between full-term and premature infants with white matter disorder', *Human Movement Science*, 22(6), pp. 729–748. doi: 10.1016/j.humov.2004.02.001.
32. Fiss, A. L. *et al.* (2019) 'Validity of the Early Activity Scale for Endurance and the 6-Minute

Walk Test for Children With Cerebral Palsy', *Pediatric Physical Therapy*. Pediatr Phys Ther, 31(2), pp. 156–163. doi: 10.1097/PEP.0000000000000577.

33. Fowler, E. G. *et al.* (2009) 'Selective Control Assessment of the Lower Extremity (SCALE): development, validation, and interrater reliability of a clinical tool for patients with cerebral palsy', *Developmental Medicine & Child Neurology*, 51(8), pp. 607–614. doi: 10.1111/j.1469-8749.2008.03186.x.
34. Fowler, E. G. *et al.* (2010) 'Pediatric Endurance and Limb Strengthening (PEDALS) for Children With Cerebral Palsy Using Stationary Cycling: A Randomized Controlled Trial', *Physical Therapy*, 90(3), pp. 367–81. doi: 10.2522/ptj.20080364.
35. Fowler, E. G. and Goldberg, E. J. (2009) 'The effect of lower extremity selective voluntary motor control on interjoint coordination during gait in children with spastic diplegic cerebral palsy', *Gait & Posture*, 29(1), pp. 102–107. doi: 10.1016/j.gaitpost.2008.07.007.
36. Fowler, E. G., Staudt, L. A. and Greenberg, M. B. (2010) 'Lower-extremity selective voluntary motor control in patients with spastic cerebral palsy: increased distal motor impairment', *Developmental Medicine & Child Neurology*, 52(3), pp. 264–269. doi: 10.1111/J.1469-8749.2009.03586.X.
37. Freund, H. J. (2003) 'Somatosensory and motor disturbances in patients with parietal lobe lesions', *Advances in Neurology*, 93, pp. 179–193. Available at: https://europepmc.org/article/med/12894408 (Accessed: 7 October 2022).
38. Glenn, D. A. *et al.* (2007) 'Diffusion tensor MR imaging tractography of the pyramidal tracts correlates with clinical motor function in children with congenital hemiparesis', *American Journal of Neuroradiology*. AJNR Am J Neuroradiol, 28(9), pp. 1796–1802. doi: 10.3174/AJNR.A0676.

39. Goldberg, E. J., Fowler, E. G. and Oppenheim, W. L. (2012) 'Case Reports: The Influence of Selective Voluntary Motor Control on Gait After Hamstring Lengthening Surgery', *Clinical Orthopaedics and Related Research*, 470(5), pp. 1320–1326. doi: 10.1007/s11999-011-2028-2.
40. Goldberg, E. J., Requejo, P. S. and Fowler, E. G. (2011) 'Joint moment contributions to swing knee extension acceleration during gait in individuals with spastic diplegic cerebral palsy', *Gait & Posture*, 33(1), pp. 66–70. doi: 10.1016/j.gaitpost.2010.09.026.
41. Hodge, J. *et al.* (2017) 'Segmental Diffusion Properties of the Corticospinal Tract and Motor Outcome in Hemiparetic Children with Perinatal Stroke', *Journal of Child Neurology*, 32(6), pp. 550–559. doi: 10.1177/0883073817696815.
42. Hoon, A. H. *et al.* (2009) 'Sensory and motor deficits in children with cerebral palsy born preterm correlate with diffusion tensor imaging abnormalities in thalamocortical pathways', *Developmental Medicine & Child Neurology*, 51(9), pp. 697–704. doi: 10.1111/j.1469-8749.2009.03306.x.
43. Huisman, T. A. G. M. (2010) 'Diffusion-weighted and diffusion tensor imaging of the brain, made easy', *Cancer Imaging*. Cancer Imaging, 10 Spec no(1A), pp. S163-171. doi: 10.1102/1470-7330.2010.9023.
44. Inoue, T. and Yokoi, Y. (2020) 'Characteristics of selective motor control of the lower extremity in adults with bilateral spastic cerebral palsy', *Journal of Physical Therapy Science*. J Phys Ther Sci, 32(5), pp. 348–351. doi: 10.1589/JPTS.32.348.
45. Jain, K. K. *et al.* (2014) 'Cerebral Blood Flow and DTI metrics changes in children with cerebral palsy following therapy', *Journal of Pediatric Neuroradiology*, 3(2), pp. 63–73. doi: 10.3233/PNR-14088.

46. Jiang, H. *et al.* (2019) 'Early diagnosis of spastic cerebral palsy in infants with periventricular white matter injury using diffusion tensor imaging', *American Journal of Neuroradiology*, 40(1), pp. 162–168. doi: 10.3174/ajnr.A5914.
47. Jiang, H. *et al.* (2021) 'Structural network performance for early diagnosis of spastic cerebral palsy in periventricular white matter injury.', *Brain Imaging and Behavior*. Springer, 15(2), pp. 855–864. doi: 10.1007/S11682-020-00295-6.
48. Karababa, F. *et al.* (2015) 'Microstructural Changes of Anterior Corona Radiata in Bipolar Depression', *Psychiatry Investigation*, 12(3), pp. 367–371. doi: 10.4306/PI.2015.12.3.367.
49. Karlsgodt, K. H. *et al.* (2012) 'Alterations in white matter microstructure in neurofibromatosis-1', *PLoS ONE*. PLoS One, 7(10). doi: 10.1371/JOURNAL.PONE.0047854.
50. Kennedy, P. R. (1990) 'Corticospinal, rubrospinal and rubro-olivary projections: a unifying hypothesis', *Trends in Neurosciences*, 13(12), pp. 474–479.
51. Kim, J. H., Kwon, Y. M. and Son, S. M. (2015) 'Motor function outcomes of pediatric patients with hemiplegic cerebral palsy after rehabilitation treatment: a diffusion tensor imaging study', *Neural Regeneration Research*, 10(4), pp. 624–630. doi: 10.4103/1673-5374.155438.
52. Kinney, H. C. (2005) 'Human myelination and perinatal white matter disorders', *Journal of the Neurological Sciences*, 228(2), pp. 190–192. doi: 10.1016/J.JNS.2004.10.006.
53. Koerte, I. *et al.* (2011) 'Anisotropy of transcallosal motor fibres indicates functional impairment in children with periventricular leukomalacia', *Developmental Medicine & Child Neurology*, 53(2), pp. 179–186. doi: 10.1111/j.1469-8749.2010.03840.x.
54. Kwon, J. Y. *et al.* (2014) 'Changes in diffusion tensor tractographic findings associated with

constraint-induced movement therapy in young children with cerebral palsy', *Clinical Neurophysiology*, 125(12), pp. 2397–2403. doi: 10.1016/J.CLINPH.2014.02.025.

55. Lakhani, B. *et al.* (2016) 'Motor Skill Acquisition Promotes Human Brain Myelin Plasticity', *Neural Plasticity*. doi: 10.1155/2016/7526135.
56. Lazari, A. and Lipp, I. (2021) 'Can MRI measure myelin? Systematic review, qualitative assessment, and meta-analysis of studies validating microstructural imaging with myelin histology', *NeuroImage*, 230. doi: 10.1016/J.NEUROIMAGE.2021.117744.
57. Lee, J. D. *et al.* (2011) 'Motor pathway injury in patients with periventricular leucomalacia and spastic diplegia', *Brain*, 134(Pt 4), pp. 1199–1210. doi: 10.1093/brain/awr021.
58. Li, Y. *et al.* (2016) 'Changes of Brain Connectivity in the Primary Motor Cortex After Subcortical Stroke: A Multimodal Magnetic Resonance Imaging Study', *Medicine*, 95(6). doi: 10.1097/MD.0000000000002579.
59. Liu, J. *et al.* (2015) 'Enhanced Interhemispheric Functional Connectivity Compensates for Anatomical Connection Damages in Subcortical Stroke', *Stroke*, 46(4), pp. 1045–1051. doi: 10.1161/STROKEAHA.114.007044/-/DC1.
60. MacWilliams, B. A. *et al.* (2022) 'Causal factors affecting gross motor function in children diagnosed with cerebral palsy', *PLoS ONE*. Edited by Y. Lee, 17(7). doi: 10.1371/JOURNAL.PONE.0270121.
61. Mailleux, L. *et al.* (2020) 'The relationship between neuroimaging and motor outcome in children with cerebral palsy: A systematic review—Part B diffusion imaging and tractography', *Research in Developmental Disabilities*, 97. doi: 10.1016/j.ridd.2019.103569.
62. Mayston, M. J., Harrison, L. M. and Stephens, J. A. (1999) 'A Neurophysiological Study of Mirror Movements in Adults and Children', *Annals of Neurology*, 45(5), pp. 583–594. doi:

10.1002/1531-8249(199905)45:5<583::AID-ANA6>3.0.CO;2-W.

63. Mori, S. *et al.* (2008) 'Stereotaxic white matter atlas based on diffusion tensor imaging in an ICBM template', *NeuroImage*, 40(2), pp. 570–582. doi: 10.1016/j.neuroimage.2007.12.035.
64. Mundkur, N. (2005) 'Neuroplasticity in Children', *Indian Journal of Pediatrics*, 72(10), pp. 855–857.
65. Nass, R. (1985) 'Mirror movement asymmetries in congenital hemiparesis: The inhibition hypothesis revisited', *Neurology*, 35(7), pp. 1059–1062. doi: 10.1212/wnl.35.7.1059.
66. Natali, A. L., Reddy, V. and Bordoni, B. (2021) *Neuroanatomy, Corticospinal Cord Tract*, *StatPearls [Internet]*. Treasure Island, FL: StatPearls Publishing. Available at: https://www.ncbi.nlm.nih.gov/books/NBK535423/ (Accessed: 2 October 2022).
67. Nemanich, S. T., Mueller, B. A. and Gillick, B. T. (2019) 'Neurite orientation dispersion and density imaging quantifies corticospinal tract microstructural organization in children with unilateral cerebral palsy', *Human Brain Mapping*, 40(17), pp. 4888–4900. doi: 10.1002/hbm.24744.
68. Noble, J. J., Gough, M. and Shortland, A. P. (2019) 'Selective motor control and gross motor function in bilateral spastic cerebral palsy', *Developmental Medicine & Child Neurology*, 61(1), pp. 57–61. doi: 10.1111/dmcn.14024.
69. Nolze-Charron, G. *et al.* (2020) 'Tractography of the external capsule and cognition: A diffusion MRI study of cholinergic fibers', *Experimental Gerontology*, 130. doi: 10.1016/J.EXGER.2019.110792.
70. Palisano, R. J. *et al.* (2007) 'Stability of the Gross Motor Function Classification System', *Developmental Medicine & Child Neurology*, 48(6), pp. 424–428. doi: 10.1111/J.1469-8749.2006.TB01290.X.

71. Palisano, R. J. *et al.* (2008) 'Content validity of the expanded and revised Gross Motor Function Classification System', *Developmental Medicine & Child Neurology*, 50(10), pp. 744–750. doi: 10.1111/j.1469-8749.2008.03089.x.

72. Peacock, W. J. and Staudt, L. A. (1990) 'Spasticity in Cerebral Palsy and the Selective Posterior Rhizotomy Procedure', *Journal of Child Neurology*, 5(3), pp. 179–185. doi: 10.1177/088307389000500303.

73. Poduslo, S. E. and Jang, Y. (1984) 'Myelin development in infant brain', *Neurochemical Research*, 9(11), pp. 1615–1626.

74. Reed, A. *et al.* (2017) 'Changes in White Matter Integrity following Intensive Voice Treatment (LSVT LOUD®) in Children with Cerebral Palsy and Motor Speech Disorders', *Developmental Neuroscience*, 39(6), pp. 460–471. doi: 10.1159/000478724.

75. Rickards, T. *et al.* (2014) 'Diffusion Tensor Imaging Study of the Response to Constraint-Induced Movement Therapy of Children With Hemiparetic Cerebral Palsy and Adults With Chronic Stroke', *Archives of Physical Medicine and Rehabilitation*, 95(3), pp. 506–514. doi: 10.1016/J.APMR.2013.08.245.

76. Riddell, M. *et al.* (2019) 'Mirror movements in children with unilateral cerebral palsy due to perinatal stroke: clinical correlates of plasticity reorganization', *Developmental Medicine & Child Neurology*, 61(8), pp. 943–949. doi: 10.1111/DMCN.14155.

77. Rosen, M. G. and Dickinson, J. C. (1992) 'The incidence of cerebral palsy', *American Journal of Obstetrics and Gynecology*, 167(2), pp. 417–423. doi: 10.1016/S0002-9378(11)91422-7.

78. Russell, D. J. *et al.* (2004) 'Gross Motor Function Measure User's Manual (GMFM-66 & GMFM-88)', *Physical & Occupational Therapy in Pediatrics*.

79. Safadi, Z. *et al.* (2018) 'Functional Segmentation of the Anterior Limb of the Internal Capsule: Linking White Matter Abnormalities to Specific Connections', *The Journal of Neuroscience*, 38(8), pp. 2106–2117. doi: 10.1523/JNEUROSCI.2335-17.2017.
80. Sakzewski, L., Ziviani, J. and Boyd, R. N. (2011) 'Best responders after intensive upper-limb training for children with unilateral cerebral palsy', *Archives of Physical Medicine and Rehabilitation*. Arch Phys Med Rehabil, 92(4), pp. 578–584. doi: 10.1016/J.APMR.2010.12.003.
81. Salem, Y. and Godwin, E. M. (2009) 'Effects of task-oriented training on mobility function in children with cerebral palsy', *NeuroRehabilitation*. NeuroRehabilitation, 24(4), pp. 307–313. doi: 10.3233/NRE-2009-0483.
82. Sanger, T. D. *et al.* (2003) 'Classification and Definition of Disorders Causing Hypertonia in Childhood', *Pediatrics*, 111(1), pp. 89–97.
83. Sardoğan, C. *et al.* (2021) 'Determining the relationship between the impairment of selective voluntary motor control and gait deviations in children with cerebral palsy using simple video-based analyses', *Gait & Posture*. Elsevier, 90, pp. 295–300. doi: 10.1016/J.GAITPOST.2021.08.019.
84. Scheck, S. M. *et al.* (2015) 'Structural connectivity of the anterior cingulate in children with unilateral cerebral palsy due to white matter lesions', *NeuroImage: Clinical*. Elsevier, 9, pp. 498–505. doi: 10.1016/J.NICL.2015.09.014.
85. Scheck, S. M., Boyd, R. N. and Rose, S. E. (2012) 'New insights into the pathology of white matter tracts in cerebral palsy from diffusion magnetic resonance imaging: a systematic review', *Developmental Medicine & Child Neurology*. Dev Med Child Neurol, 54(8), pp. 684–696. doi: 10.1111/J.1469-8749.2012.04332.X.

86. Senova, S. *et al.* (2020) ‘Anatomy and function of the fornix in the context of its potential as a therapeutic target’, *Journal of Neurology, Neurosurgery & Psychiatry*. BMJ Publishing Group Ltd, 91(5), pp. 547–559. doi: 10.1136/JNNP-2019-322375.
87. Shang, Q. *et al.* (2015) ‘Clinical study of cerebral palsy in 408 children with periventricular leukomalacia’, *Experimental and Therapeutic Medicine*, 9(4), pp. 1336–1344. doi: 10.3892/etm.2015.2222.
88. Shapiro, S. S. and Wilk, M. B. (1965) ‘An Analysis of Variance Test for Normality (Complete Samples)’, *Biometrika*. JSTOR, 52(3/4), p. 611. doi: 10.2307/2333709.
89. Shattuck, D. W. and Leahy, R. M. (2002) ‘Brainsuite: An automated cortical surface identification tool’, *Medical Image Analysis*. Med Image Anal, 6(2), pp. 129–142. doi: 10.1016/S1361-8415(02)00054-3.
90. Shortland, A. (2011) ‘Editorial: Strength, gait and function in cerebral palsy’, *Gait & Posture*. Gait Posture, 33(3), pp. 319–320. doi: 10.1016/J.GAITPOST.2010.10.086.
91. Smith, S. M. *et al.* (2006) ‘Tract-based spatial statistics: Voxelwise analysis of multi-subject diffusion data’, *NeuroImage*, 31(4), pp. 1487–1505. doi: 10.1016/j.neuroimage.2006.02.024.
92. Smith, S. M. and Nichols, T. E. (2009) ‘Threshold-Free Cluster Enhancement: Addressing problems of smoothing, threshold dependence and localisation in cluster inference’, *NeuroImage*, 44(1), pp. 83–98. doi: 10.1016/j.neuroimage.2008.03.061.
93. Song, S. K. *et al.* (2002) ‘Dysmyelination Revealed through MRI as Increased Radial (but Unchanged Axial) Diffusion of Water’, *NeuroImage*, 17(3), pp. 1429–1436. doi: 10.1006/nimg.2002.1267.
94. Staudt, L. A. and Peacock, W. J. (1989) ‘Selective Posterior Rhizotomy for Treatment of Spastic Cerebral Palsy’, *Pediactric Physical Therapy*, 1(1), pp. 3–9.

95. Staudt, M. *et al.* (2003) 'Pyramidal tract damage correlates with motor dysfunction in bilateral periventricular leukomalacia (PVL)', *Neuropediatrics*, 34(4), pp. 182–188. doi: 10.1055/s-2003-42206.

96. Sun, J. M. *et al.* (2017) 'Effect of Autologous Cord Blood Infusion on Motor Function and Brain Connectivity in Young Children with Cerebral Palsy: A Randomized, Placebo-Controlled Trial', *Stem Cells Translational Medicine*, 6(12), pp. 2071–2078. doi: 10.1002/sctm.17-0102.

97. Thomas, B. *et al.* (2005) 'Quantitative diffusion tensor imaging in cerebral palsy due to periventricular white matter injury', *Brain*. Brain, 128(Pt 11), pp. 2562–2577. doi: 10.1093/BRAIN/AWH600.

98. Thompson, R. M. *et al.* (2020) 'MRI safety and imaging artifacts evaluated for a cannulated screw used for guided growth surgery', *Magnetic Resonance Imaging*, 66, pp. 219–225. doi: 10.1016/J.MRI.2019.11.005.

99. Tobin, J. (1958) 'Estimation of Relationships for Limited Dependent Variables', *Econometrica*, 26(1), pp. 24–36. Available at: https://www.jstor.org/stable/pdf/1907382.pdf (Accessed: 10 November 2022).

100. Trivedi, R. *et al.* (2008) 'Treatment-Induced Plasticity in Cerebral Palsy: A Diffusion Tensor Imaging Study', *Pediatric Neurology*, 39(5), pp. 341–349. doi: 10.1016/j.pediatrneurol.2008.07.012.

101. Trivedi, R. *et al.* (2010) 'Correlation of quantitative sensorimotor tractography with clinical grade of cerebral palsy', *Neuroradiology*. Neuroradiology, 52(8), pp. 759–765. doi: 10.1007/S00234-010-0703-8.

102. Ueda, R. *et al.* (2021) 'White matter changes follow low-frequency repetitive transcranial

magnetic stimulation plus intensive occupational therapy for motor paralysis after stroke: a DTI study using TBSS', *Acta Neurologica Belgica*, 121(2), pp. 387–396. doi: 10.1007/S13760-019-01150-2/TABLES/5.

103. Volpe, J. J. (2009) 'Brain injury in premature infants: a complex amalgam of destructive and developmental disturbances', *Lancet Neurology*, 8(1), pp. 110–124. doi: 10.1016/S1474-4422(08)70294-1.

104. Vos, S. B. *et al.* (2012) 'The influence of complex white matter architecture on the mean diffusivity in diffusion tensor MRI of the human brain', *NeuroImage*. Neuroimage, 59(3), pp. 2208–2216. doi: 10.1016/J.NEUROIMAGE.2011.09.086.

105. Vuong, A. *et al.* (2021) 'Selective Motor Control is a Clinical Correlate of Brain Motor Tract Impairment in Children with Spastic Bilateral Cerebral Palsy', *American Journal of Neuroradiology*, 42(11), pp. 2054–2061. doi: 10.3174/ajnr.A7272.

106. Wahl, M. *et al.* (2007) 'Human Motor Corpus Callosum: Topography, Somatotopy, and Link Between Microstructure and Function', *The Journal of Neuroscience*, 27(45), pp. 12132–12138. doi: 10.1523/JNEUROSCI.2320-07.2007.

107. Wakana, S. *et al.* (2007) 'Reproducibility of quantitative tractography methods applied to cerebral white matter', *NeuroImage*. Neuroimage, 36(3), pp. 630–644. doi: 10.1016/J.NEUROIMAGE.2007.02.049.

108. Wheeler-Kingshott, C. A. M. and Cercignani, M. (2009) 'About "axial" and "radial" diffusivities', *Magnetic Resonance in Medicine*. Magn Reson Med, 61(5), pp. 1255–1260. doi: 10.1002/MRM.21965.

109. Winklewski, P. J. *et al.* (2018) 'Understanding the Physiopathology Behind Axial and Radial Diffusivity Changes-What Do We Know?', *Frontiers in Neurology*, 9(92). doi:

10.3389/fneur.2018.00092.

110. Wu, Y.-N. *et al.* (2010) 'Efficacy of Robotic Rehabilitation of Ankle Impairments in Children with Cerebral Palsy', *Annual International Conference of the IEEE Engineering in Medicine and Biology Society*, 2010, pp. 4481–4484. doi: 10.1109/IEMBS.2010.5626043.

111. Wu, Y.-N. *et al.* (2011) 'Combined Passive Stretching and Active Movement Rehabilitation of Lower-Limb Impairments in Children With Cerebral Palsy Using a Portable Robot', *Neurorehabilitation and Neural Repair*, 25(4), pp. 378–385. doi: 10.1177/1545968310388666.

112. Yeargin-Allsopp, M. *et al.* (2008) 'Prevalence of Cerebral Palsy in 8-Year-Old Children in Three Areas of the United States in 2002 : A Multisite Collaboration', *Pediatrics*, 121(3), pp. 547–554. doi: 10.1542/peds.2007-1270.

113. Zhang, L. *et al.* (2021) 'DTI Tract-Based Quantitative Susceptibility Mapping: An Initial Feasibility Study to Investigate the Potential Role of Myelination in Brain Connectivity Change in Cerebral Palsy Patients During Autologous Cord Blood Cell Therapy Using a Rotationally-Invar', *Journal of Magnetic Resonance Imaging*, 53(1), pp. 251–258. doi: 10.1002/JMRI.27286.

114. Zhao, M. *et al.* (2019) 'Hand, foot and lip representations in primary sensorimotor cortex: a high-density electroencephalography study', *Scientific Reports*, 9(1). doi: 10.1038/s41598-019-55369-3.

115. Zhou, J. Y. *et al.* (2019) 'Influence of impaired selective motor control on gait in children with cerebral palsy', *Journal of Children's Orthopaedics*. British Editorial Society of Bone and Joint Surgery, 13(1), pp. 73–81. doi: 10.1302/1863-2548.13.180013/ASSET/IMAGES/LARGE/10.1302_1863-2548.13.180013-FIG2.JPEG.